1-1-1982

Structure-property relationships in polybutadiene polyurethanes.

Christine M. Brunette
University of Massachusetts Amherst

STRUCTURE-PROPERTY RELATIONSHIPS IN POLYBUTADIENE POLYURETHANES

A Dissertation Presented

by

CHRISTINE M. BRUNETTE

Submitted to the Graduate School of the
University of Massachusetts in partial fulfullment
of the requirements for the degree of

DOCTOR OF PHILOSOPHY

May 1982

Polymer Science and Engineering

STRUCTURE-PROPERTY RELATIONSHIPS IN POLYBUTADIENE POLYURETHANES

A Dissertation Presented

By

CHRISTINE M. BRUNETTE

Approved as to style and content by:

Dr. William J. MacKnight, Chairperson of Committee

Dr. Shaw L. Hsu, Member

Dr. Robert E. Lenz, Member

Dr. William J. MacKnight
Department Head
Polymer Science and Engineering

To Mike and Anne

for their encouragement and sacrifices

throughout the course of my education

ACKNOWLEDGEMENTS

I wish to acknowledge the advice, guidance and continual encouragement given to me by Professor William J. MacKnight throughout this research endeavor. I am also indebted to Professor Shaw L. Hsu who offered many helpful criticisms and suggestions and to Professor Robert W. Lenz and Dr. N.S. Schneider for their enthusiastic support and valuable discussions.

I would like to acknowledge the time and talents expended in behalf of this this research by many of my fellow graduate students. In particular, my sincere appreciation is extended to Mark Rossman and Bruce Bengston for preparing the samples examined throughout this research and to Don Burchell for his patience and assistance with the FT-IR experiments.

Many thanks go to: the faculty and staff of the Polymer Science and Engineering Department for their professional encouragement and assistance; the Materials Research Laboratory and Army Materials and Mechanics Research Center for supporting my studies at the University of Massachusetts.

Finally, my warmest appreciation to friends and colleagues for making my stay here enjoyable and memorable.

PREFACE

The work in this dissertation is presented in six separate chapters, each of which includes a brief introduction, experimental and self-contained reference section. The overall objective was to investigate the relations between composition, phase segregation, hydrogen bonding and the properties of segmented polyurethanes based on polybutadiene soft segments. The absence of hydrogen bonding to the soft segment was expected to simplify considerations both by restricting all hydrogen bonding to the hard segment structure and by promoting phase segregation. A brief introduction and review of the structure and properties of segmented polyurethanes is presented in Chapter I. In Chapter II, the effects of hydrogenation and aromatic chain extenders on the dynamic mechanical, stress-strain, and thermal transition behavior of crosslinked polybutadiene polyurethanes is presented. Structure-property studies are extended to linear systems comprised of amorphous and (semi)crystalline hard segments in Chapters III and IV with emphasis on the time-dependent recovery of the properties. In Chapters V and VI, hydrogen bonding in these polymers and model hard segment compounds is investigated using infrared spectroscopy. Much of the work represented in Chapters II through V has been previously published.

ABSTRACT

Structure-Property Relationships of Polybutadiene Polyurethanes

(April 1981)

Christine Mary Brunette

B.S., Boston College
M.S., University of Massachusetts
Ph.D., University of Massachusetts

Directed by: Professor William J. MacKnight

The nature of hydrogen bonding, phase segregation, and hard segment organization is studied in a series of segmented polyurethanes based on hydroxy terminated polybutadiene (HTPBD) soft segments and hard segments consisting of either 2,4- or 2,6-toluene diisocyanate (TDI) and 1,4-butanediol (BDL). The existence of two phase morphology is deduced from dynamic mechanical relaxation and thermal analysis. All polymers exhibit a soft segment glass transition very close to Tg of free HTPBD homopolymer and independent of hard segment structure and concentration. The high temperature transitions, corresponding to the glass transition in 2,4-TDI polymers and melting in the 2,6-TDI polymers are strongly dependent upon hard segment concentration and average hard segment length. The unusual occurrence of two hard segment transitions in the 2,4-TDI series is related, in part, to the exceptionally high degree of phase segregation with the lower glass transition resulting from localization of shorter hard segment units and the higher transition from domains containing longer hard segment units. An inversion of the continuous and dispersed phases is reflected in both stress-strain and

dynamic mechanical properties above a 40 weight percent of hard segment. Thermal history is found to have negligible effect on the position of the soft segment glass transition and, therefore, in the degree of phase segregation for all materials studied. The time-dependence in dynamic mechanical and thermal properties is related to physical changes within the hard segment domains, independent of the soft segment matrix.

An analysis of hydrogen bonding in a selection of HTPBD polyurethanes and model compounds based on 2,4- and 2,6-TDI and p,p'-diphenylmethane diisocyanate (MDI) and BDL hard segments is made using Fourier Transform Infrared Spectroscopy (FTIR). Changes in the frequency, half-width and intensity of the bonded N-H absorption band resulting from thermal treatment are correlated to structural changes as evidenced by differential scanning calorimetry (DSC); variations in behavior are related to differences in packing and the ability and ease at which crystallization and reorganization of the hard segment repeat unit occurs. Resolution of the N-H band into its hydrogen bonded and non-bonded components indicates 80 to 90 percent of the N-H groups are hydrogen bonded at room temperature. Since hydrogen bonded interactions are limited to the hard segment components in PBD-containing polyurethanes, the results provide a quantitative measure of the extent of microphase segregation. Temperature-dependent studies indicate that the onset temperature for hydrogen bond dissociation occurs at 25 to 75°C in the 2,4-TDI polymers and at about 130°C in the 2,6-TDI polymers, close to the transition temperatures for the amorphous and crystalline domain structure, respectively. Heat of dissociation is about

4 kcal/mole for the former series and 7-8 kcal/mole for the latter. Overall, the results indicate that the thermal behavior of hydrogen bonding is sensitive to structure organization and correlate well with other properties studied via calorimetry and dynamic mechanical relaxation.

TABLE OF CONTENTS

LIST OF TABLES

LIST OF FIGURES

C H A P T E R I

INTRODUCTION AND REVIEW

A. Structure and Properties of Segmented Polyurethanes

Considerable attention has been devoted toward an understanding of the property-structure relationships in segmented polyurethanes in recent years. In general, these materials derive their unusual properties from the thermodynamic incompatibility of the component polymer segments and consequent phase separation. Typically, the "soft" segments are composed of a rubbery polymer (i.e. polyester or polyether) with its glass transition temperatures, Tg_s, well below the use temperature. The "hard" segments, which are generally formed from the extension of an aromatic diisocyanate with a low molecular weight diol provide physical crosslinking and reinforcement for the soft phase and are responsible for the higher temperature performance. Much of the interest in these materials arises from their thermal reversibility which allows them to be processed conventionally as thermoplastics at high temperatures but behave like crosslinked elastomers upon cooling.

The existence of phase segregation, caused by the clustering of hard and soft segments into separate domains, has been well documented (1-3). Consequently, many of the physical and mechanical properties (i.e. enhanced modulus, high extensibility, and resiliency) have been interpreted in terms of a two phase morphology. Both soft and hard domains can be amorphous and/or partially crystalline depending on the

compositional variables. For partially crystalline systems, the ordered hard segment phase is thought to be composed of fringed lamellae domains of thickness equal to the hard segment length and lateral width of less than a few hundred Angstroms (4). Occasionally there is a spherulitic superstructure (4,5).

Using small angle x-ray scattering (SAXS), Clough, Schneider, and King (1) reported that a reasonable amount of SAXS is present in non-crystalline samples based on 2,4-TDI polyurethanes. Moreover, they found that the domain size and organization of domains increased with increasing hard segment length. Wilkes and Yusek (6) extended such SAXS studies to include the deformation behavior. Noncrystalline materials gave maxima in the SAXS at a spacing of 15 nm while the crystalline material gave a maximum at 22 nm. Bonart (3,7) studied polymers with "paracrystalline" and/or crystalline hard segments by x-ray techniques. He found that on elongation, the paracrystalline hard segments oriented initially transverse to the stretch direction. At higher strains, the original ordered regions were disrupted and segmental orientation into the stretch direction occurred. Highly crystalline hard segments oriented transversely at all elongations and were described as acting more as inert fillers. The soft segment or noncrystalline domains, having weaker interactions, were found to orient into the stretch direction at all elongations. Similar conclusions were reported by Cooper et al. using infrared dichroism (8-10).

Extensive studies concerning the effects of the chemical structure, the molecular weight, and molecular weight distribution of the soft and

the hard segments on the extent of phase segregation, domain formation and thus polymer properties have been reported. Harrell (11) demonstrated that narrowing of the hard segment size distribution drastically increased the modulus and permanent set while narrowing the soft segment distribution mildly increased the modulus but also gave a drastic increase in permanent set. Subsequent studies of the orientation behavior of these materials (8), however, suggest that there is little effect of polydispersity other than the effect associated with change in crystallinity.

Seefried, Koleske, and Critchfield (12-14) have carried out systematic studies on MDI polyurethanes with polycaprolactone soft segments over a wide range of soft segment molecular weight and hard segment concentration. They found that the glass transition shifted to lower temperatures as the soft segment chain length increased and, that for the highest molecular weight polyesters, soft segment crystallization occurred. The Tg of the lower molecular weight soft segment samples increased with increasing hard segment content while the Tg of the higher molecular weight materials was unchanged until extreme amounts of hard segments were introduced. A higher degree of phase separation between blocks was postulated in the latter materials. This group also illustrated that MDI-polyurethanes, in contrast to TDI urethanes (based on the two isomers) possess a more perfect domain organization due to short range order including crystallinity and consequently show a higher extent of segregation between hard and soft segment.

An extensive study of TDI polyurethanes, one based on the asymmetric 2,4-TDI structure and the other on the symmetrical 2,6-TDI isomer has been carried out by Schneider and coworkers by DSC, TMA, and SAXS (15-18). The glass transition temperature of 2,4-TDI polymers with polyether soft segments of 1000 M_n showed a strong dependence on composition. The authors attributed this behavior to extensive hard and soft segment mixing in these amorphous materials. The corresponding polyurethanes based on the 2,6-TDI structural isomer displayed a higher degree of phase segregation as indicated by a concentration invariant Tg and high melting endotherms, associated with well ordered and crystalline hard semgnt domains. An increase in soft segment molecular weight from 1000 to 2000 induced phase segregation in both TDI series with some crystallinity in the soft segment developing in the 2,6-TDI series. This group also made a comparison of TDI urethanes based on polyether and polyester soft segments. They concluded that a higher degree of hard-soft segment mixing occurs in polyester than in polyether urethanes but they could not measure it quantitatively. More recently, a SAXS investigation of these polyurethanes (19) showed that the average interfacial thicknesses of the domains were 5-7 Å and 10-12 Å for the polyether and polyester urethanes, respectively, thus supporting the above conjecture that polyether urethanes lead to better phase separation.

B. Hydrogen Bonding in Polyurethane Elastomers

Segmented polyurethanes are extensively hydrogen bonded. In all cases, the NH group of the urethane serves as the proton donor while the

acceptor group may include the carbonyl and adjacent oxygen atom in the urethane group as well as the ester carbonyl or ether oxygen of the soft segment. Much of the research on hydrogen bonding has been made using infrared spectroscopy, being detected by absorption bands lower in frequency than the free NH and carbonyl absorbances (20). Resolution of these bands into their free and bonded components has served as a semi-quantitative measure of the degree of phase separation. Even before the concept of two-phase morphology was established by Cooper and Tobolsky (21) studies of the IR spectra of polyester and polyether-based urethanes by Bogarchuk et al. (20) showed that there were more hydrogen bonding interactions between the soft and hard segments in the polyester than polyether. On the basis of these findings, the authors suggest that some form of hard segment aggregation occurs in the polyether urethane, while in the polyester urethane the hard segments are dispersed throughout the soft segment matrix. Later infrared studies showed that interurethane bonding is favored both as urethane concentration and soft segment length are increased (22,23).

Studies of a series of MDI polyurethanes by Seymour and coworkers (24) have shown that virtually all NH groups were hydrogen bonded at room temperature, but that only 60% of the urethane carbonyls participated in hydrogen bond formation. The remaining hydrogen bonds were associated with the soft segment. This was accounted for by incompleteness in phase separation due to mixing of hard and soft segments or by interactions at the domain-matrix interface.

Infrared analysis on hydrogen bonding in TDI polyurethanes have

been reported by Sung and Schneider (17). At room temperature, almost all the urethane NH groups in both 2,6-TDI and 2,4-TDI series were reported to form hydrogen bonds. However, about 80 and 50% of urethane carbonyl groups were hydrogen bonded in the 2,6-TDI and in the comparable 2,4-TDI polyurethanes, respectively. This evidence suggested that the degree of phase segregation is higher in the symmetric isomer, thus supporting their earlier studies. However, quantitative determination of hard and soft segment interactions were complicated by the number of proton acceptor groups possible in these materials.

The temperature dependence of hydrogen bonding in polyurethanes has been studied in order to relate hydrogen bond dissociation to domain morphology. Working on a series of MDI-based segmented polyurethanes, Seymour and coworkers (25) showed that the transitions observed by DSC could be moved to higher temperatures whereas the onset temperature for hydrogen bond dissociation, obtained from infrared analysis, remained unchanged at 70 to 80°C. These results lead to the conclusion that the dissociation of hydrogen bonding is insensitive to the degree of order present.

The thermal behavior of hydrogen bonding in nonsegmented polyurethane homopolymers based on aliphatic and aromatic diisocyanates were examined by MacKnight and Yang (26). They found that below Tg there were no free NH groups in the aliphatic polyurethanes where 25-30% of free NH were found in the aromatic series. Moreover, the integrated absorbance of the NH stretching vibration showed discontinuities at

temperatures corresponding to Tg, T_m, and in the case of the aliphatic series, to first order crystal-crsytal phase transition T_t.

Subsequent temperature dependent IR work on TDI polyurethanes (15) showed that the onset temperature for the dissociation of hydrogen bonded NH and carbonyl in 2,6-TDI polyurethanes occurs at about 65°C, independent of urethane content and well below the melting temperature of the crystalline hard segment structure. For the 2,4-TDI elastomers, hydrogen bonded NH groups began to dissociate at temperatures of 40 to 60°C while the carbonyl fraction changed insignificantly to 150°C. The higher stability of interurethane hydrogen bonded in the latter materials was suggested as due to the high steric hindrance caused by the methyl group in the 2,6-TDI polymers. Heats of hydrogen bond dissociation were reported to be about 4 Kcal/mole for both the 2,4-TDI and 2,6-TDI series.

The temperature variation of hydrogen bonding in polyether and polyester MDI segmented elastomers (27) revealed that the extent of interurethane hydrogen bonding was higher in materials having better phase separation. Hard to soft segment bonding was found to be weaker and dissociate first on heating. The ΔH of hydrogen bond dissociation was shown to increase with increasing hard and soft segment length and thus used as a measure of hard domain perfection.

Arguments based on hydrogen considerations have also been used to describe the internal structure of domains and deformation behavior of polyurethane elastomers. Bonart et al. (3,7,28) have analyzed the wide angle x-ray diagrams on MDI-based urethanes and proposed a model based

on a system of hydrogen bridged between hard segments. An interference in the WAXS at 12 A^{-1} was attributed to a quasiperiodical or paracrystalline arrangement of the hard segments. These models were based on maximization of hydrogen bonding to conform with the structural information obtained by WAXS and lamellar arrangement of hard segments. During the application of stress, the author speaks of "restructuration" of physical crosslinking involving the breakage and reformation of hydrogen bonds. Tanaka, Yokoyama, and Kaku (29) presented a small amount of data indicating a slight slippage of the hydrogen bonds with stress, followed by a rather slow recovery. More recent deformation studies by Seymour and coworkers (23) showed little break up of hydrogen bonding at elongations up to 300%. They concluded that changes in the extent of hydrogen bonding do not play an important role in determining observed elastic properties.

An inherent difficulty in studying the role of hydrogen bonding in influencing the properties of polyurethane elastomers, the nature of the hard segment structure and of phase segregation is the fact that in most instances hydrogen bonding occurs not only in the hard segment but between the hard segment and the soft segment as well (i.e. polyester and polyether urethanes). Therefore, the present study was undertaken to gain additional insight into such phenomena in segmented polyurethanes where this complexity is excluded. The polyurethanes studies include those based on a non-polar polybutadiene soft segment. A schematic representation of the polymers is shown in Figure 1-1.

Soft Segment

Hard Segment

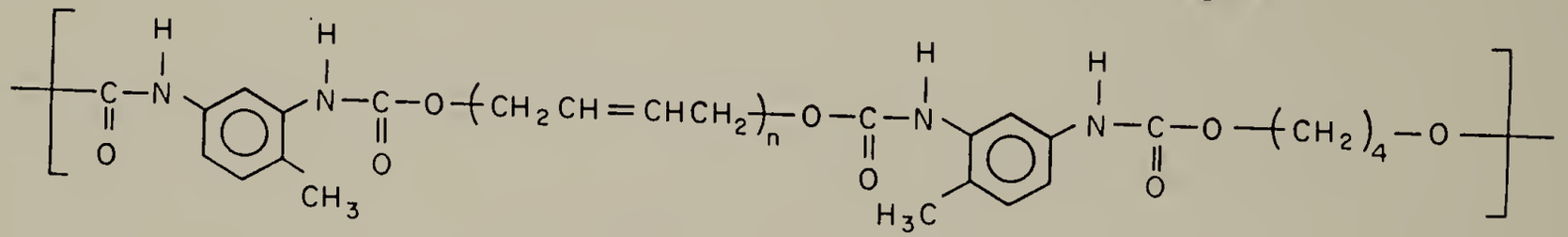

2,4 - TDI - BDL - PBD Polyurethane

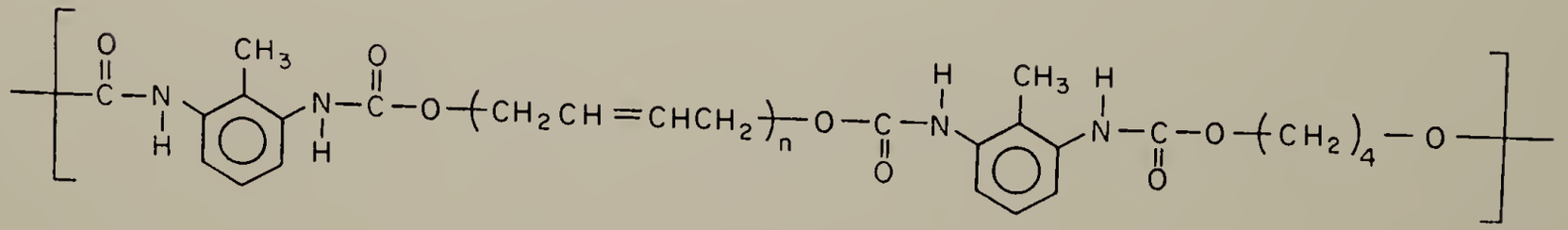

2,6 - TDI - BDL - PBD Polyurethane

Fig. 1-1. Structure of PBD-polyurethane elastomers.

References

1. S.B. Clough, N.S. Schneider and A.O. King, J. Mcromol. Sci., B2, 641 (1968).
2. G.M. Estes, S.L. Cooper and A.V. Tobolsky, J. Macromol. Sci., Rev. Macromol. Chem. C4 (1), 167 (1970).
3. R. Bonart, L. Moribitzer and G. Hentze, J. Macromol. Sci., B3 (2), 337 (1969).
4. N.S. Schneider, C.R. Desper, J.L. Illinger, A.O. King, and D. Barr, J. Macromol. Sci.-Phys. B11, 527 (1975).
5. J.A. Koutsky, N.V. Hein, S.L. Cooper, J. Polym. Sci., Polym. Lett. Ed. 8. 353 (1970).
6. C.E. Wilks and C.S. Yusek, J. Macromol. Sci.-Phys., B7(1), 157 (1973).
7. R. Bonart, L. Morbitzer and E.H. Muller, J. Macromol. Sci.-Phys., B3(2), 447 (1974).
8. H.N. Ng, A.E. Allegrezza, Jr., R.W. Seymour and S.L. Cooper, Polymer, 14, 255 (1973).
9. G.M. Estes, R.W. Seymour and S.L. Cooper, Macromolecules, 4, 452 (1971).
10. R.W. Seymour, A.E. Allegrezza, Jr. and S.L. Cooper, Macromolecules, 6, 89;6 (1973).
11. L.L. Harrell, Jr., Macromolecules, 2(6), 607 (1969).
12. C.G. Seefried, J.V. Koleske and F.E. Critchfield, J. Appl. Polym. Sci., 19, 2493 (1975).

13. C.G. Seefried, J.V. Koleske and F.E. Critchfield, J. Appl. Polym. Sci., 19, 2503 (1975).

14. C.G. Seefried, J.V. Koleske, F.E. Critchfield and J.L. Dodd, Polym. Eng. Sci., 15, 646 (1975).

15. C.S. Paik Sung and N.S. Schneider, Macromolecules, 10, 452 (1972).

16. N.S. Schneider, C.S. Paik Sung, R.W. Matton and S.L. Illinger, Macromolecules, 8, 62 (1975).

17. C.S. Paik Sung and N.S. Schneider, Macromolecules, 8, 68 (1975).

18. N.S. Schneider and C.S. Paik Sung, Polym. Eng. Sci., 17, 73 (1977).

19. Z. Ophir, J. Polym. Sci.-Phys., 18, 1469 (1980).

20. Y.M. Boyarchuk, L.Y. Rappoport, V.N. Mikitin and N.P. Apukhtine, Polym. Sci. USSR, 7, 859 (1965).

21. S.L. Cooper and A.V. Tobolsky, J. Appl. Polym. Sci., 10, 1837 (1966).

22. T. Tanaka, T. Yokeyama, and Y. Yamaguchi, J. Polym. Sci., Part A-1, 6, 2137 (1968).

23. K. Nakayama, T. Ino and I. Matsubura, J. Macromol. Sci. Chem., A3(5), 1005 (1969).

24. R.W. Seymour, G.M. Estes and S.L. Cooper, Macromolecules, 3, 579 (1970).

25. R.W. Seymour and S.L. Cooper, Macromolecules, 6, (48) (1973).

26. W.J. MacKnight and M. Yang, J. Polym. Sci., Polym. Symp. Ser., 42, 817 (1973).

27. V.W. Srichatrapimuk and S.L. Cooper, J. Macromol. Sci.-Phys., B15(2), 267 (1978).

28. R. Bonart, J. Macromol. Sci.-Phys., B2(1), 115 (1968).

29. T. Tanaka, T. Yokoyama and K. Kaku, Mem. Fac. Sci., Kyushu Univ., 23, 113 (1963).

CHAPTER II

STRUCTURAL AND MECHANICAL PROPERTIES OF CROSSLINKED POLYBUTADIENE POLYURETHANES AND THEIR HYDROGENATED DERIVATIVES

Introduction

Segmented polyurethanes incorporating a hydroxy terminated polybutadiene (HTPBD) soft segment offer the advantage of low moisture permeability and have been the subject of several studies aimed at exploiting this property for adhesives and electrical potting compounds (1-3). In addition, these polyurethanes exhibit improved hydrolytic stability over polyester and polyether polyurethanes, as well as excellent resistance to strong acids or bases. The HTPBD (R-45M) in common use is prepared by a free radical polymerization and consists of about 60% trans, 20% cis, and 20% vinyl content. The average hydroxyl functionality is greater than 2 and frequently in the range of 2.1-2.4.

Several recent publications have appeared which deal with the structure and properties of HTPBD polyurethanes. A study by Legasse (4) was concerned with the morphology, transition behavior and especially the time dependent recovery of the hard segment transition after heating in samples cured with p,p'diphenylmethane diisocyanate (MDI) and butanediol, but some aspects of the behavior reported were probably conditioned by the nature of the commercial coating formulation which was examined. The influence of HTPBD molecular weight on the mechanical properties of both nonsegmented and segmented polyurethane copolymers

was studied by Ono and coworkers (5). They demonstrated that superior properties were obtained with segmented copolymers, reflecting the contribution of domain structure. In addition, it was shown that the tensile strength and related mechanical properties increased significantly below 3,000 HTPBD molecular weight, which corresponds to the molecular weight of the most commonly available HTPBD prepolymer (Arco R-45M).

The present work is concerned with three related series of HTPBD samples, in one of which the HTPBD has been partially hydrogenated, the other of which an aromatic chain extender is used. Hydrogenation of the HTPBD was undertaken both as a means of improving the oxidative stability to meet the need of polyurethanes for long term encapsulation and to study the influence on polyurethane properties. The use of N,N-dihydroxyethylaniline as chain extender in place of the more commonly used 1,4 butanediol is recommended as giving somewhat higher mechanical properties (6). Results are presented for the structural, thermal, dynamic mechanical and stress-strain properties of these HTPBD polyurethanes, and, where possible, correlations are made.

Experimental

Materials and polymerization conditions. The synthesis was carried out by a two step method involving endcapping the hydroxyl-terminated polybutadiene (PBD) (Arco, R45M) with a 5% molar excess of toluene-2,4-diisocyanate (TDI) (Aldrich) followed by reaction with the chain

extender, 1,4 butanediol (BDL) (Aldrich) or N,N-dihydroxyethylaniline (HEA) (Aldrich). Since some crosslinking occurs through the excess functionality of R45M, the resulting polymers are not soluble or truly thermoplastic.

A 100 ml reaction vessel equipped with a mechanical stirrer and vacuum outlet was charged with liquid prepolymer, evaculated and immersed in an oil bath at 120°C. After one hour, a weighed amount of TDI was added. The mixture was then stirred for one hour under constant nitrogen flow, after which the temperature was lowered to 80°C. Following the addition of the chain extender, the reaction mixture was degassed, poured between teflon sheets and cured in the press (3 MPa pressure) at 120°C for 17 hours.

Hydrogenation of Prepolymer. HTPBD (100 g) was dissolved in 500 ml of toluene in a 2 liter reactor sleeve. Approximately 0.5 g of Pd on activated charcoal catalyst was added and the sleeve was placed in the pressure reactor bomb assembly to which a hydrogen cylinder was connected. The vessel was purged with H_2 for 15 minutes and then pressurized with H_2. The reaction was allowed to proceed until a pressure drop was attained which corresponded to the desired level of hydrogenation. The mixture was then filtered through a Buchner funnel and the catalyst residues were removed. The solvent was evaporated with a rotary evaporator, isolating the hydrogenated polybutadiene prepolymer (HYPBD).

The extent of hydrogenation was determined by microanalysis for carbon and hydrogen and by proton nuclear magnetic resonance (NMR).

Infrared Analysis. Infrared spectra (400-4000 cm^{-1}) were obtained with a Nicolet 7199 Fourier Transform Infrared spectrometer. One hundred scans at 2 cm^{-1} resolution were signal averaged and stored on a disk for further analysis. Spectra of the prepolymer and its hydrogenated form were obtained from films cast from chloroform solution on KBr disks. Usually this technique yields sufficiently thin films for quantitative analysis. The criteria for the analysis is that Beer's law be obeyed; hence low absorptions are needed (7). Identical infrared spectra were also obtained for films cast as formed at 25°C. However, this technique usually yields thicker films, and hence higher absorbance values.

Thermal Analysis. Measurements of the soft segment glass transition temperature were made with the Perkin Elmer DSC-2, purged with He and chilled with liquid nitrogen. The DSC was calibrated for low temperatures using the crystal-crystal transformation of cyclohexane at 186°K. Runs were conducted on polymer samples of about 15 mg at a heating rate of 20°C/min and an attenuation of 2 mcal/sec. The higher temperature runs were carried out in a Perkin Elmer DSC-2 equipped with a two stage mechanical refrigeration unit. Scans were conducted from 240 to 420°K at 20°C/min using an attenuation of 2 mcal/sec. The samples were usually the same as those previously run in the low temperature DSC measurements. Glass transition temperatures were determined as the temperature corresponding to one half the increase in heat capacity at the transition.

Dynamic mechanical measurements. All measurements were carried out using a Vibron Dynamic Viscoelastometer (Toyo Measuring Instrument Co.) Model DDV II at a fixed frequency of 11 Hz. The temperature range was from -130°C to 150°C and the samples were heated at a nominal rate of 1.5 deg/min under a dry nitrogen atmosphere.

Tensile testing. Stress-strain data were obtained on an Instron TM-SM table model universal testing instrument at an extension rate of 40 mm/min. Specimens were die-cut from a sheet of the polyurethane film .015 in. thick. A specimen gage length was about 1.5 in. long and .12 in. in width. In cyclic stress-strain experiments, a single sample was submitted to increasing amounts of prestrain. The sample was extended by increments up to 20%, allowed to relax at zero load for 5 minutes, extended to 40%, etc. This test provides data at 0, 20, 40, 60, and 80% of the extension at break (ε_b). All data reported are averages of at least 5 tests on different samples.

Results and Dissussion

Three series of polyurethanes were prepared. Series I samples were based on HTPBD-TDI-BDL, series II on HYPBD-TDI-BDL and series III on HTPBD-TDI-HEA. Each series consisted of samples with increasing molar ratios of TDI-BDL(HEA) to HTPBD at an NCO/OH ratio of approximately 1.05, assuming a functionality of 2.2 hydroxyls per molecule for the prepolymer (see Table 2.1).

Table 2-1

Composition of HTPBD-Polyurethanes and Hydrogenated Derivatives

Sample		Molar Composition TDI/BDL(HEA)/PBD	Urethane wt. %
Series I TDI-BDL-PBD	R-50	4.2/3.1/1.0	27
	R-51	6.5/5.3/1.0	38
	R-52	8.4/6.9/1.0	44
	R-53	10.1/9.0/1.0	50
Series II TDI-BDL-HYPBD	HY-50	4.1/2.9/1.0	26
	HY-51	6.4/5.2/1.0	37
	HY-52	8.3/7.3/1.0	43
	HY-53	10.2/8.9/1.0	48
Series III TDI-HEA-PBD	S-1	3.5/2.4/1.0	28
	S-2	4.2/2.7/1.0	35
	S-3	5.7/4.5/1.0	42
	S-4	8.0/6.7/1.0	51
	S-5	11.4/9.3/1.0	62

The percent hydrogenation of the prepolymer as determined by microanalysis and NMR was 65 percent. The functionality was found to be the same as the nonhydrogenated material (8), assuming the slight change in molecular weight due to the hydrogenation to be negligible. In contrast to HTPBD prepolymer which was clear, the hydrogenated product (HYPBD) was opaque.

Characterization of the Hydrogenated PBD. The infrared spectra confirmed the composition expected for the prepolymer. The strong 970 cm^{-1} and 910 cm^{-1} bands are generally associated with the C-H out of plane motion in the trans and 1,2 vinyl units, respectively (9). In addition, the 995 cm^{-1} band was used to analyze the cis content (10). These normal motions are very localized and, therefore, suitable for quantitative analysis (9).

After hydrogenation, significant changes in the ratios of these bands are observed. For example, as shown in Figure 2-1, the integrated intensity of the 910 cm^{-1} band, assignable to 1,2 vinyl groups, decreased substantially compared to trans segments; the ratio of the integrated intensities of 910 cm^{-1}/970 cm^{-1} decreasing from about 0.35 to 0.11 in the hydrogenated form. The preferential hydrogenation of the vinyl groups is in accord with the fact that this moiety occurs in a pendant position on the polymer and should be more accessible to hydrogen. This finding is consistent with that of Mango et al. in that the rate of hydrogenation of the vinyl double bond is greater than that of the internal olefin (11). The cis units were also preferentially hydrogenated over the trans, although to a lesser extent than the vinyl

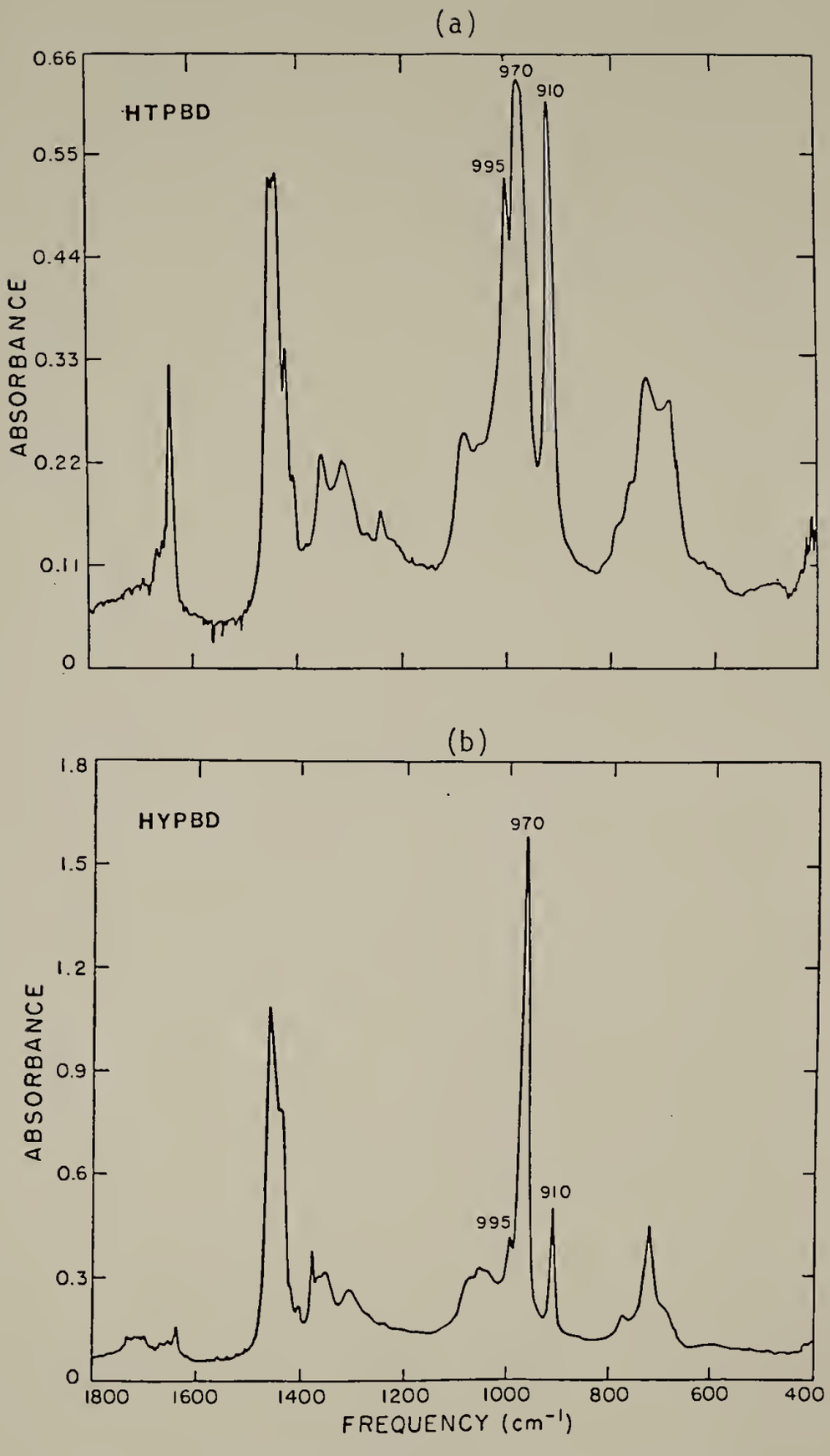

Fig. 2-1. Infrared spectra of nonhydrogenated (a) and hydrogenated (b) PBD prepolymer.

group. In addition, the 1377 cm^{-1} band associated with methyl rocking motion was detected after hydrogenation (12).

The sequence length of the methylene units in the hydrogenated samples was also of interest. A medium intense band was found at 720 cm^{-1}, which is commonly associated with amorphous polyethylene (13,14). This observation suggests that hydrogenation is quite extensive, consistent with the NMR studies, which showed a 65% saturation. In addition, a very weak band was observed at 729 cm^{-1} as shown in Figure 2-2. This band is the CH_2 rocking vibration component arising from the crystal field splitting associated with methylene sequences in an orthorhombic unit cell (15). The lack of extensive crystallinity as evidenced by the weak absorption band is probably due to the random placement of the hydrogenated 1,2 vinyl groups and residual unsaturated segments within the polymer chain.

The DSC scan of the hydrogenated PBD shows complex behavior (Figure 2-3). A well defined Tg is observed at -70°C, about 11°C higher than the Tg of its unsaturated precursor. Above the Tg there is a diffuse but marked endothermal region extending from about -50 to 25°C and a broad but well defined endotherm with a peak at 39°C. The broadly distributed endothermal region, presumably due to melting of crystalline structure, suggests that the size distribution of the crystals is very large and that a preponderance of small imperfect crystals exists. The crystals have a polyethylene-like structure based on the infrared results. The behavior shown in Figure 5 is repeatable on cooling and rescanning.

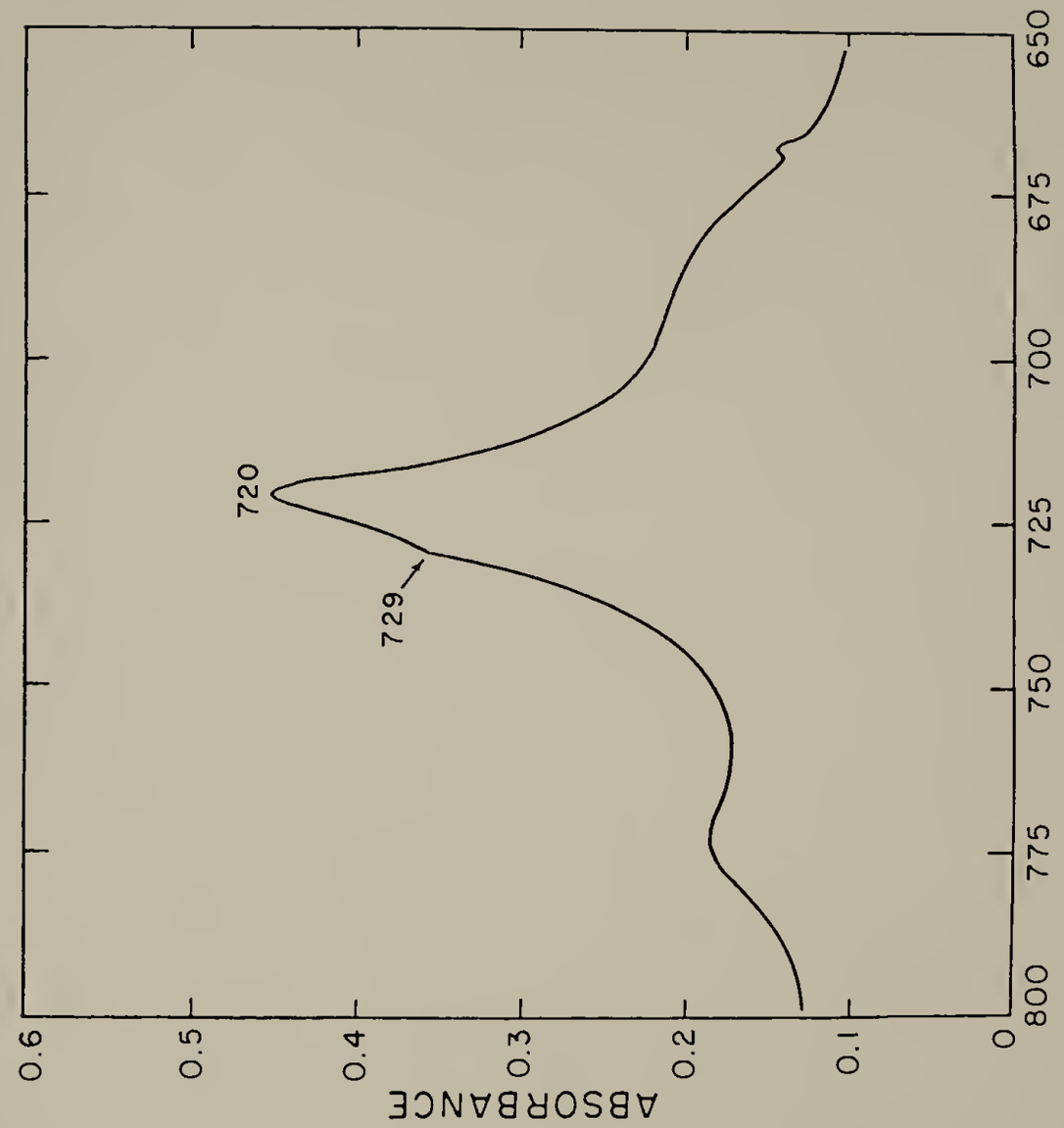

Fig. 2-2. Infrared spectrum of hydrogenated HTPBD prepolymer showing the 720 cm^{-1} band.

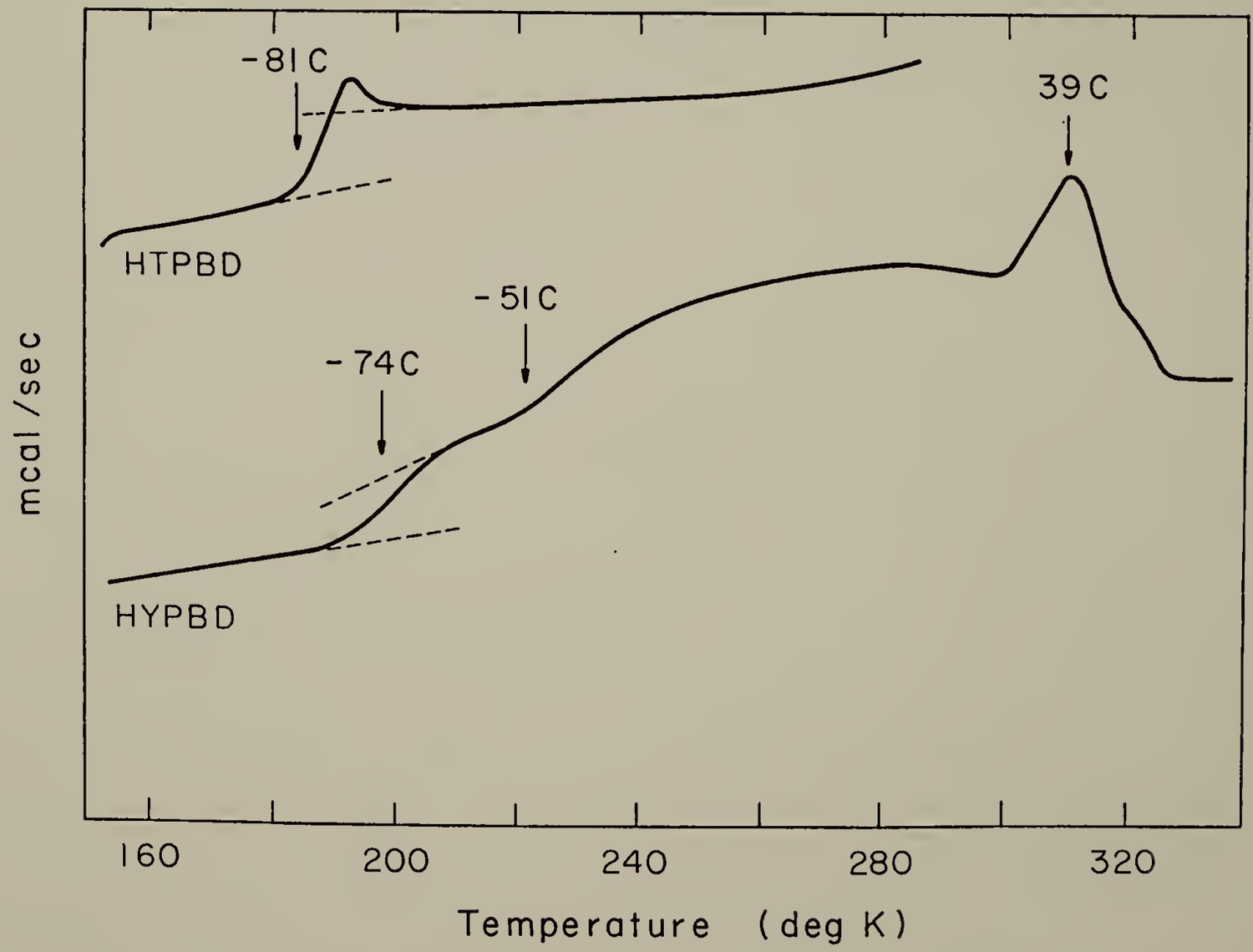

Fig. 2-3. DSC scan (160 to 340°K) on hydroxyl terminated polybutadiene (PBD) and its hydrogenated derivative (HYPBD).

Thermal Analysis of Series I-III Polyurethanes. The DSC results for the various PBD polyurethanes are summarized in Table 2-2. The soft segment glass transition temperature in all these PBD polyurethanes was reproducible and well defined. The Tg values are insensitive to the increasing hard segment content. This behavior, together with the fact that the average value of Tg is less than 10°C higher than that obtained for the pure HTPBD or HYPBD, indicates that phase segregation is essentially complete in these materials. The slight elevation in Tg above that obtained for the pure homopolymer which occurs in these polyurethanes can be accounted for by only 7% of hard segment mixing with the soft segment phase, as calculated from the copolymer equation and/or the tying in of the end groups of the PBD soft segments.

Above the soft segment Tg in the hydrogenated polyurethanes there is the endothermal region which also appears in the free HYPBD, but here the upper limit of the endotherm is 10° compared to 25°C with the free HYPBD and the melting peak at 39°C is absent. The absence of this melting peak in the polyurethane samples suggests that either the additional constraints on mobility or the very slight amount of phase mixing interferes with crystallization.

Higher temperature transitions associated with the hard segment phase are observed for all three series of poyurethanes. As indicated in Table 2-2, the transition behavior shows a strong and systematic dependence on the increasing urethane content. In general, a diffuse Tg is observed between 20 and 55°C and a second Tg, dominated by a marked excess enthalpy peak appears between 65 and 100°C. The presence

Table 2-2

Summary of DSC Transition Tempertures (DEG C) in HTPBD Polyurethanes and Hydrogenated Derivatives

Sample	Tg	T_1	T_2
R-50	-75	35	65
R-51	-74	40	70
R-52	-75	--	80
R-53	-75	--	84
HY-50	-68	40	74
HY-51	-72	37	71
HY-52	-69	38	74
HY-53	-66	59	78
S-1	-73	20	--
S-2	-72	53	85
S-3	-71	51	87
S-4	-72	56	90
S-5	-73	--	100
PBD	-81		
HYPBD	-70 T_m (Diffuse) - 50 to +25°, T_m (Peak) 39°		

of two distinct transitions indicates that there may be segregation of the shorter and longer hard segment units. These characteristics have been reported earlier in other PBD-containing polyurethanes (16) and are examined more extensively in Chapter III. While the thermal behavior is generally similar among the three series, it is noted that the temperature of the hard segment transitions are as much as 20°C higher in samples cured with HEA, than in the corresponding samples cured with BDL, as is the case for the hard segment analogs.

Dynamic Mechanical Measurements. Figures 2-(4-6) represent the temperature dependence of the tensile storage and loss moduli (E' and E") for the various PBD and HYPBD containing polyurethanes. All series display a single major relaxation, labeled α, and are characterized by a decrease in modulus from about 1000 to 10 MPa over a narrow temperature range. The α relaxation occurs at -74°C for both series of unsaturated polymers and at -69°C for the hydrogenated ones, all determined at 11 Hz from the poition of the E" loss maximum. These values are in good agreement with DSC results reported earlier (see Table 2-3). Further examination of Figure 2-8 shows that as hard segment content increases, the storage modulus at temperatures above the α relaxation temperature also increases. This is characteristic of incompatible systems whereby the hard segment domains behave as filler particles and act as reinforcement. The trend, however, is much less obvious in the case of the hydrogenated polymer than in the unsaturated polymers. The softening temperature (taken as the temperature at which the limit of rheovibron measurement was reached) also showed a

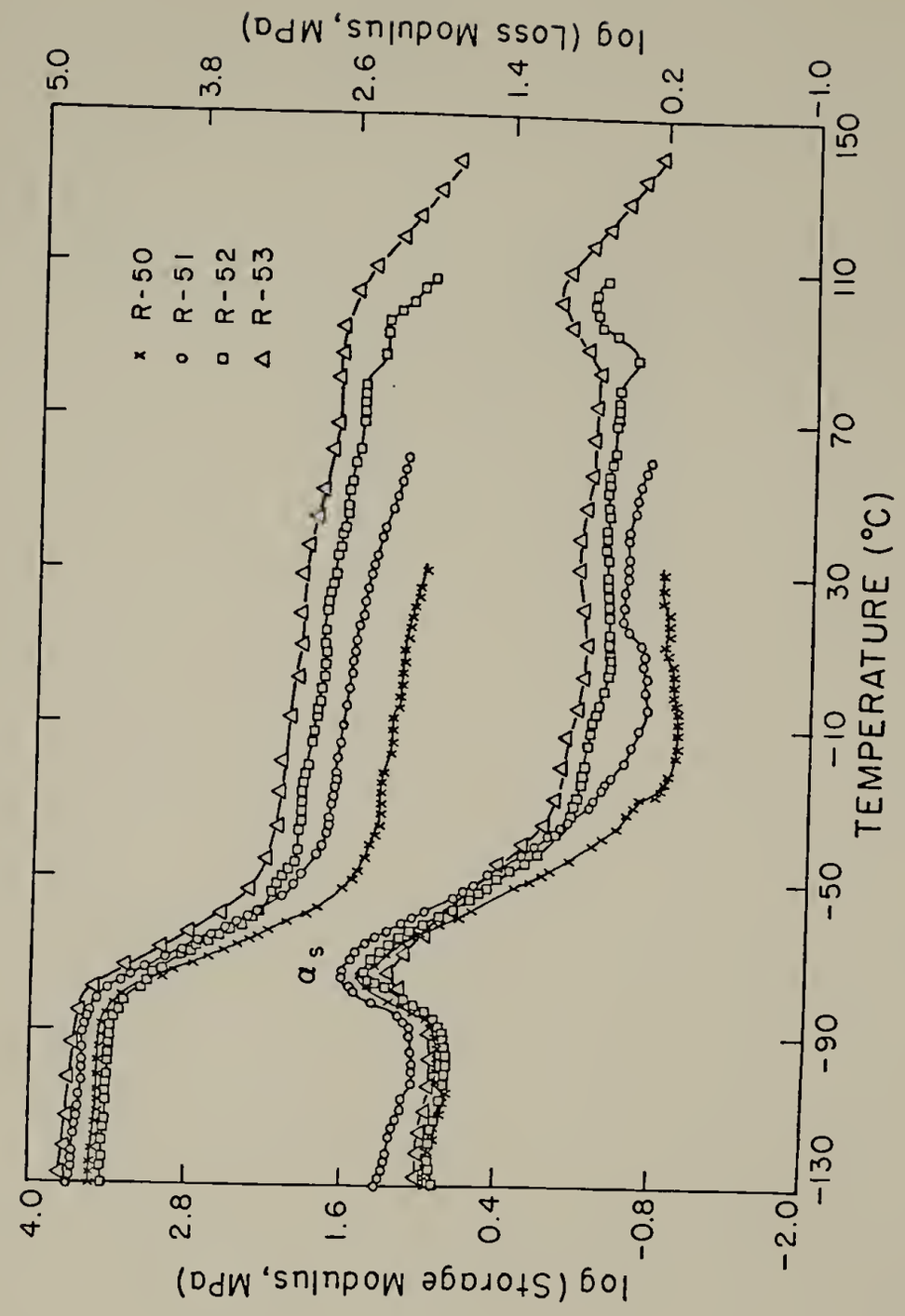

Fig. 2-4. Temperature dependence of the storage and loss modulus for TDI-BDL-PBD polyurethanes.

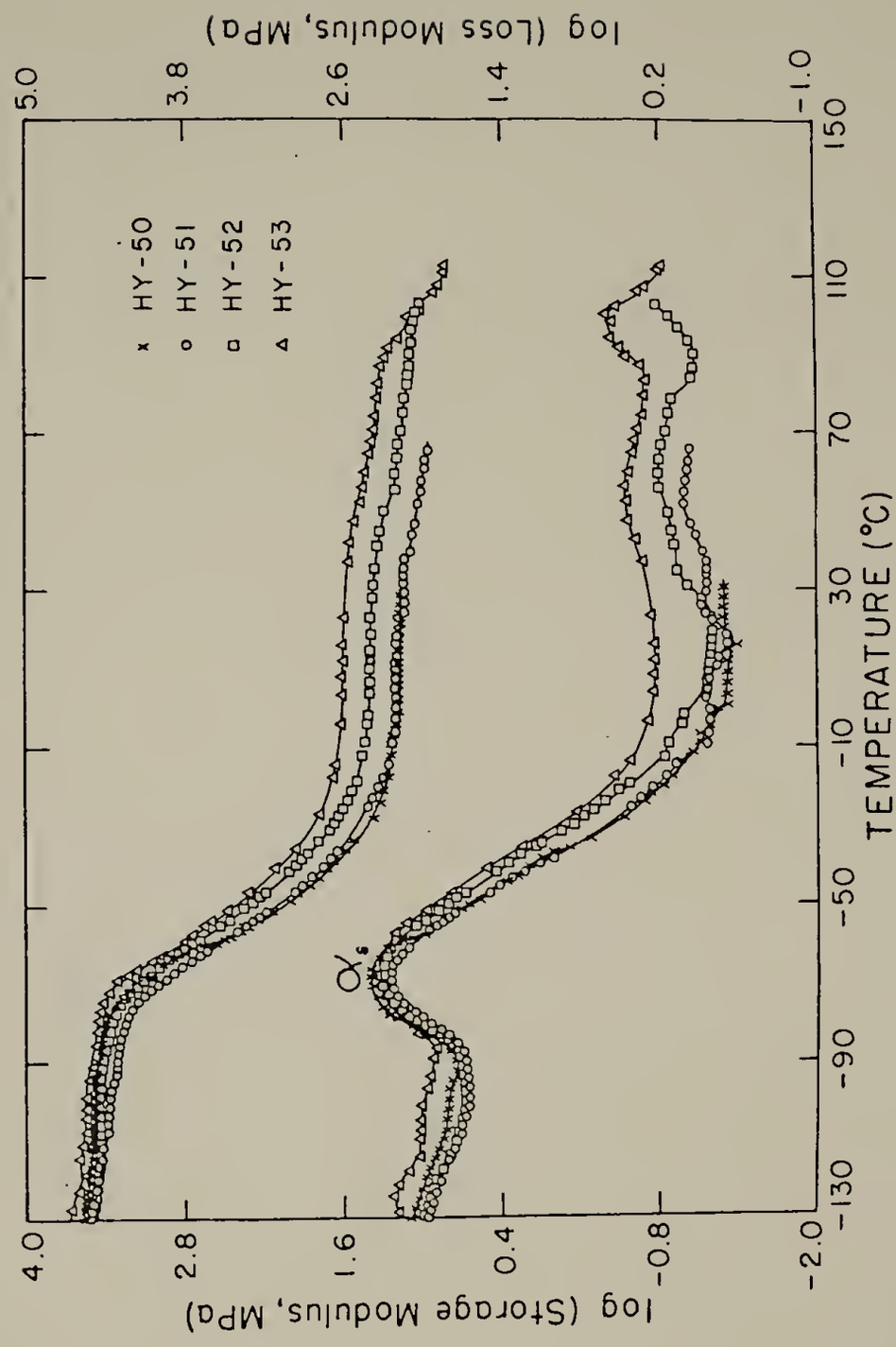

Fig. 2-5. Temperature dependence of the storage and loss modulus for TDI-BDL-HYPBD polyurethanes.

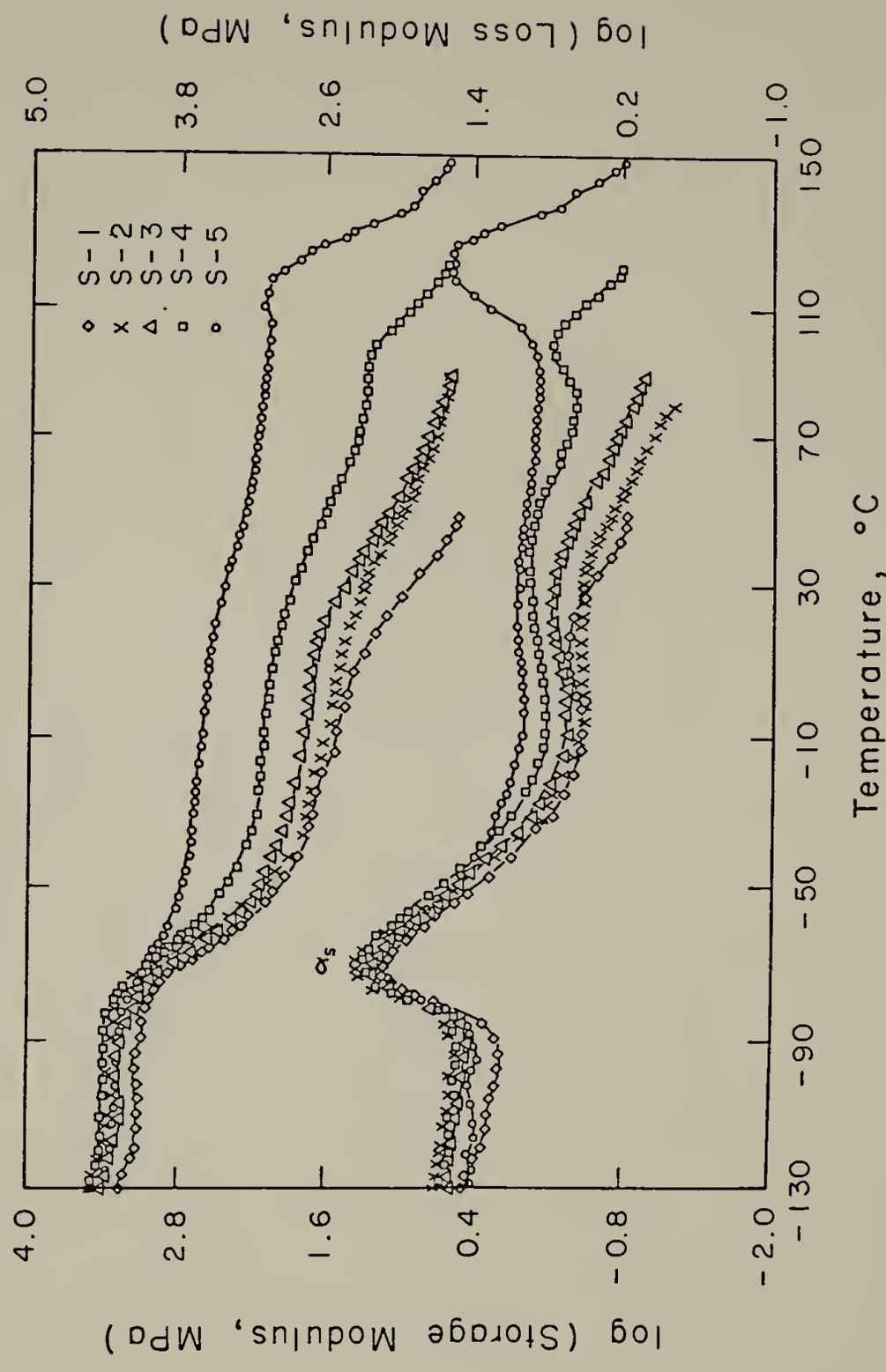

Fig. 2-6. Temperature dependence of the storage and loss modulus for TDI-HEA-PBD polyurethanes.

Table 2-3

Summary of Dynamic Mechanical Relaxation Regions

in HTPBD-Polyurethanes and Hydrogenated Derivatives

Sample	Relaxation Temperatures[a] (°C) From E''_{max}		Softening Temperature
R-50	-74 (-65)[b]		30
R-51	-74 (-63)		61
R-52	-74 (-65)		107
R-53	-72 (-64)		119
HY-50	-69 (-54)		30
HY-51	-70 (-53)		66
HY-52	-69 (-53)		103
HY-53	-69 (-54)		114
S-1	-73 (-62)		50
S-2	-73 (-63)	20	80
S-3	-73 (-62)	20	92
S-4	-72 (-62)	40, 94	125
S-5	-72 (-63)	114	150

[a]All determined at 1 1 11 Hz.

[b]Values in ( ) from tan δ_{max}.

corresponding increase with hard segment content for all series. It is noted that in samples cured with HEA, the storage modulus (as well as the softening temperature) is some 70% higher than the corresponding samples cured with BDL, due to an increased filler effect imparted by the aromatic chain extender.

A more direct comparison between the hydrogenated and nonhydrogenated polymers can be made by inspection of the temperature dependence of the loss tangent shown in Figures 2-7 for the various samples. It is at once apparent that all the hydrogenated polymers show a decrease in intensity and a broadening of the tan δ peak compared to the unsaturated polymers. Moreover, the temperature of this relaxation is shifted to higher temperatures by approximately 10°C in the hydrogenated series. This effect may be attributed to the presence of soft segment crystallinity in the hydrogenated polyurethanes. The soft segment crystallinity acts to increase the temperature of the α relaxation and to change its shape. Such effects are also observed in other semicrystalline polymers such as polyethylene, polypropylene and poly(ethylene terephthalate) (17,18). Soft segment crystallization and melting in these hydrogenated polymers were also observed in our thermal studies.

No conclusive evidence of a hard segment glass transition, which was found to occur between 30 and 100°C by DSC determination, is observable in the various dynamic mechanical relaxation measurements of both hydrogenated and unsaturated polymers of series I and II. In series III, however, hard segment relaxations are apparent in all samples

Fig. 2-7. Temperature dependence of the loss tangent for (a) TDI-BDL-PBD and (b) TDI-BDL-HYPBD polyurethanes.

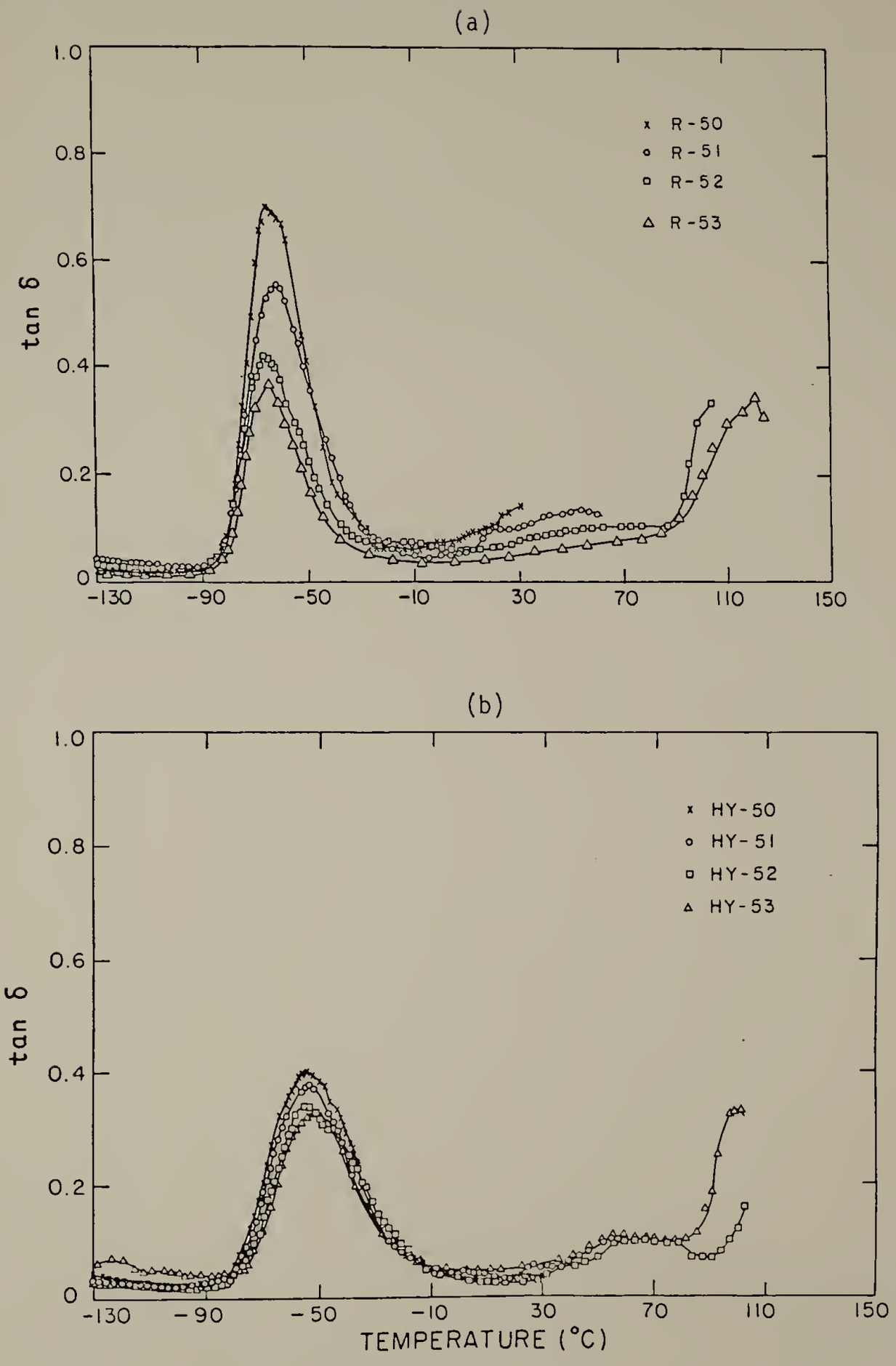
(a)
1.0
0.8
0.6
0.4
0.2
0
tan δ
R-50
R-51
R-52
R-53
-130
-90
-50
-10
30
70
110
150
(b)
1.0
0.8
0.6
0.4
0.2
0
tan δ
HY-50
HY-51
HY-52
HY-53
-130
-90
-50
-10
30
70
110
150
TEMPERATURE (°C)

above a 30 wt. percent urethane. This effect can be attributed to an increase in hard segment density and, possibly, improved organization of the hard segment structure in these HEA-cured materials.

Stress-Strain Measurements. The results of tensile tests performed at room temperature on films of hydrogenated and unsaturated polyurethanes are shown in Figure 2-8 and summarized in Table 2-4. In all series, as the percentage of hard segment increases, several systematic changes occur in the tensile properties. First, the initial modulus (slope of stress-strain curve) increases, indicating the greater rigidity imposed by the hard segment. The stress level during extension also increases with hard segment content, again showing the effects of the less mobile hard segment domains which have difficulty sliding past one another. As expected, the ultimate elongation values for the three series of polymers decreases with increasing weight fraction of hard segment. While the tensile strengths (σ_b) and elongations (ε_b) are comparable for series I and III polyurethanes, the initial moduli are significantly higher for samples cured with HEA, presumably a consequence of the more rigid hard segments.

With the exception of sample 51, the initial modulus and stress level at break (σ_b) was higher in the hydrogenated samples than in the unsaturated ones. The ultimate elongations were also significantly higher. The two concurrent effects give rise to an increase in the toughness of the material, as determined by the areas under the curves. This improvement in properties is presumably due to crystallization and and/or higher degree of orientation in the hydrogenated soft segments

Fig. 2-8. Stress-strain response of HTPBD-TDI-BDL polyurethanes (——) and their hydrogenated derivatives (----).

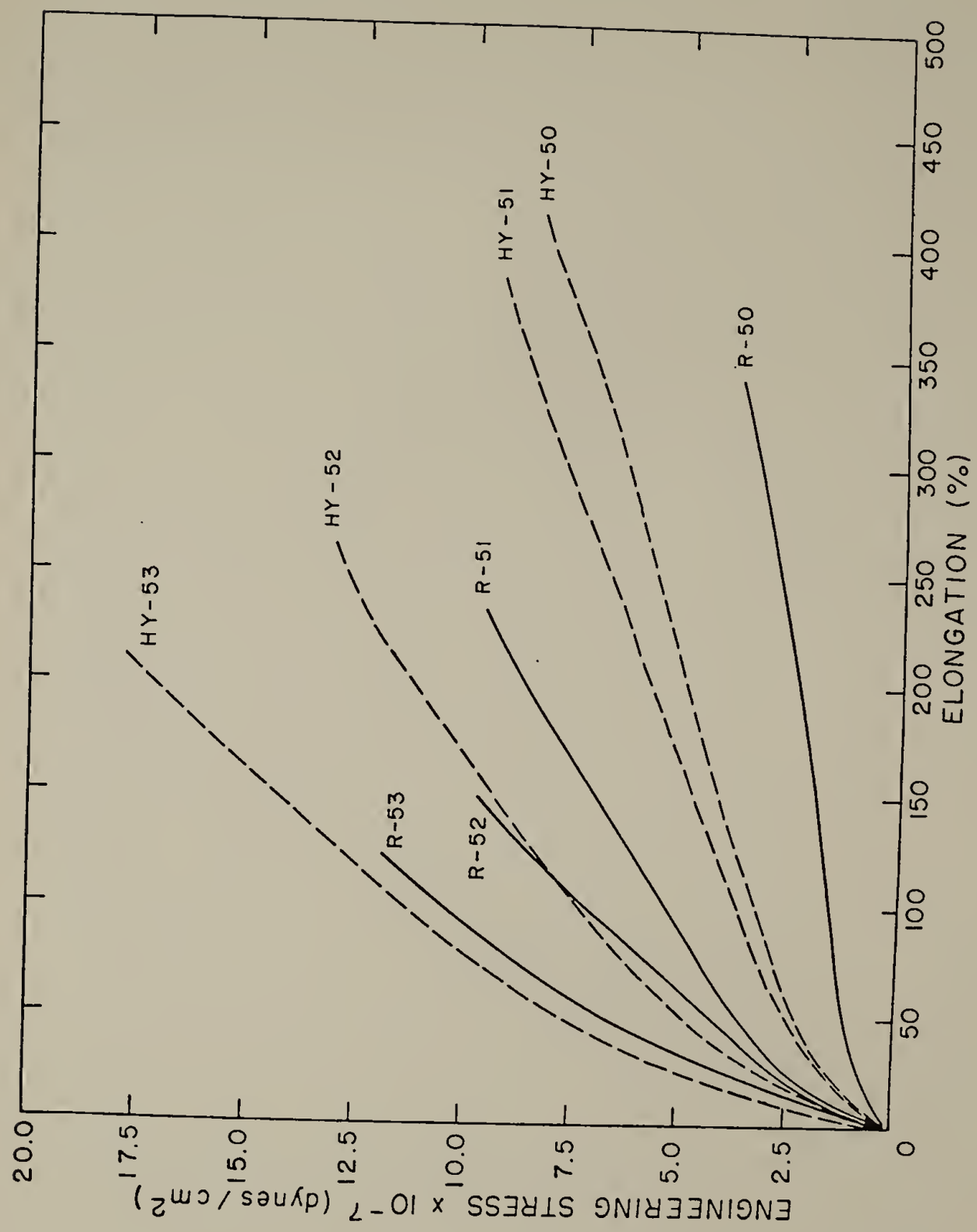
ENGINEERING STRESS x 10⁻⁷ (dynes/cm²)
20.0
17.5
15.0
12.5
10.0
7.5
5.0
2.5
0
50
100
150
200
250
300
350
400
450
500
ELONGATION (%)
HY-53
HY-52
HY-51
HY-50
R-53
R-52
R-51
R-50

Table 2-4

Stress-Strain Properties of HTPBD-Polyurethanes and Hydrogenated Derivatives

Sample	Engineering Stress (σ_b) psi	Elongation (ε_b) percent
R-50	570	340
R-51	1390	230
R-52	1410	150
R-53	1520	130
HY-51	1220	410
HY-52	1350	380
HY-53	1920	260
HY-54	2900	250
S-1	260	850
S-2	1020	420
S-3	1000	540
S-4	800	210
S-5	610	20

[a]All determined at 90% ε_b.

which develop on extension. Similar improvements in elastomeric properties of hydrogenated polybutadiene polyurethanes were also noted by Camberlin and coworkers (19).

Cyclic Instron tests were also performed on these samples (see Figure 2-9. Readily apparent are two characteristics of stress softening. First, upon subsequent straining, lower stress levels are observed at all extensions lower than the maximum previously applied, and second, at strain levels higher than those previously reached, the stress levels are apparently unaffected by prestraining. Both the hydrogenated and unsaturated materials behave similarly in this respect, the only noticeable difference is that HY-51 and S-3 show more permanent set than R-51. This stress-softening behavior is characteristic of phase separated materials and several interpretations of the phenomena are cited, including disruption of the polymer structure and of the reinforcing mechanism, chain slippage and chain breakage (20).

Conclusions

The results obtained for the soft segment Tg by DSC and rheovibron measurements (E" or tan δ) are in good agreement. The low value of Tg for both the PBD and HYPBD-containing polyurethane, very close to the respective values for the free PBD or HYPBD, and the invariance of Tg with increasing urethane content attest to the fact that these samples are well phase segregated.

As observed in the IR spectra, the partial hydrogenation (65% by NMR) of the prepolymer involves preferential saturation of 1,2 vinyl

Fig. 2-9. Cyclic stress-strain curves for (a) R-51 (HTPBD-containing polyurethane) and (b) HY-51 (hydrogenated derivative).

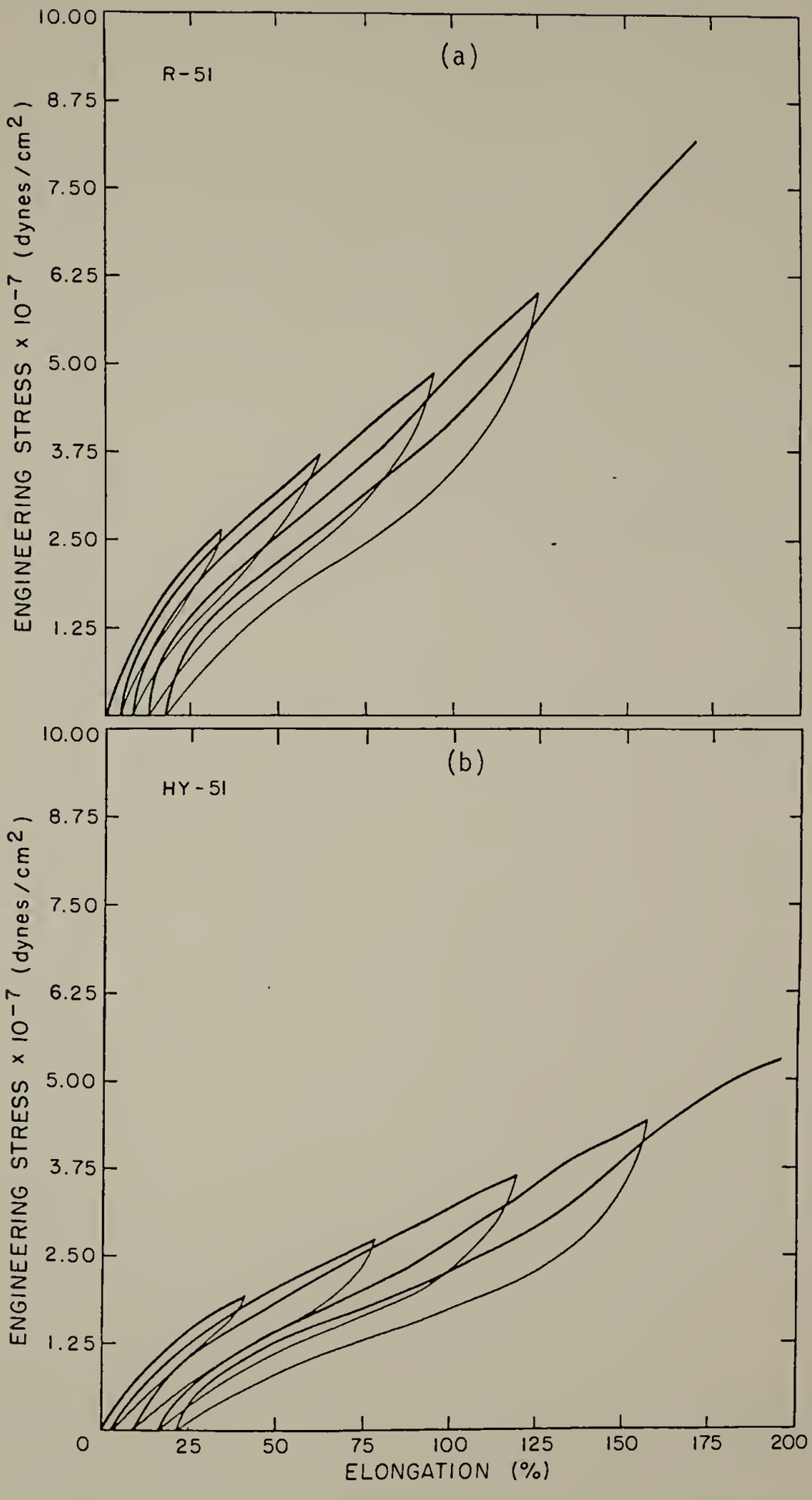
(a)
R-51
(b)
HY-51
ENGINEERING STRESS x 10⁻⁷ (dynes/cm²)
10.00
8.75
7.50
6.25
5.00
3.75
2.50
1.25
0
25
50
75
100
125
150
175
200
ELONGATION (%)

and cis double bonds. It is surprising under the circumstances that any crystallinity develops. Nonetheless, the DSC measuremnts indicate a broad melting peak at 39°C. Since the chain structure is chemically heterogeneous, the crsytalline material must involve only small regions of the chain leading to very small crystallite sizes. Only a very weak infrared absorption can be detected at 729 cm^{-1}, which is a characteristic absorption for crystalline polyethylene. In the HYPBD polyurethane samples the broad low temperature melting process is observed but not the melting peak, suggesting that either the additional constraints on mobility or the very slight amount of phase mixing interferes with crystallization.

In the dynamic mechanical results only the low temperature Tg is clearly evident in samples cured with BDL while in the HEA cured materials, the hard segment relaxations are also evident. This may be due to a higher hard segment density, and possibly an improved urethane domain structure in the latter materials. The main effect of increasing hard segment content is to increase the storage modulus above the glass transition and also the upper limit at which the vibron measurements can be made. The broadening of the tan δ peak for the HYPBD containing polyurethanes probably reflects the interplay of the Tg and the broad melting process observed by DSC.

More important evidence of the effect of soft segment hydrogenation is seen in the comparison of mechanical properties. Generally, it appears that hydrogenation of the soft segment results in a significant increase in the ultimate elongation and the breaking strength and, therefore, in the toughness of these polyurethanes measured as the area

under the stress-strain curve. In view of the low tensile and tear strength of the PBD polyurethanes, this is a welcome improvement in properties. The gain is presumably due to crystallinity within the soft segment which develops upon hydrogenation of the precursor prepolymer; the presence of crystallites in the soft segment of the hydrogenated urethane polymers results in the enhancement of the stress values at a given strain due to these regions acting as tie-points. The comparable levels of hysteresis observed in the cyclic stepwise extension curves for PBD and HYPBD polyurethanes, however, indicate that the small level of crystallinity does not interfere with the elastic recovery of the HYPBD-containing polyurethanes.

References

1. C. Arnold, Jr., J. Elastomers Plastics, 6, 238 (1974).
2. R.D. Elmore, Use of EN-y to Encapsulate Analyzer Assemblies, PDO 6989189, Sept. 1974.
3. G.B. Wood, Evaluation of Conformal Coatings of Microelectronic Circuitry in Fuse Applications, MDL-TR-1777, March 1977.
4. R.R. Legasse, J. Appl. Polym. Sci., 21, 2489 (1977).
5. K. Ono, H. Shimada, T. Nishimuro, S. Yamashita, H. Okamoto and Y. Minoura, J. Appl. Polym. Sci., 21, 3222 (1977).
6. ARCO Chemical co. Product Bulletin BD-1 (March 1974), BD-2 (March 1974) and BD-3 (October 1974).
7. J. Strassburger and I.T. Smith, Appl. Spectros., 33, 283 (1979).
8. M.B. Rossman, M.S. Thesis, University of Massachusetts (1981).
9. S.L. Shu, W.H. Moore and S. Krimm, J. Appl. Phys., 46, 4185 (1975).
10. J.L. Binder, J. Polym. Sci., A3, 1587 (1965).
11. L.A. Mango and R.W. Lenz, Makromol. Chem., 163, 13 (1973).
12. R.G. Snyder and J.H. Schachtschneider, Spectrochim. Acta, 19, 85 (1963).
13. R.G. Snyder, J. Chem. Phys., 47, 1316 (1967).
14. R.G. Snyder, J. Mol. Spectrosc., 7, 116 (1961).
15. R.S. Stein and G.B.B.M. Sutherland, J. Chem. Phys., 22, 1993 (1954).
16. N.S. Schneider and R.W. Matton, Polym. Eng. Sci., 19, 1122 (1979).
17. K.H. Illers, Kolloid Z.Z. Polym., 250, 426 (1972).
18. T.R. Earnest, Jr. and W.J. MacKnight, Macromol., 10, 206 (1977).

19. Y. Camberlin, J. Cole, and J.P. Pascault, submitted to Angewand. Makromol. Chem.

20. G.M. Estes, S.L. Cooper and A.V. Tobolsky, J. Macromol. Sci., Rev. Macromol. Chem., C4, 313 (1970).

CHAPTER III

THERMAL, MECHANICAL AND TIME-DEPENDENT PROPERTIES OF LINEAR SEGMENTED POLYURETHANES WITH BUTADIENE SOFT SEGMENTS

Introduction

Considerable attention has been devoted toward an understanding of the property-structure relationships in segmented polyurethanes in recent years. In general, these materials derive their unusual properties from the thermodynamic incompatibility of the component polymer segments and consequent phase separation. Through techniques such as differential thermal analysis, dynamic mechanical measurements, and x-ray studies, models of phase segregation and domain structure have been developed which are reasonably successful in accounting qualitatively for the many features of segmented polyurethanes (1-3). However, in most polyurethanes previously investigated, difficulties arise because the phenomena of interest are obscured by one or more of the following competing effects: 1.) specific interactions between the hard and soft segment phase, via hydrogen-bonding, 2.) crystallinity occurring in either or both the soft and hard segment phases, and 3.) chemical crosslinking. It is therefore of interest to examine the structure-property relations in a series of segmented polyurethanes in which these added complexities are excluded.

This study continues the examination of polyurethanes based on a polybutadiene soft segment (4,5) to eliminate polar and hydrogen bonding

interactions between hard and soft segment units. As in the prior study (Chapter II), the hard segment is based on 2,4 toluene diisocyanate and butanediol which is completely amorphous under all conditions. The distinguishing feature of the present work is the use of an anionically polymerized hydroxy terminated polybutadiene. This macroglycol has an average hydroxyl functionality of 1.97 which avoids crosslinking through the soft segment phase, a problem with the previously studied materials based on the free radical polybutadiene (ARCO R-45M). In addition, the microstructure of the present macroglycol precludes the occurence of any soft segment crystallinity. Thus, the structure of the hard domains, the nature of phase segregation and other morphological features can be studied in a simplified manner. The characterization techniques performed on these polymers include dynamic mechanical relaxation, stress-strain measurements and differential scanning calorimetry. Also, the thermal history dependence of these polybutadiene polyurethanes is studied and the results are compared to analogous polyurethanes containing polyether and polyester soft segments.

Experimental

Materials. The hydroxyl-terminated polybutadiene (HTPBD) used in this study was kindly provided by the Japan Synthetic Rubber Co. Infrared analysis yielded a vinyl content of 55%, a trans content of 35% and a cis content of 10%. The details of this analysis have been described

previously (5). Gel permeation chromatography in tetrahydrofuran using a polystyrene calibration gave a number average molecular weight M_n=2200 and weight average molecular weight M_w=3290.

The synthesis was carried out in bulk by a two step method involving end capping the HTPBD with a 5% molar excess of 2,4-toluenediisocyanate (TDI) followed by reaction with the chain extender, 1,4 butanediol (BDL), the same procedure employed in the previous study (Chapter II). The composition and some characteristic properties of the resulting polyurethane samples are summarized in Table 3-1. This series of six samples ranges from a 2 to 1 to 10 to 1 equivalent ratio of TDI to HTPBD at a fixed NCO/OH ratio of approximately 1.05.

Measurements. Dynamic mechanical measurements were carried out on a Vibron Dynamic Viscoelastometer, Model DDV-II (Toyo Measuring Instruments Co.). The temperature range was from -160 to 150°C and the frequencies employed were 3.5, 11, and 110 Hz. Samples were heated at a nominal rate of 1.5 deg/min under a dry nitrogen atmosphere.

Thermal analysis of the soft segment glass transition temperature was made with the Perkin Elmer DSC-2, purged with He and chilled with liquid nitrogen. The DSC was calibrated for low temperatures using the crystal-crystal transformation of cyclohexane at 186°K. Runs were conducted on polymer samples of about 15 mg at a heating rate of 20°c/min and an attenuation of 5mcal/sec. Heat capacity mesurements at the soft segment glass transition were calibrated using a sapphire standard. The higher temperature scans were conducted from 250 to 450°K using the

Table 3-1

Composition and Properties of HTPBD-Polyurethanes

Sample	Molar Composition TDI/BDL/PBD	Hard Segment Weight %	Properties
JSR-2	2.1/1.2/1.0	18	clear, soft, tacky rubber
JSR-3	3.0/1.9/1.0	25	translucent, rubbery, tough
JSR-4	4.1/3.1/1.0	32	
JSR-6	6.2/5.0/1.0	42	translucent, slightly elastic tough
JSR-8	8.4/7.2/1.0	49	opaque, hard, slightly flexible
JSR-10	10.0/8.8/1.0	55	opaque, hard

DSC-2 equipped with a two stage mechanical refrigerator unit. Glass transition temperatures were determined as the temperature corresponding to one half the increase in heat capacity at the transition.

Stress-strain data were obtained on an Instron Universal testing machine at an extension rate of 2 cm/min. Rectangular-shaped specimens of the approximate average dimensions 50 x 3 x .40 mm were used. In cyclic stress-strain experiments, a single sample was submitted to increasing amounts of prestrain. The sample was extended by increments up to 20%, allowed to relax at zero load for 5 minutes, extended to 40%, etc. All data reported are averages of at least 5 tests on different samples.

Results

Dynamic Mechanical Measurements. As shown in Figure 3-1, the relaxation behavior clearly illustrates the two phase nature of these HTPBD-containing polyurethanes of varying hard segment concentrations. All polymers of this family exhibit a constant low temperature relaxation at about -56°C, determined at 11 Hz from the temperature of the E" loss maximum. This α_s relaxation is due to the onset of micro-brownian segmental motion associated with the glass transition of the soft butadiene phase. Neither the temperature nor the activation energy, E_a, of the α_s relaxation varies with urethane content over the concentration range examined (see Table 3-2). This indicates that

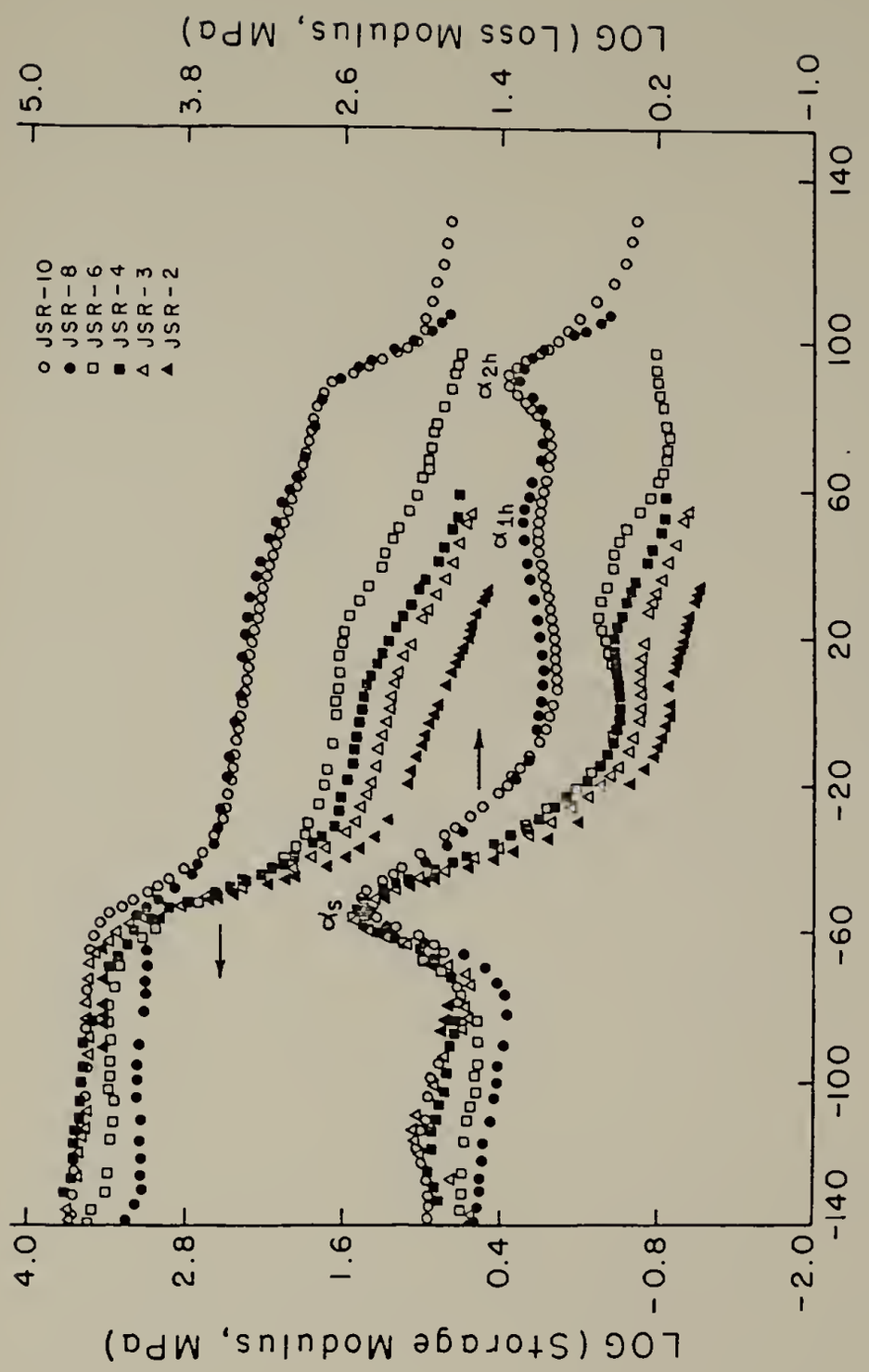

Fig. 3-1. Temperature dependence of the storage and loss modulus for HTPBD-polyurethanes.

Table 3-2

Summary of Dynamic Mechanical Relaxation

Regions in HTPBD-Polyurethanes

Sample	Relaxation	Temperature[a] (°C)	Activation[b] Energy (kJ/mole)	Softening Temperature (°C)
JSR-2	α_s	-57 (-45)	120±20	35
JSR-3	α_s	-56 (-46)	140±20	51
	α_{1h}	20	---	
JSR-4	α_s	-56 (-46)	110±20	62
	α_{1h}	20	---	
JSR-6	α_s	-56 (-47)	110±20	99
	α_{1h}	35	240±10	
	α_{2h}	76 (84)	280±20	
JSR-8	α_s	-56 (-48)	120±30	114
	α_{1h}	56	---	
	α_{2h}	91 (102)	280±20	
JSR-10	α_s	-55 (-47)	120±10	138
	α_{1h}	60	---	
	α_{2h}	93 (105)	340±10	

[a]All determined at 11 Hz from E_{max}; ( ) from $\tan\delta_{max}$.

[b]Determined from an Arrhenius dependent of frequency (3.5, 11, and 110 Hz) on temperature, to the 95% confidence level.

the development of a hard segment phase which gives rise to an additional relaxation (later to be discussed) has no effect on the mechanism of the α_s relaxation. The α_s relaxation is also characterized by a decrease in storage modulus of at least two orders of magnitude.

Above ambient temperatures, the loss processes vary systematically with urethane content. Samples of the lowest urethane concentration display a single weak transition at about 20°C, designated α_{1h}. At 42 wt. % hard segment, a second relaxation, designated α_{2h}, occurs at 75°C. As the hard segment content is further increased, the α_{2h} relaxation becomes much more prominent while the positions of both α_{1h} and α_{2h} relaxation are shifted some 15° to higher temperatures. The temperatures and activation energies for these transitions are summarized in Table 3-2. It is reasonable to believe that such transitions result from motions occurring within the hard segments. This could be supported by noting also difference in E_a for α_s and α_h.

Consistent with findings for other phase segregated systems, the level of the storage modulus above α_s and the softening temperature increases with hard segment content. These effects, as well as the increase in the α_h relaxation temperature, can be directly attributed to an increase in the hard segment length and a more well developed glassy urethane domain structure which occurs with increasing hard segment content.

A final point to note lies in the temperature dependence of the mechanical loss (tanδ) illustrated in Figure 3-2. As the hard segment content increases, the magnitude of the α_s relaxation decreases while

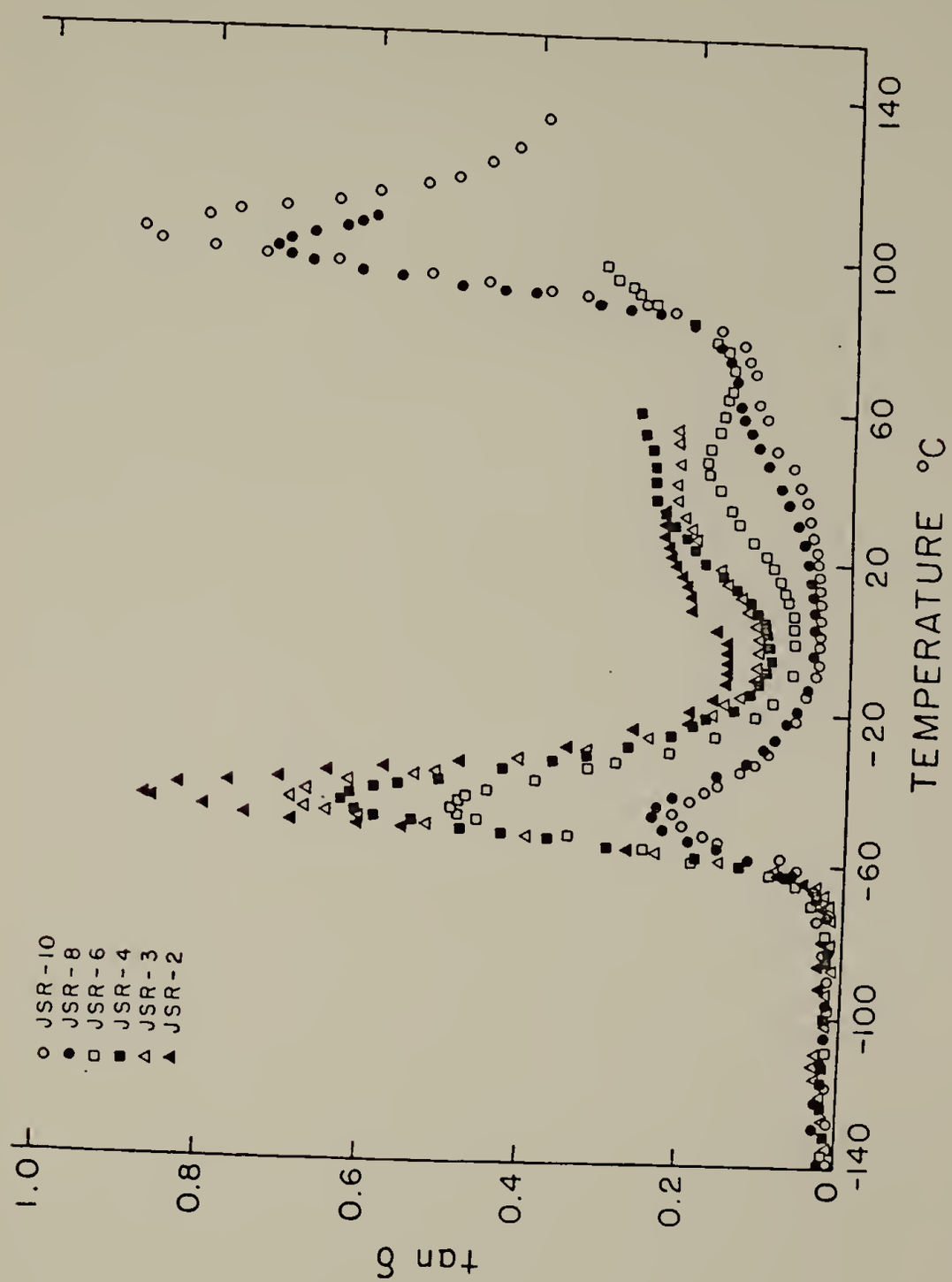

Fig. 3-2. Temperature dependence of the loss tangent for HTPBD-polyurethanes.

that of the α_{2h} relaxation increases. In fact, the magnitude of the α_{2h} relaxation at the highest urethane content (JSR-10) is nearly equal to that of the α_s relaxation of the lowest urethane content (JSR-2). Such changes in the damping behavior of these materials clearly reflect changes in the relative amounts of the constituent phases present and a gross change in the character of the polymer. Further evidence for this behavior is presented in stress-strain data, to be discussed later.

Unlike the behavior of other polyurethanes (6,7), the dynamic mechanical properties of HTPBD-based polyurethanes were unaffected by thermal history. Samples were quenched to room temperature from 150°C and immediately retested and were also stored for one month prior to retesting. Figure 3-3 shows that the values of the various viscoelastic functions were essentially unchanged. The invariance of the activation energy, shape and temperature of the α_s relaxation suggest there is little, if any, change in the composition of the soft segment phase on heating.

Thermal Analysis. A summary of the DSC transition temperatures for the six HTPBD-containing polyurethanes and the HTPBD prepolymer is presented in Table 3-3. These results are in good agreement with the dynamic mechanical studies. The soft segment glass transition is well defined and reproducible and appears at -56±2°C in all samples. Like the height of the α_s mechanical loss peak, the magnitude of the step change in the specific heat, (ΔCp), accompanying the soft segment glass transition decreases with increasing wt. % of urethane. These ΔCp values are listed in Table 3-3 and plotted versus weight fraction of hard segment in Figure 3-4. Note that the intercept of the line lies

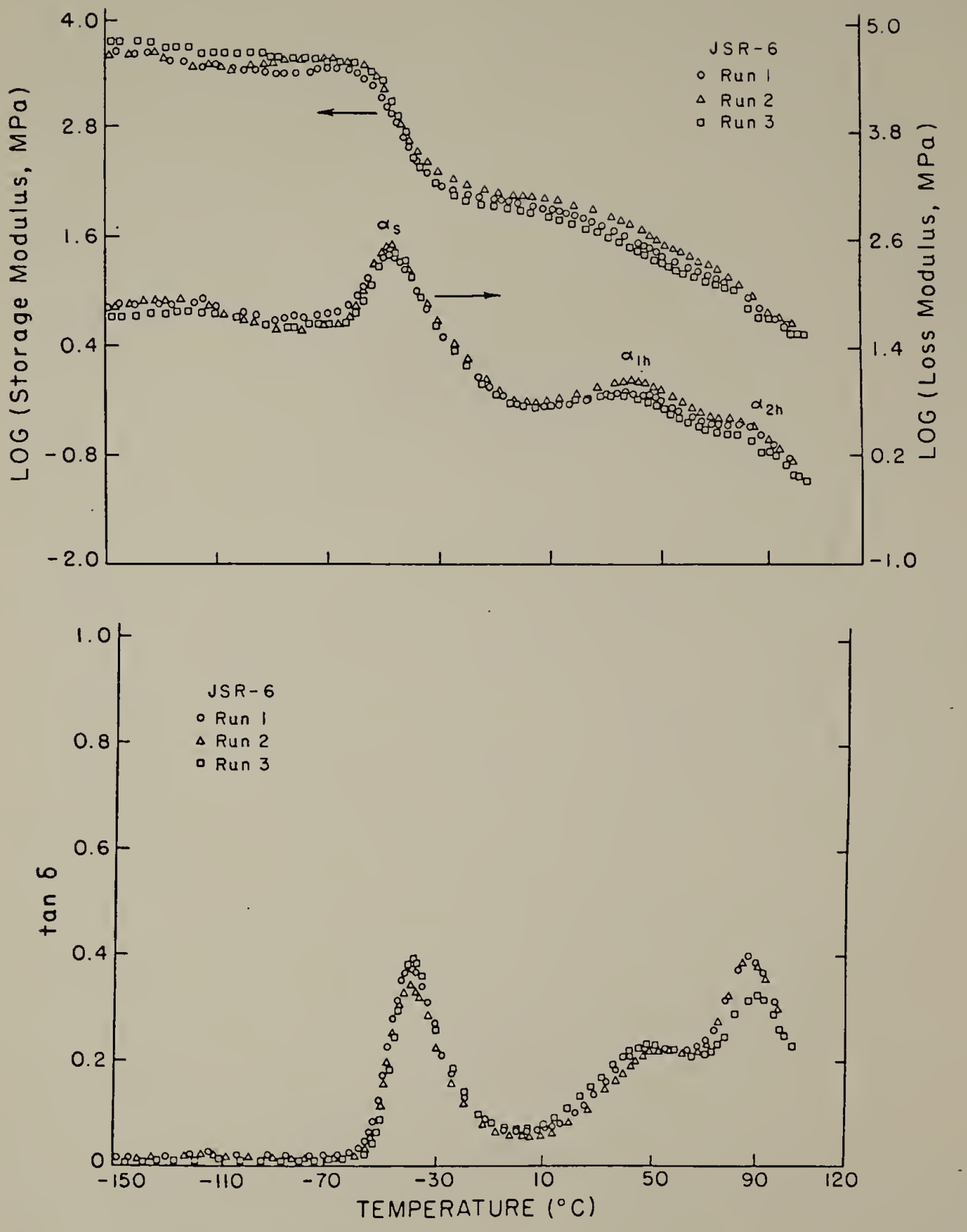

Fig. 3-3. Dynamic mechanical response of JSR-6: (a) initial run, (b) quenched from 150°C and retested immediately, (c) quenched from 150°C and retested after one month.

very close to the ΔCp value of the HTPBD prepolymer.

Since DSC gives quantitative results and since interactions between hard and soft segments are assumed sufficiently small that they may be ignored, the following equation based on a simple two-phase model can be used to calculate soft segment content:

$$f_{SS} = \frac{\Delta Cp_{Tg}}{\Delta C^{\circ}_{p}Tg} = 1 - f_{HS} \qquad (3\text{-}1)$$

where f_{SS} = soft segment fraction present per unit mass

ΔCp_{Tg} = observed heat capacity change at Tg_S for the polymer

$\Delta C^{\circ}_{p}Tg$ = the experimentally determined or extrapolated heat capacity change at Tg_S for 100% soft segment phase

and f_{HS} = hard segment weight fraction

Using Equation 3-1, the ΔCp values of the six polymers normalized to the ΔCp of pure HTPBD are also plotted in Figure 3-4 and are shown to lie very close to the ideal two-phase line.

This type of treatment has also been applied to semicrystalline polymers (8,9). However, unlike these HTPBD-polyurethanes, deviations from the ideal two-phase behavior are generally observed indicating that interactions between the phases are important. In polyester and polyether urethanes where crystallinity is often present as is hydrogen bonding interactions between the two phases deviations are also expected due to additional constraints imposed on the soft segment phase (7,10).

The higher temperature transition behavior follows a general pattern, the details of which depend upon urethane content (see Table 3-3 and Figure 3-5). The DSC scans for samples of the lowest

Table 3-3

Effect of Thermal History on Transitions in HTPBD-Polyurethanes by DSC

Sample	Tg_s (°C)	ΔCp (cal g^{-1} $°K^{-1}$)	Upper Transitions, T_1 and T_2 (°C)[a] 1st Run		After 24 hrs.		After 24 days	
JSR-2	-58 (-57)	.125	20(d)		20w		20(d)	
JSR-3	-56 (-56)	.118	20(d)		20w		20(d)	
JSR-4	-58 (-58)	.097	20(20)	55(58w)	22	54	20(22)	54(57)
JSR-6	-55 (-54)	.084	40(a)	65(80)	42	74	39(a)	64(83)
JSR-8	-55 (-54)	.076		74(84)	83			74(82)
JSR-10	-56 (-54)	.070		75(84)	83			74(84)
JHTPBD	-65 (-65)	.155						

[a]Values in bracket, transition observed in second scan; d - indicates the transition was diffuse; w - that it was weak; a - that it was absent.

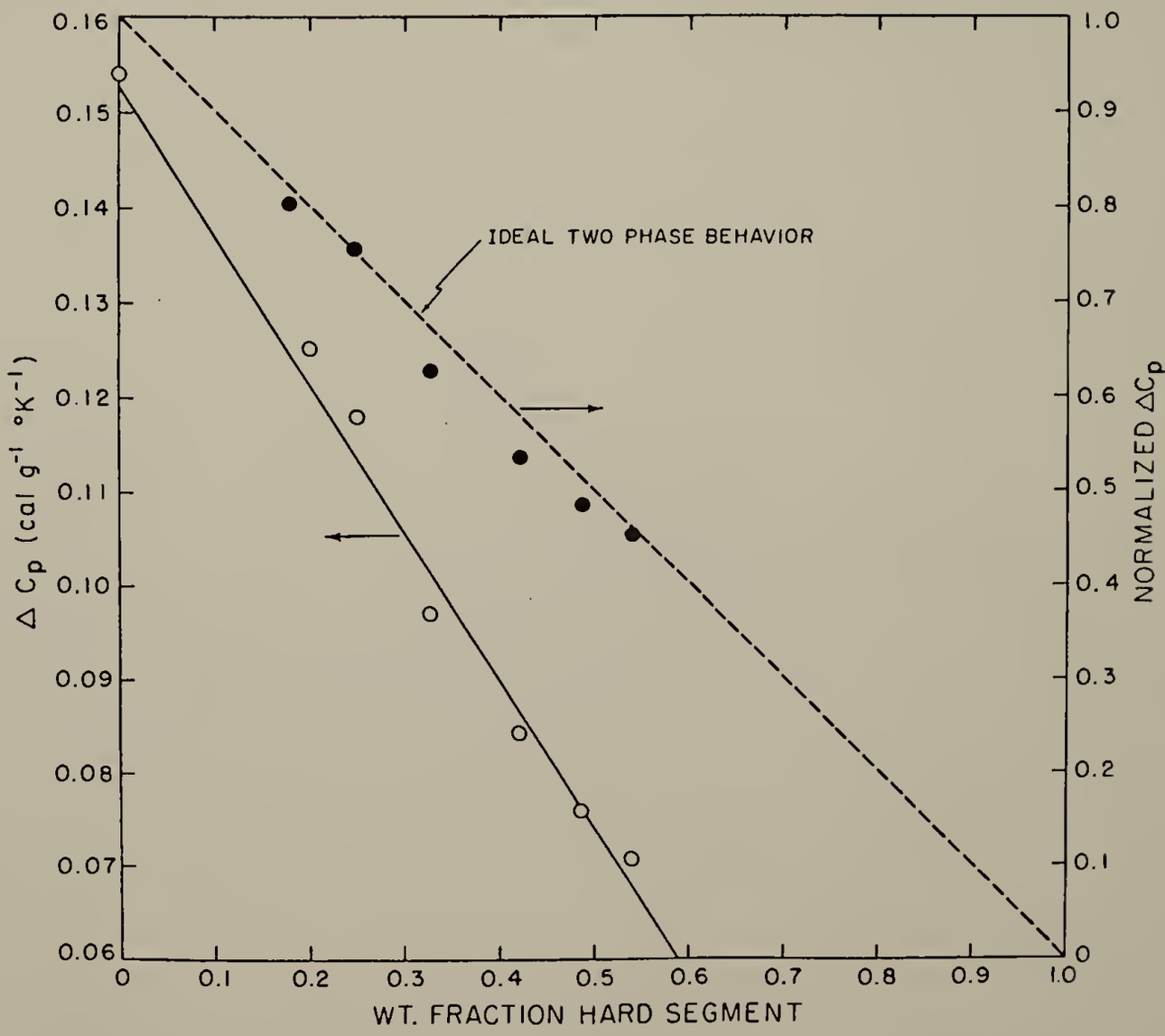

Fig. 3-4. Observed heat capacity change at Tg_S for JSR samples of varying hard segment content, (open circles); normalized heat capacity change compared to ideal two-phase behavior, (closed circles).

urethane content (JSR-2 and JSR-3) show only a single, diffuse transition in the vicinity of 20°C. This transition is reproducible in subsequent scans. For JSR-4, the initial trace shows two transition regions; a weak transition at 20°C (T_1) and a strong endothermic peak at 55°C (T_2). In the second scan, both transitions reappear but the excess enthalpy peak at T_2 disappears and the transition occurs about 5° higher. As mentioned earlier, both of these transitions can be attributed to the hard phase. In the following sample there is a further increase in the strength of T_2 accompanied by a marked weakening of T_1 in the second scan. These two transitions appear at 40 and 65°C. Only one transition is evident in samples of the highest urethane concentration (JSR-8 and JSR-10) which appears at 75°C on first scan and 84°C on repeated scanning. The glass transiton temperature of the pure TDI/BDL homopolymer (bottom trace) occurs at about 110°C.

The behavior observed for the hard segment transitions by DSC (and hard segment relaxations by rheovibron measurements) is related, in part, to the very high degree of phase segregation which occurs in these materials as compared to polyester or polyether urethanes. Since only the T_1 transition at 20°C occurs in samples with the lowest hard segment content (which corresponds to the shortest hard segment length), this suggests that T_1 is associated with the T_g of the short hard segment units. The systematic reduction in the strength and permanence of the T_1 transition with increasing hard segment content further supports the conjecture that T_1 is due to phase segregated structures made up of shorter hard

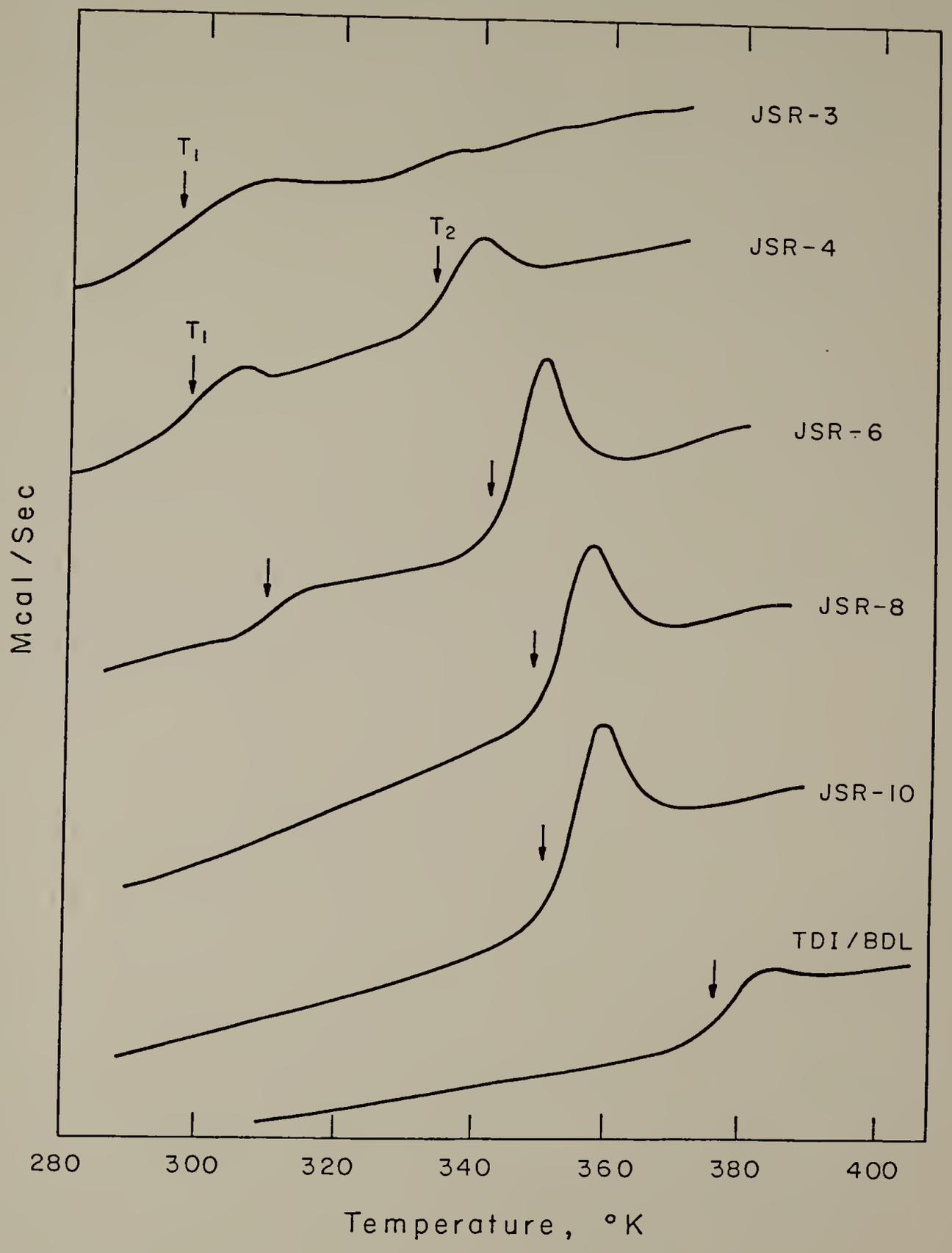

Fig. 3-5. DSC scans for HTPBD-polyurethanes.

segment units and, therefore, T_2 to phase segregated structures containing the longer hard segment units. Why two different populations of hard segments should occur in an amorphous system remains unclear. Actually, the broadness of T_1 transition region suggests that the transition is due to the combined contribution of regions having a range of transition temperatures. This is presumably related to the polydispersity of the hard segment length, inherent in these materials. Similar transition behavior has also been observed in other HTPBD-containing polyurethanes under conditions where the lower transition was clearly identifiable with shorter hard segments containing up to three TDI repeat units (4). In contrast to these PBD-containing polyurethanes, it seems likely that in the polyester and polyether urethanes these shorter hard segments which are not incorporated in the domain would be mixed with and hydrogen bonded to soft segment units, and contribute to the increase in soft segment Tg, which is often observed.

The effect of thermal history on Tg_s, T_1 and T_2 was also studied. Thermal cycling of the materials to 150°C produces no change either in the position or shape of Tg_s. The absence of thermal history effects on Tgs is consistent with the dynamic mechanical results reported earlier. The effects of thermal history on T_1 and T_2 are illustrated in Figure 3-6. Scans were made after different storage times at 25°C as noted on the figure. As mentioned earlier, two transitions are observed in samples of intermediate composition. For JSR-4, the T_1 transition region is only slightly affected by thermal treatment, recovering readily after the initial scan. The time scale for recovery of the

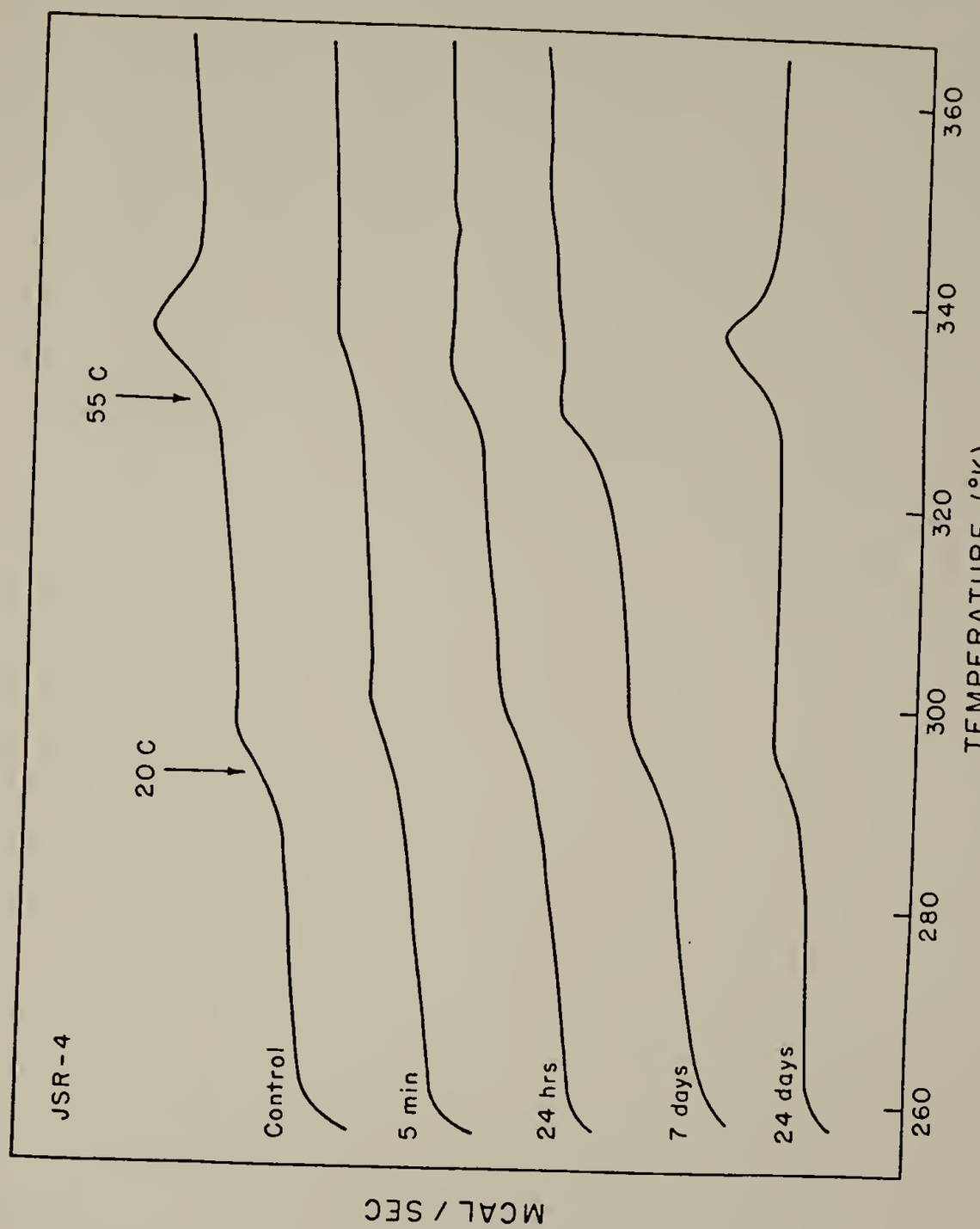

Fig. 3-6. DSC scans of JSR-4 taken at different times following quenching.

endothermic peak at T_2, however, is far longer. Following heat treatment, this endothermic peak is replaced by a weak step change in specific heat, characteristic of the glass transition, that increases in strength over a period of approximately 24 days before assuming its original appearance. This time-dependent behavior is believed to be caused by a simple densification process within the amorphous hard segment domains (11) and not to reordering phenomena commonly observed in MDI-based segmented polyurethanes. A comparable time scale was required for the recovery of the T_2 transition in the higher urethane samples. It is noted that this endothermic peak recovers much sooner (2-4 h) on annealing at temperatures about 10° below the transition following quenching.

Stress-Strain Measurements. The effect of hard segment content on the stress-strain behavior of these polyurethanes was also investigated. The results are summarized in Table 3-4.

From Figure 3-7 it is clear that the mechanical properties of these materials change only slightly when the hard segment content increases from 18 to 32 wt. % but change profoundly between 32 (JSR-4) and 42 wt. % hard segment (JSR-6). In fact, below 32 wt. % the polymers are clearly elastomeric with extensions of >1000% and recover almost completely when the stress is removed. Above 42 wt. % hard segment, they exhibit elongations to break, ε_b, of less than 80% and show permanent set. Such a marked change in the characteristics of the polymer is probably due to inversion of hard and soft phases. Very likely, the films have a different morphology consisting of soft segment domains in a hard

Table 3-4

Stress-Strain Properties of HTPBD Polyurethanes

Sample	Tensile Strength (σ_b) psi True σ_b	Engineering σ_b	Elongation (ϵ_b) %	%Recovery[a]
JSR-2	4,440	410	1000	95
JSR-3	10,060	600	1620	90
JSR-4	6,010	480	1160	89
JSR-6	3,310	620	430	85
JSR-8	650	390	70	75
JSR-10	440	390	15	-

[a]All determined at 90% ϵ_b.

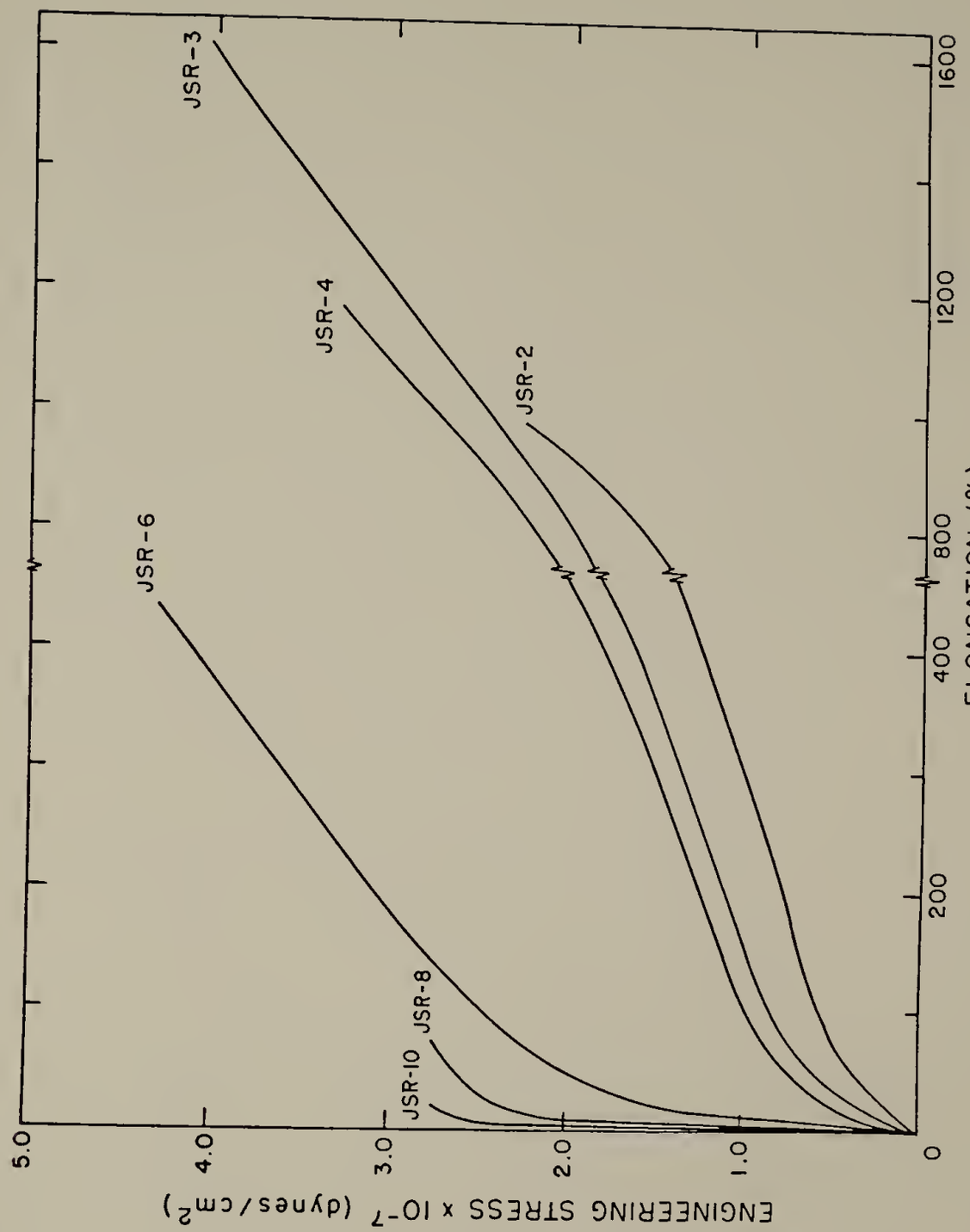

Fig. 3-7. Stress-strain response of HTPBD-polyurethanes.

segment rich matrix.

In agreement with our dynamic mechanical and DSC studies, the stress-strain behavior of these PBD-based polyurethanes is unaffected by thermal treatment. Here the samples were annealed at 150°C for as long as two hours followed by air quenching. In contrast, the mechanical properties of a series of polyester and polyether polyurethanes were shown to be highly time dependent (i.e. materials harden with time and increase in toughness) when tested under similar conditions (10).

Cyclic Instron tests were also performed on these materials. If the sample is not strained to break, but relaxed to zero stress, stress softening or hysteresis is observed (see Figure 3-8). With the exception of JSR-10 which was too brittle to test, all samples show a decrease in stress on repeated straining. Moreover, the higher the hard segment content, the higher the percent hysteresis, presumably due to greater plastic deformation occurring within the hard phase.

Discussion

Based on the chemically dissimilar nature of the hard and soft segment components in PBD-containing polyurethanes, the existence of compositionally pure phases in these materials is not surprising. The purity of the PBD soft segment in this study as well as in the previous one (Chapter II) is verified by the low and composition insensitive soft segment glass transition temperature (see Figure 3-9). The differences in these temperatures and those of the corresponding free PBD

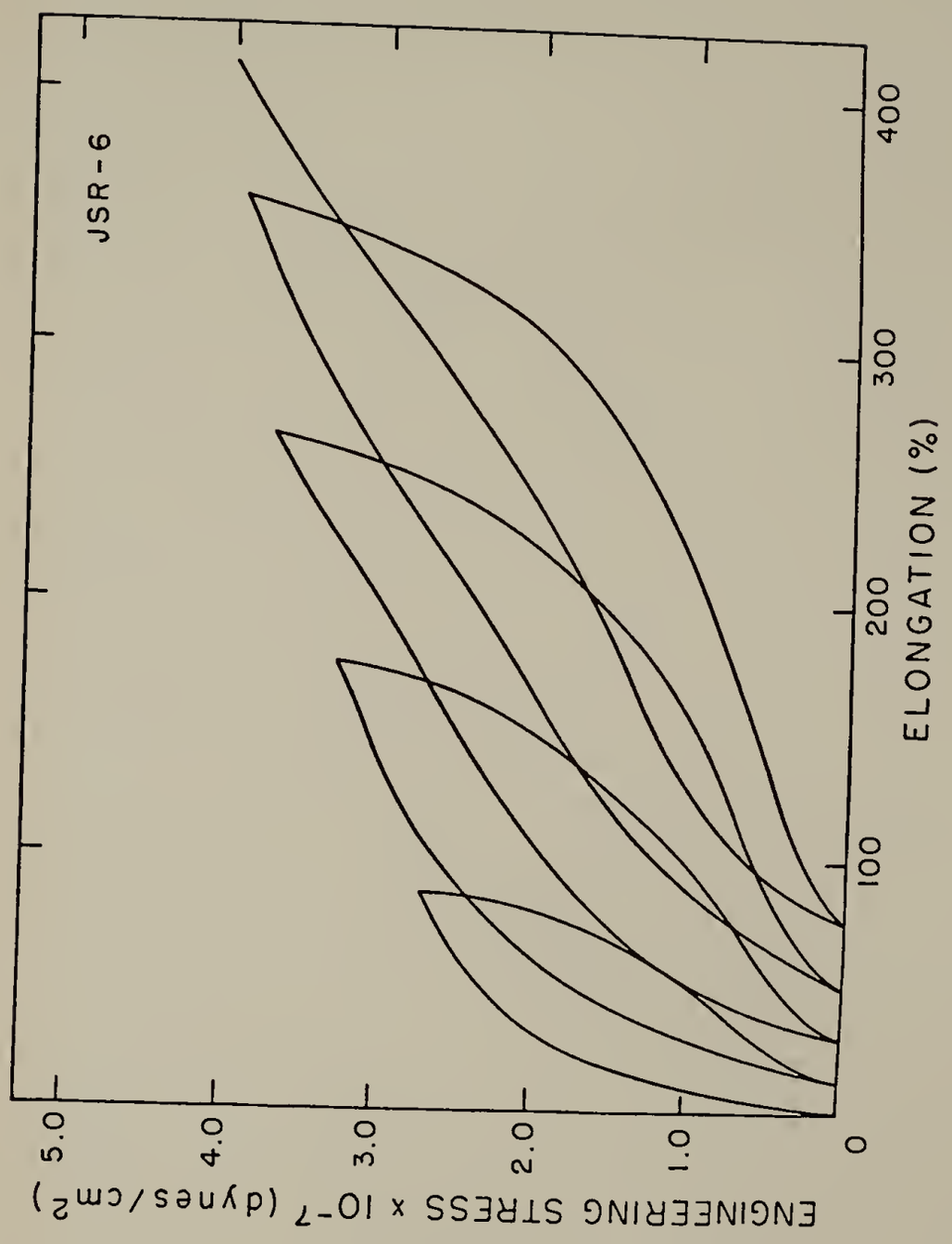

Fig. 3-8. Cyclic stress-strain curve for JSR-6 extended 20, 40, 60 and 80% ε_b.

homopolymer are, in fact, the smallest ever reported in segmented polyurethanes.

The glass transition temperature of the hard segment, however, shows a strong dependence on composition in all 2,4-TDI polyurethanes studied here. As shown in Figure 3-9, the Tg of the hard segment domain increases from about 20° to 100°C with increasing urethane content and asymptotically approached the Tg of the corresponding hard segment homopolymer. This result has been interpreted as meaning that the amorphous hard segment domain structure improves with increasing urethane content, based on small angle x-ray scattering studies which provided independent evidence of domain structure above a 35-40 weight percent hard segment (12). In polyester and polyether urethanes, this trend of improving domain structure with increasing urethane content is accompanied by a decrease in the amount of solubilized soft segment in the hard domain, thus leading to an improvement in phase segregation. The lower values of Tg_H in the lower hard segment materials has thus been accounted for, in part, by increased mixing of soft segment in the hard segment phase. This would also result in the elevation of the soft segment Tg, commonly observed for these materials. In contrast, the hard segment phase in these PBD-polyurethanes is relatively pure even for the short hard segment length (based on the mole ratio composition of the urethane components) as indicated by the very low value of the soft segment Tg. Moreover, previous IR analysis indicates that 80-85 percent of the NH groups are hydrogen bonded for all compositions (5). Since hydrogen bonding interactions are limited to the hard

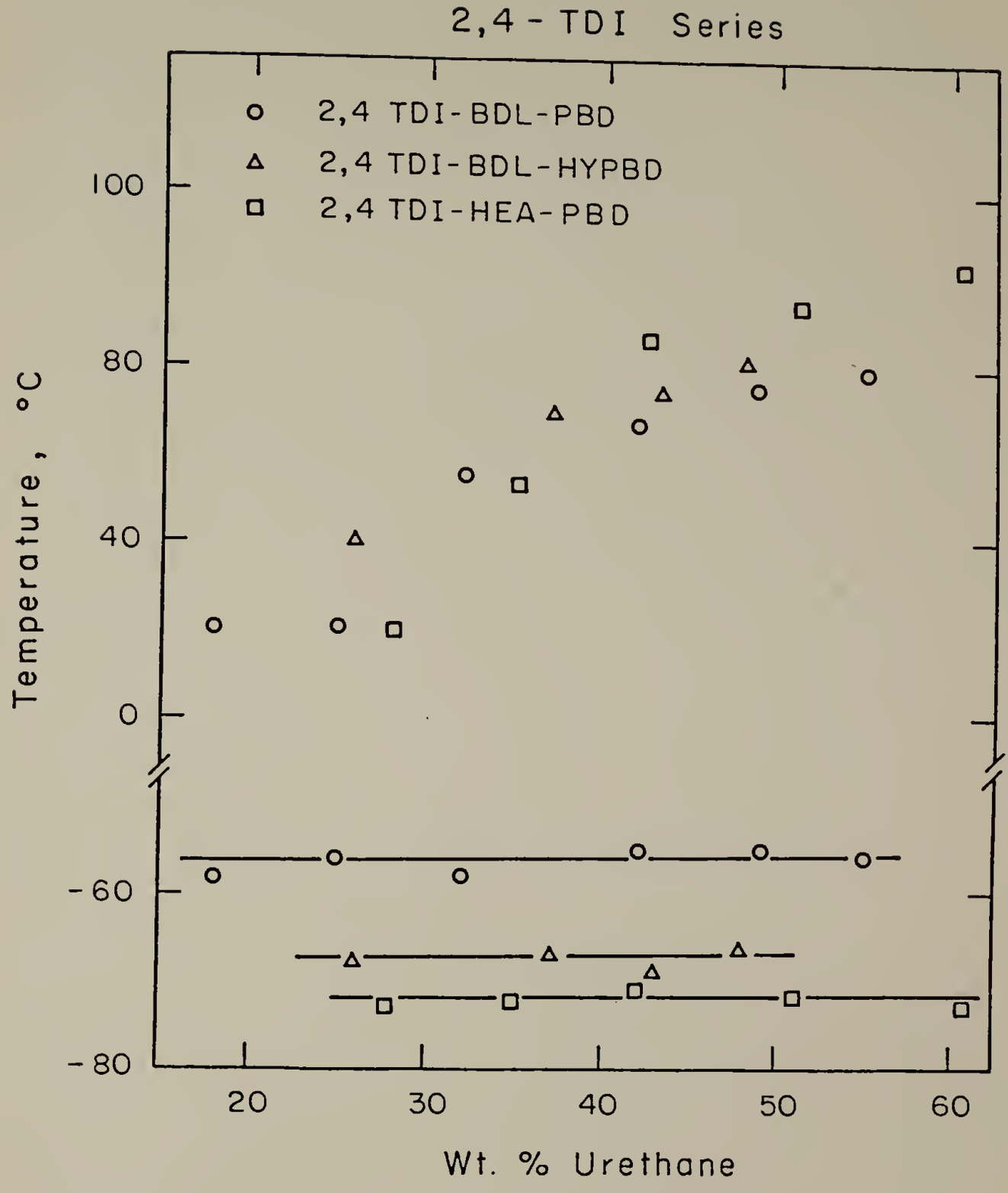

Fig. 3-9. Comparison of glass transition temperatures of HTPBD-polyurethanes as a function of hard segment content.

segment components, the high extent of interurethane hydrogen bonding serves as additional evidence that the hard segment phase in these polyurethanes is relatively free of intermixed soft segments. Consequently, the observed shift of the hard segment glass transition temperature relative to the Tg of the TDI/BDL homopolymer can be more accurately ascribed to the shorter block length and thus lower molecular weight of the urethane as the hard segment content decreases in these polymers.

It is also noted that, unlike the more typical polyester or polyether polyurethanes, modifications within the soft segment phase (i.e. hydrogenation, chain microstructure, molecular weight) and/or hard segment phase (i.e. structure of the diisocyanate, chain extender, hard segment length) have negligible effect on the degree of phase segregation in PBD-polyurethanes; changes in the overall thermal and mechanical properties are related to changes within the individual hard and soft segment regions. This behavior is undoubtedly attributed to the extreme incompatibility of the apolar soft segment and strongly polar hard segment units. Moreover, there is no hydrogen bonding contribution to increase the compatibility between the two phases.

The morphology of PBD-polyurethanes, as shown by Legasse (11) and inferred from our results resembles that of styrene-butadiene and styrene-isoprene block copolymers. In these systems, the hard and soft segments undergo microphase separation to form individual domains largely composed of one type of segment (i.e. hard segment domains dispersed in a soft segment matrix) (13,14). The morphology of such a

domain structure may be contrasted to that of polyester and polyether polyurethanes. Experimental evidence suggests that for these materials, separation into discrete microphase regions does not occur but rather the hard segments form an interlocking continuous network with regions rich in soft segments (15,16). Consequently, the inherent properties of the individual segments i.e. crystallinity, chemical structure, molecular weight, etc., are likely to be determinants of the extent of phase separation and resultant morphology. This line of reasoning is further exemplified in their time-dependent thermal and mechanical behavior. For polyester and polyether urethanes, changes in soft segment glass transition temperature, degree of phase separation and room temperature modulus are observed following heat treatment. These results have been attributed to the temporary disruption of domain structure and increased mixing of hard and soft segments (6). This mixing process is promoted in part by hydrogen bonding between the urethane segments and ester or ether functional groups of the soft segment (17). While this model explains well time-dependent phenomena in polyester and polyether urethanes, it bears little application to HTPBD-based polyurethanes where the lower transition temperature remains insensitive to thermal cycling. The reversible thermal history dependence in these HTPBD systems is related to physical changes within the hard segment domains and independent of the soft segment matrix. Since no thermally activated mixing occurs between the two phases, two distinct regions prevail rather than a continuum of compositions. Although this behavior has been attributed to either the

presence of chemical crosslinks or absence of hydrogen bonding to the soft segment (11,18), this present study on linear HTPBD-urethanes confirms the latter - that the absence of hydrogen bonding between hard and soft segments must account for the absence of thermal history effects in these polymers as compared to polyester and polyether polyurethanes.

Finally, some comments should be made concerning the relatively poor mechanical properties of PBD-polyurethanes as compared to polyether or polyester polyurethanes. The work of Ono et al. (18) indicates that the molecular weight of HTPBD is too high for optimal properties since they noted a strong improvement in many properties with decreasing molecular weight starting at M_n=3,000. The highest value of the tensile strength achieved, about 3,400 psi, however, still falls below the value of 6,000 psi or more which can be obtained in conventional polyurethanes based on polyether or polyester soft segments of equivalent molecular weight. There are other factors which also might contribute to lower properties. Studies of the distribution of hydroxyl functionality (19) have indicated that the lower molecular weight species in HTPBD might have a functionality very much less than two. These molecules would represent network defects that lower the properties. Another likely explanation is that which is also responsible for the absence of thermal history effects, namely the absence of interdomain hydrogen bonding and consequent separate domain morphology in PBD-polyurethanes. It may be speculated that separate domain morphology comprising alternating regions of hard

and soft segments would exhibit lower ultimate tensile properties than interconnecting or interlocking domain morphology, suggested for polyester and polyether polyurethanes.

Conclusions

The glass transition temperature of the HTPBD soft segment appears at -56°C by both DSC and rheovibron measurements. The value of Tg_s in these polyurethanes as compared to a value of -64°C for the pure HTPBD and its invariance with increasing urethane content indicate that phase segregation is very nearly complete. Since TDI-BD form amorphous hard segment regions, the driving force for phase segregation must come from the extreme incompatibility of the apolar soft segment and the strongly polar hard segment units. In addition, there is no hydrogen bonding contribution to increase the compatibility between the two phases.

The unusual transition behavior above ambient temperatures is related to the nature of the dispersed hard segment phase. Only a T_1 (α_{1h}) transition region is evident in samples of lowest urethane content; both T_1 and T_2 (α_{2h}) appear in samples of intermediate content while only T_2 appears in highest urethane samples. These transitions above Tgs are also the result of the extreme degree of phase segregation, with T_1 arising from the localization of shorter hard segment units, which in polyester or polyether polyurethanes would remain soluble in the soft segment phase and T_2 from domains containing longer hard segment units. This systematic change in transition

behavior with urethane content is also reflected in stress-strain properties whereby the polyurethane changes from a tough elastomeric material to a more brittle, though low modulus, plastic. This is undoubtedly due to inversion of the continuous and dispersed phases which occurs in the system at approximately 40-50 weight percent of hard segment.

Another significant feature of these HTPBD-polyurethanes is their completely reversible nature following thermal treatment. In contrast with previous findings on polyester and polyether urethanes, the time dependence in dynamic mechanical and thermal behavior was not accompanied by any measurable change in the Tg of the soft segment phase. This difference in behavior is largely attributed to the absence of urethane hydrogen bonding to the soft segment in HTPBD-based polyurethanes.

References

1. S.B. Clough, N.S. Schneider and A.O. King, J. Macromol. Sci., B2, 641 (1968).
2. G.M. Estes, S.L. Cooper and A.V. Tobolsky, J. Macromol. Sci., Rev. Macromol. Chem., C4 (1), 167 (1970).
3. R. Bonart, L. Morbitzer and G. Hentze, J. Macromol. Sci., B3 (2), 337 (1969).
4. N.S. Schneider and R.W. Matton, Polym. Eng. Sci., 19, 1122 (1979).
5. C.M. Brunette, S.L. Hsu, W.J. MacKnight and N.S. Schneider, Polym. Eng. Sci., 21, 163 (1981).
6. G.L. Wilkes and R. Wildnaur, J. Appl. Phys., 46 (10), 4148 (1975).
7. G.A. Senich and W.J. MacKnight, Adv. Chem. Ser., No. 176 (1979).
8. J.M. O'Reilly and F.E. Karasz, ACS Polymer Properties, 5 (2), 351 (1964).
9. M. Sh. Yagfarov, Vysokomol. soyed., A11, 1195 (1969).
10. N.S. Schneider and C.S. Paik Sung, Polym. Eng. Sic., 17 (2), 73 (1977).
11. R.R. Lagasse, J. Appl. Polym. Sci., 21, 2489 (1977).
12. C.S. Paik Sung and N.S. Schneider, Macromolecules, 10, 452 (1977).
13. D.J. Meier, J. Polym. Sci., Part C, 26, 81 (1969).
14. E. Helfand and Y. Tagami, J. Chem. Phys., 56, 3592 (1972).
15. R.W. Seymour, A.E. Allegrezza and S.L. Cooper, Macromolecules, 4, 452 (1971).
16. R.W. Seymour and S.L. Cooper, Rubber Chem. Technol., 47, 19 (1974).

17. C.S. Paik Sung and N.S. Schneider, Macromolecules, 8, 68 (1975).

18. R.A. Azzink, J. Polym. Sci.-Phys. 15, 59 (1977).

19. K. Ono, H. Shimadu, T. Nishimuro, S. Yamashita, M. Okamoto and Y. Minour, J. Appl. Polym. Sci., 21, 3223 (1977).

20. S.K. Baczek, J.N. Anderson and H.E. Adams, J. Appl. Polym. Sci., 19, 2269 (1975).

C H A P T E R I V

THERMAL TRANSITION AND RELAXATION BEHAVIOR OF POLYBUTADIENE POLYURETHANES BASED ON 2,6-TOLUENE DIISOCYANATE

Introduction

In the previous chapter, studies of segmented polyurethanes based on polybutadiene (PBD) soft segments and hard segments comprised of 2,4 toluene diisocyanate (2,4-TDI) and butanediol (BDL) have been reported. This present study is concerned with PBD-polyurethanes based on 2,6-toluene diisocyanate (2,6-TDI) and BDL hard segments. In contrast to the completely amorphous systems, the symmetrical structure of the 2,6-TDI isomer results in crystalline hard segment domains (1). Though a high degree of phase segregation is also expected (since crystallization of hard segments serves as an added driving force), the nature of the hard segment domain structure will be strongly dependent on thermal history. This has been shown to be the case in segmented polyurethanes comprising crystalline hard segments as well as other semi-crystalline polymers (2,3). For example, in diphenylmethane diisocyanate (MDI) based polyurethanes (2,4), three characteristic hard segment transitions have been observed: a transition at 80°C which is attributed to the disruption of domains with limited short range order, a transition between 130 and 150° assigned to long range ordering, and a transition above 200° which is due to the melting of microcrystalline domains. Annealing studies have shown that the lower temperature

transition can be shifted continuously upward to merge with the higher temperature transition, the final state of order depending on the annealing history and sample composition.

While polyurethanes based on 2,6-TDI/BDL hard segments have been the subject of a few recent studies (1,5), a detailed analysis of the melting and crystallization behavior of the hard segment domains in these polymers is lacking. The following therefore describes experiments aimed to better understand the morphology and annealing behavior of these materials as well as to examine the effects of compositional variables on transition behavior and other related polyurethane properties. The absence of polar and hydrogen bonding interactions between the hard and soft segment phase removes a complicating factor which has obscured the results of previous studies.

Experimental

Materials. The synthesis was carried out by a two step method involving end capping the hydroxy terminated polybutadiene (HTPBD) with the diisocyanate followed by reaction with the chain extender. The details of this procedure have been described in Chapter II. The 2,6-TDI (Aldrich Chemical, 99%) was vacuum distilled and a middle 60% was isolated for the synthesis. The HTPBD (Japanese Synthetic Rubber Co.) and the BDL (Aldrich) were used as received. The molar ratio of TDI to HTPBD was varied in three equal steps from 4 to 1 to 6 to 1 at a fixed NCO/OH ratio of approximately 1.05. The three samples were designated by the

hard segment content in weight percent ranging from 30 to 50 (i.e. JSR-50). All samples used for the study were compression molded into 25 mil thick films using a pressure of 3 MPa.

Measurements. Differential scanning calorimetry (DSC) was carried out using a Perkin-Elmer DSC-2, purged with helium and chilled with liquid nitrogen for the low temperature runs (170° to 250°). Runs were conducted on polymer samples of about 15 mg at a heating rate of 20°C/min. The higher temperature scans were conducted from 250 to 500°K using dry ice and acetone to control the heating rate. Cyclohexane, indium, and tin were used as thermal standards. Heat capacity measurements at the glass transition were calibrated using a sapphire standard. The glass transition temperatures (T_g's) were taken to be the midpoint of the step in heat capacity. The temperature of maximum excursion from the base-line of the melting endotherm was taken to be the melting point (T_m). Cooling and heating rate studies were performed on the three samples using the temperature programming capability of the DSC. Samples were cooled and heated at rates of 2.5, 5, 10, 20, 40, 80, 160, and 320 deg/min and DSC scans taken immediately.

Wide angle x-ray diffraction (WAXS) patterns were recorded in the symmetrical reflection technique using a Siemens D500 x-ray diffractometer equipped with a scintillation detector. A copper target in conjunction with a monochrometer mounted after the sample was used for all x-ray experiments.

Dynamic mechanical measurements were carried out on a Vibron Dynamic Viscoelastometer, Model DDV-II (Toyo Measuring Instruments Co.).

The temperature range was from -150 to 220°C and the frequencies employed were 3.5, 11, and 110 Hz. Samples were heated at 1-2°C/min under dry nitrogen. Apparent activation energies were determined for major relaxations from the Arrhenius dependence of frequency on inverse temperature. Least squares lines were fitted to plots of log (frequency) vs. T^{-1} and the activation energies to the 95% confidence limit determined from the slopes.

Results

Thermal measurements. The major DSC transitions observed for the 2,6-TDI polyurethanes of varying hard segment content and the two pure segment homopolymers, HTPBD and TDI/BDL, are summarized in Table 4-1. A soft segment glass transition, T_{gs}, occurs at about -54°C in all samples. This value is close to that reported earlier for the corresponding 2,4-TDI systems and only 8° higher than the glass transition temperture of the pure HTPBD. The heat capacity changes, ΔC_p, accompanying this transition decrease with increasing hard segment content. As in the 2,4-TDI polymers, when these values are normalized to ΔCp of the prepolymer (see Equation 1 of Chapter III) the soft segment weight fraction obtained for each polymer (Table 4-1) again indicates ideal two-phase behavior.

Above ambient temperatures, each thermogram shows a hard segment glass transition, T_{gH}, at about 62°C. On further heating, a melting endotherm occcurs between 140-150°C (T_{m1}) followed by a clear exotherm (T_c) between 145-155°C, and then a final melting process of increased

Table 4-1

Summary of DSC Transitions in HTPBD-Polyurethanes

Sample	Lower Transition, °C			Upper Transitions				
	T_{gs}	ΔC_p	$\Delta C_p/\Delta C_p^{\circ}$[a]	T_{gH}	T_{m1}	ΔH_m cal/g	T_{m2}	ΔH_m cal/g
JSR-31	-54	.071	64.3	64	142	.50	192(197)[b]	1.37(2.31)
JSR-42	-54	.065	58.9	60	144	.82	199(203)	3.72(4.63)
JSR-50	-53	.054	48.9	63	148	1.17	208(211)	5.63(6.42)
HTPBD	-63	.110						
TDI/BD							(220)	(13.78)

[a] ΔC_p of polymer normalized to that of prepolymer.

[b] Values in ( ) - samples annealed 8 h at 160°C.

area between 190-210°C (T_{m2}). Increasing the heating rate shows that only the first melting peak is characteristic of the initial crystal distribution. All later structure is caused by recrystallization which is nearly suppressed on heating at 160°/min. The precise nature of this recrystallization will be discussed later.

Unlike T_{gs} and T_{gH}, the positions of the two melting endotherms vary systematically with hard segment content. T_{m1} and T_{m2} occur 10 and 20° higher in JSR-50 as compared to JSR-31. The enthalpies of fusion normalized to the weight fraction hard segment, ΔH_m, are nearly the same for all compositions with the exception that ΔH_m corresponding to T_{m2} is some 50% lower for JSR-31 as compared to JSR-42 and JSR-50. As indicated in Table 4-1, these values are significantly higher for the higher temperature melting peak.

Time-dependence of transitions. Thermal cycling the polyurethanes to 220°C produced no change in either the temperature or shape of the T_{gs} transition. This behavior is similar to that observed earlier in the polyurethanes with 2,4-TDI hard segments and indicates that there is little, if any, change in the composition of the soft segment phase as a result of heating.

Representative DSC curves for the hard segment transitions are shown in Figure 4-1 for JSR-42. Each curve shows the DSC trace as a function of time after quenching at 320°/min to room temperature. Following the initial scan, the excess enthalpy peak occuring at T_{gH} is replaced by the characteristic step change in the specific heat which then increases in temperature and magnitude before recovering its

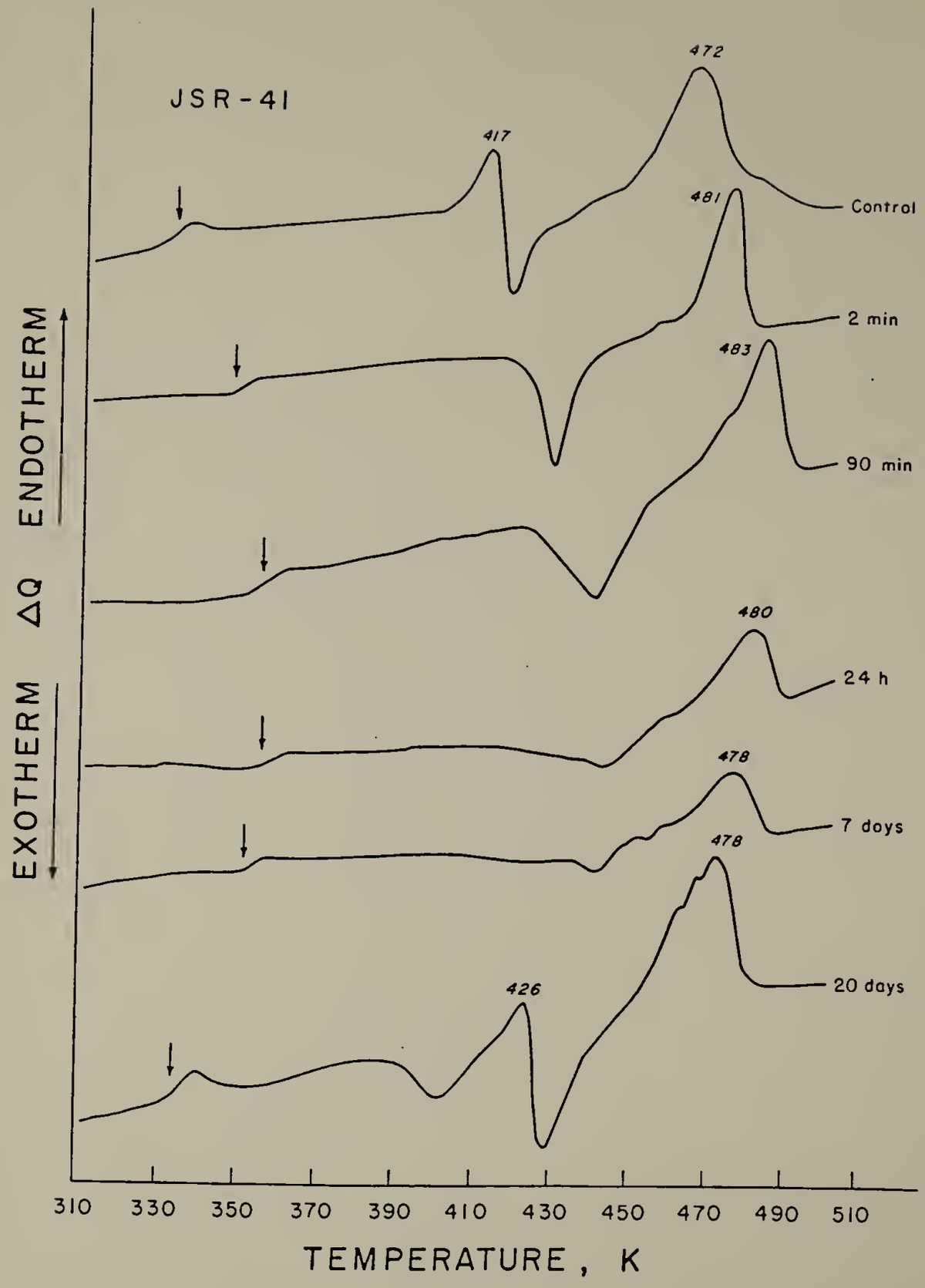

Fig. 4-1. DSC scans for JSR-41 taken at different times following quenching. (Arrow designates the position of the hard segment T_g.)

original appearance within 20 days. As in the 2,4-TDI materials, this time-dependent behavior is most probably due to a densification of the amorphous phase within the hard segment domains (6) and not to reordering phenomena commonly observed in other semicrystalline segmented polyurethanes (2,9). This will become more evident in the annealing studies to be discussed.

As shown in Figure 4-1, the endotherm, T_{m1}, is absent in the short time repeat scans. However, the crystallization exotherm, T_c, and T_{m2} reappear immediately after quenching and are shifted some 10° to higher temperatures. Cooling at slower rates (160 - 2.5°/min) resulted in similar behavior; the position of T_{m2} is essentially unchanged though its area decreases with decreasing cooling rate. Longer storage periods (ca. 24 h) result in a decrease in the areas of both peaks. Within 20 days, however, most of the original thermal behavior is restored, including the T_{m1} endotherm which now appears 10° higher than the control. It should be mentioned that this endotherm reappears much sooner (<4 h) on annealing at temperatures 10-15° lower than the transition. Similar time dependent behavior was observed in JSR-50, though in JSR-31, the T_{m1} peak is still evident immediately after quenching.

Annealing study. In Figures 4-(2-4) the effects of annealing on the melting behavior of these materials at constant DSC scanning rate (20°C/min) is reported. Each series of curves show the DSC trace for samples annealed 4 h (with the exception of the bottom trace, where the samples were annealed 8 h) at the designated temperatures. It is at

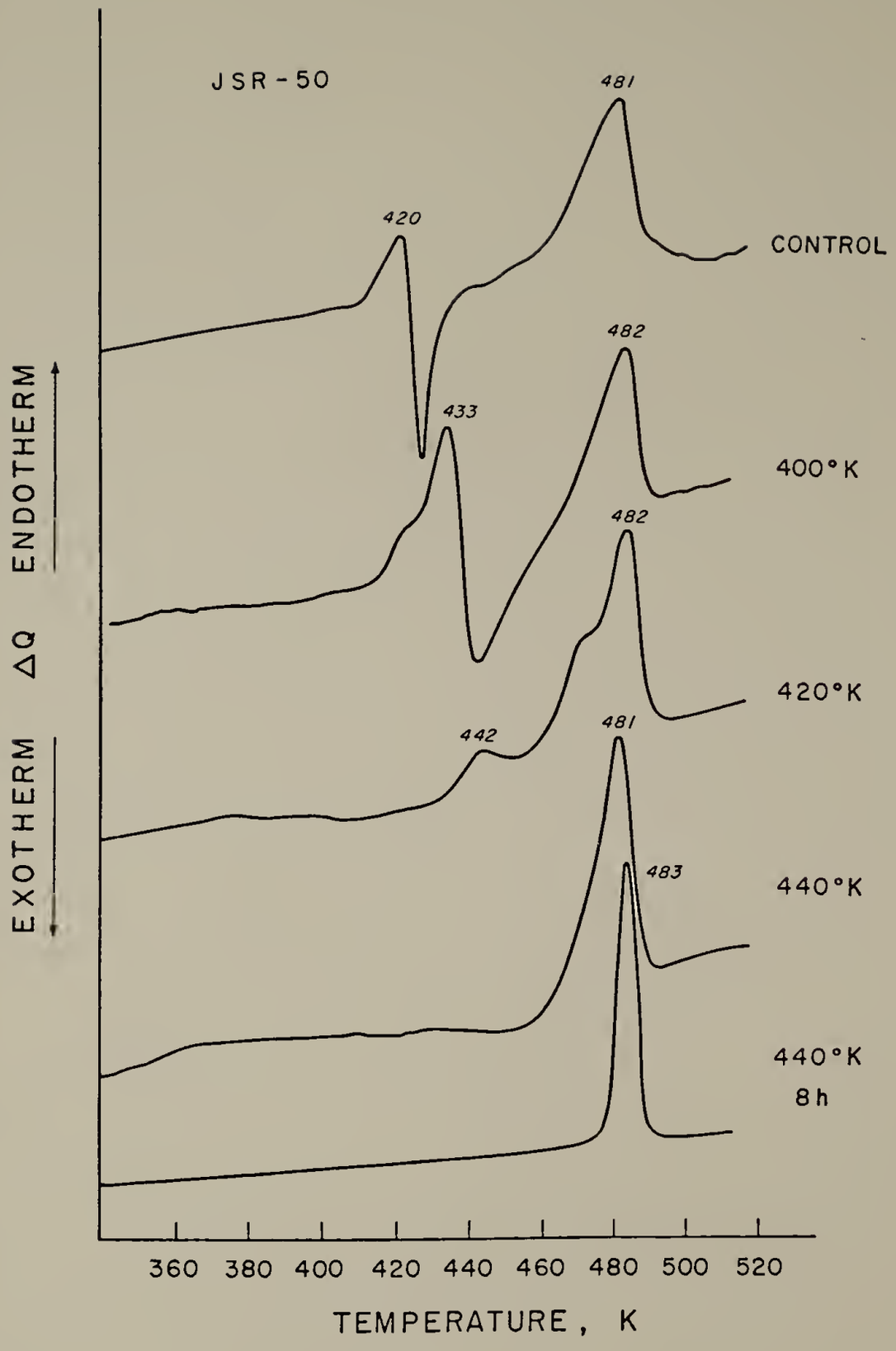

Fig. 4-2. Effect of annealing on the melting behavior of JSR-50.

once apparent that the dependence on annealing temperature, T_a, is not simple but is controlled by the compositional variables.

In JSR-50 (Figure 4-2), annealing at temperatures T_a<130°C results in an increase in the area and position of T_{m1} and corresponding decrease in the area of Tm_2. At higher annealing temperatures (T_a >150°C), the lower endotherm (T_{m1}) as well as the exotherm disappear and only the high temperature endotherm (T_{m2}) is observed. At longer annealing times (8h), the onset of melting of T_{m2} (taken as the temperature of initial departure from the baseline) increases by about 30° and the peak becomes more intense. The maximum in T_{m2}, however, is essentially unaffected by these annealing conditions. It should also be mentioned that this melting peak occurs 10° lower than that of the pure hard segment analog annealed under the same conditions.

A different series of curves are obtained for polyurethanes of 42 and 31 wt. percent hard segment (Figures 4-3 and 4-4). In JSR-42 low annealing temperatures (T_a <110°C) result in a 10° shift of T_{m1}, T_c, and T_{m2} to higher temperatures. At intermediate annealing temperatures (100°<T_a<140°) only a double endotherm of low intensity appears, intermediate in position between the original endotherms, T_{m1} and T_{m2}. At the highest annealing temperature and time (160°C, 8 h) again a double endotherm is observed but now appears some 40° higher than the previous endotherm and only 3° higher than Tm_2 in the control. Unlike JSR-50 and JSR-42, the T_{m1} endotherm in the lowest urethane sample is still apparent after prolonged annealing (8 h at 160°C) and occurs at the same temperature as in the control (though its

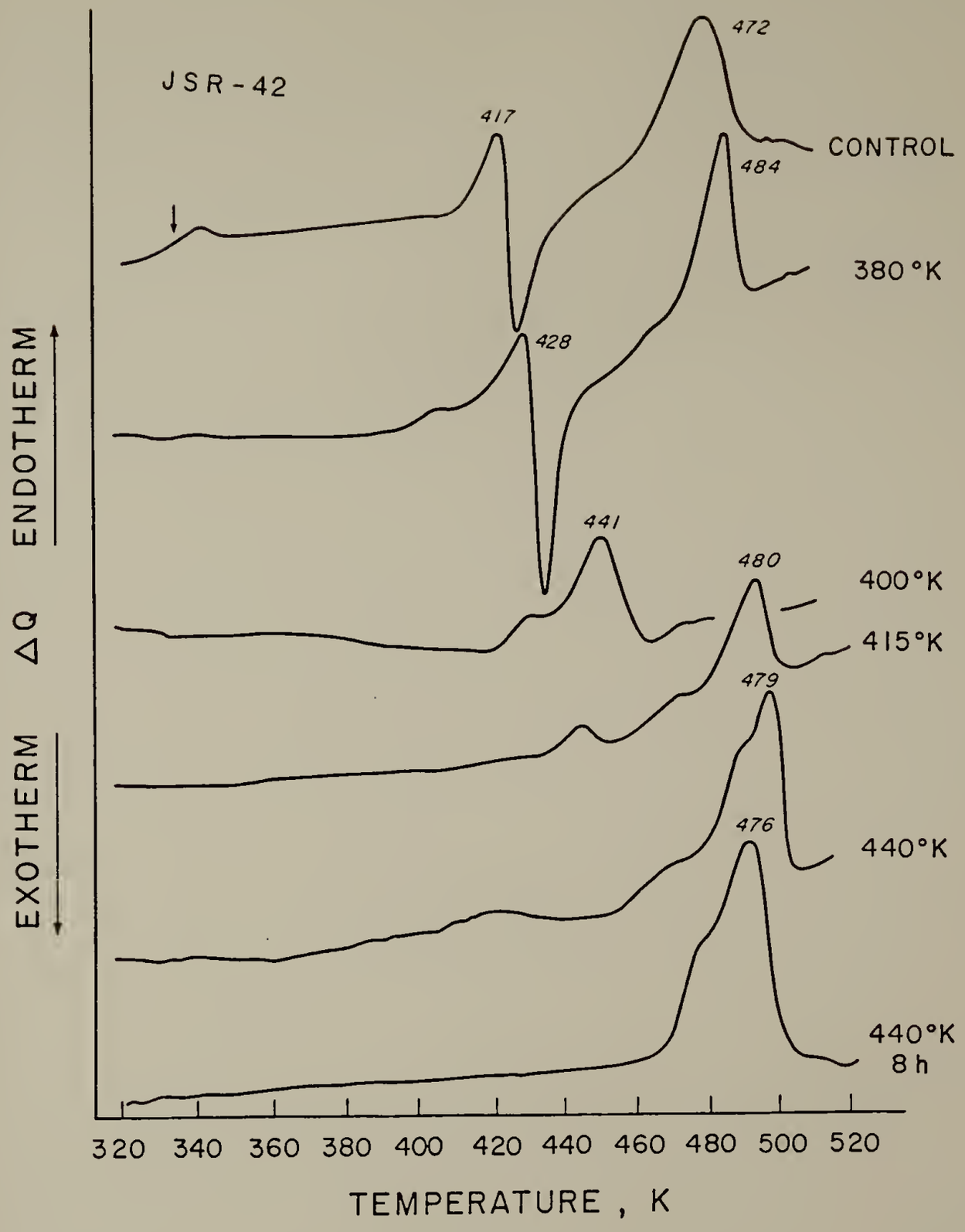

Fig. 4-3. Effect of annealing on the melting behavior of JSR-42.

area has decreased appreciably). The T_{m2} endotherm, however, increases by 5° and becomes narrower (see Figure 4-4). Further annealing resulted in negligible change in the thermal transition behavior of these samples.

It should be mentioned that unlike the melting endotherms, the position of T_{gH} was essentially unchanged by these annealing conditions. Its magnitude, however, decreases with annealing until it is no longer discernible after the most prolonged and high temperature annealing conditions. This behavior may be contrasted to that of the typical MDI-based polyurethanes (2) where annealing shifts the lower transition (ca. 80°C) upscale to merge with the next higher transition (ca. 130°C). Apparently, the degree of crystallinity in the hard segments of the 2,6-TDI polyurethanes can be greatly increased by annealing.

A final point to note lies in the enthalpies of fusion, ΔH_m, of the T_{m2} endotherm in samples annealed at the highest temperature (see Table 4-1). As in the unannealed materials, these values increase approximately linearly with hard segment content, with the corresponding values being slightly higher. Since ΔH_m stems from those hard segments which form highly ordered crystalline domains, the fraction w_c of crystalline hard segments relative to that of the fully annealed TDI/BDL homopolymer may be obtained:

$$w_c = \frac{\Delta H_m}{w_H \cdot \Delta H_m^\circ} \qquad (4\text{-}1)$$

where ΔH_m and ΔH_m° are the enthalpies of fusion of the polymer and homopolymer, respectively, and w_H is the weight fraction of hard

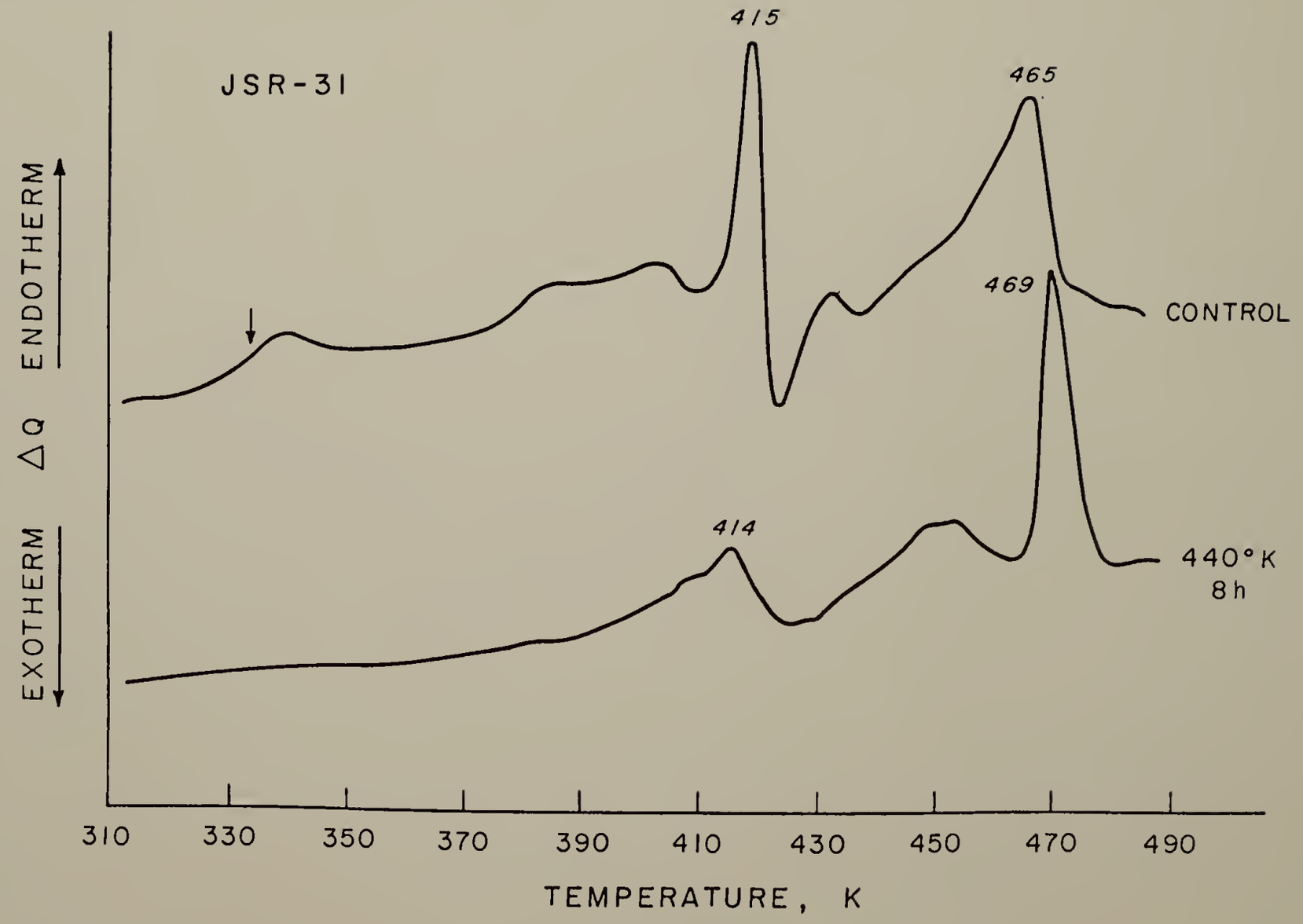

Fig. 4-4. Effect of annealing on the melting behavior of JSR-31.

segment. The values obtained are .93, .83, and .54 for JSR-50, JSR-42, and JSR-31, respectively.

Wide-angle x-ray diffraction. The wide angle x-ray scattering patterns of all three polymers indicate crystalline hard segment peaks centered at 4.6 and 3.7 Å, the same d-spacings observed for the pure hard segment sample. These d-spacings become more prominent with increasing hard segment content. Moreover, on annealing at 160°C 8h, the crystalline peaks become sharper and stronger, indicating a higher overall crystallinity and an increasing crystalline order relative to the controls, consistent with DSC studies. A representative scattering curve is shown in Figure 4-5.

Dynamic mechanical measurements. The dynamic mechanical response of these materials at 11 Hz is shown in Figure 4-6 and summarized in Table 4-2. As in the corresponding 2,4-TDI polyurethanes, the relaxation behavior clearly illustrates the two-phase nature of these PBD-urethanes. A low temperature relaxation maximum, α_S, at -54°C with an activation energy of about 140 KJ/mole is apparent for each sample, independent of hard segment concentration. These results are in good agreement with the DSC soft segment glass transition temperatures reported earlier. As expected, the magnitude of α_S decreases with increasing hard segment content while the magnitude of the storage modulus above this relaxation increases.

Above ambient temperatures, a relaxation associated with the hard segments, α_H occurs at about 45°C for all samples followed by a high temperature δ relaxation. The latter process is associated with the

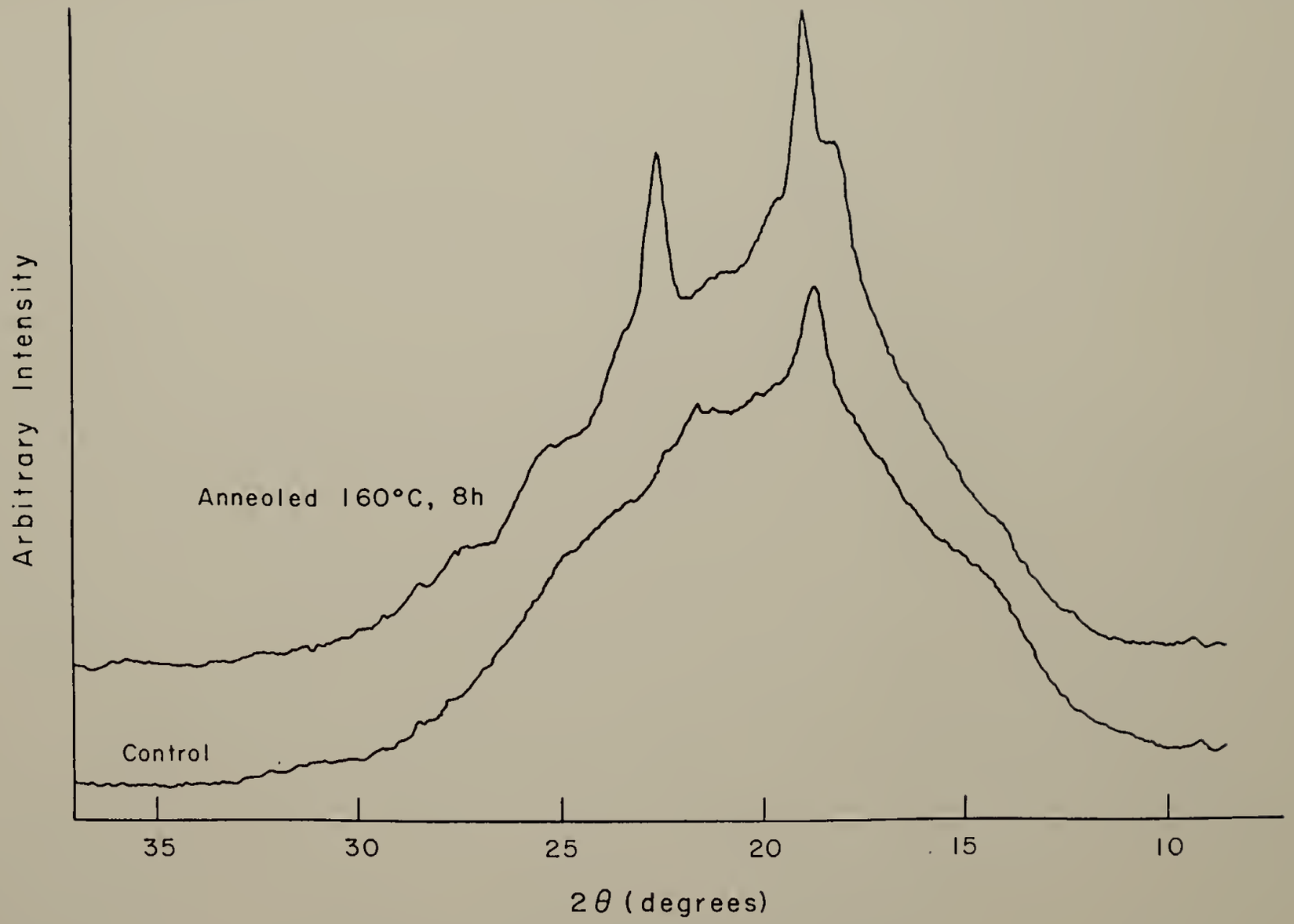

Fig. 4-5. WAXS pattern of JSR-50.

melting of hard segment crystallites. Unlike α_S and α_H, the temperature of the δ relaxation shows a strong dependence on hard segment concentration as does T_{m2} by DSC measurements; both increase with increasing hard segment content. This effect can be assigned to an increase in the hard segment block length as the hard segment content is increased.

The effects of thermal history on the dynamic mechanical properties was also investigated. For JSR-42 retested immediately after the first experiment to 200°C and one month later, the position, shape, and activation energy of the α_S relaxation is essentially unchanged. However, in contrast to the previous study based on 2,4-TDI/BDL, the storage modulus decreased by about 40% over the temperature interval from 25 to 170°C while the magnitude of the α_H dispersion increases and broadens. These effects can be attributed to the disruption of the original crystal structure, as also evident in DSC studies. After one month, however, the recovery is very near complete. The δ relaxation appears unaffected by heating to 200°C.

The effects of annealing on the relaxation behavior of all three materials are summarized in Table 4-2 (values in parentheses) and also shown in Figure 4-6 for JSR-50. As in the DSC study, samples were annealed 8 h at 160°C. Consistent with DSC results, the position of the α_S relaxation is unaffected by the annealing process, though the magnitude of this loss peak decreases as does the broad loss peak (20-200°C) associated with the α_H relaxation. In addition, the level of the storage modulus above α_S is shown to increase as much as 70%

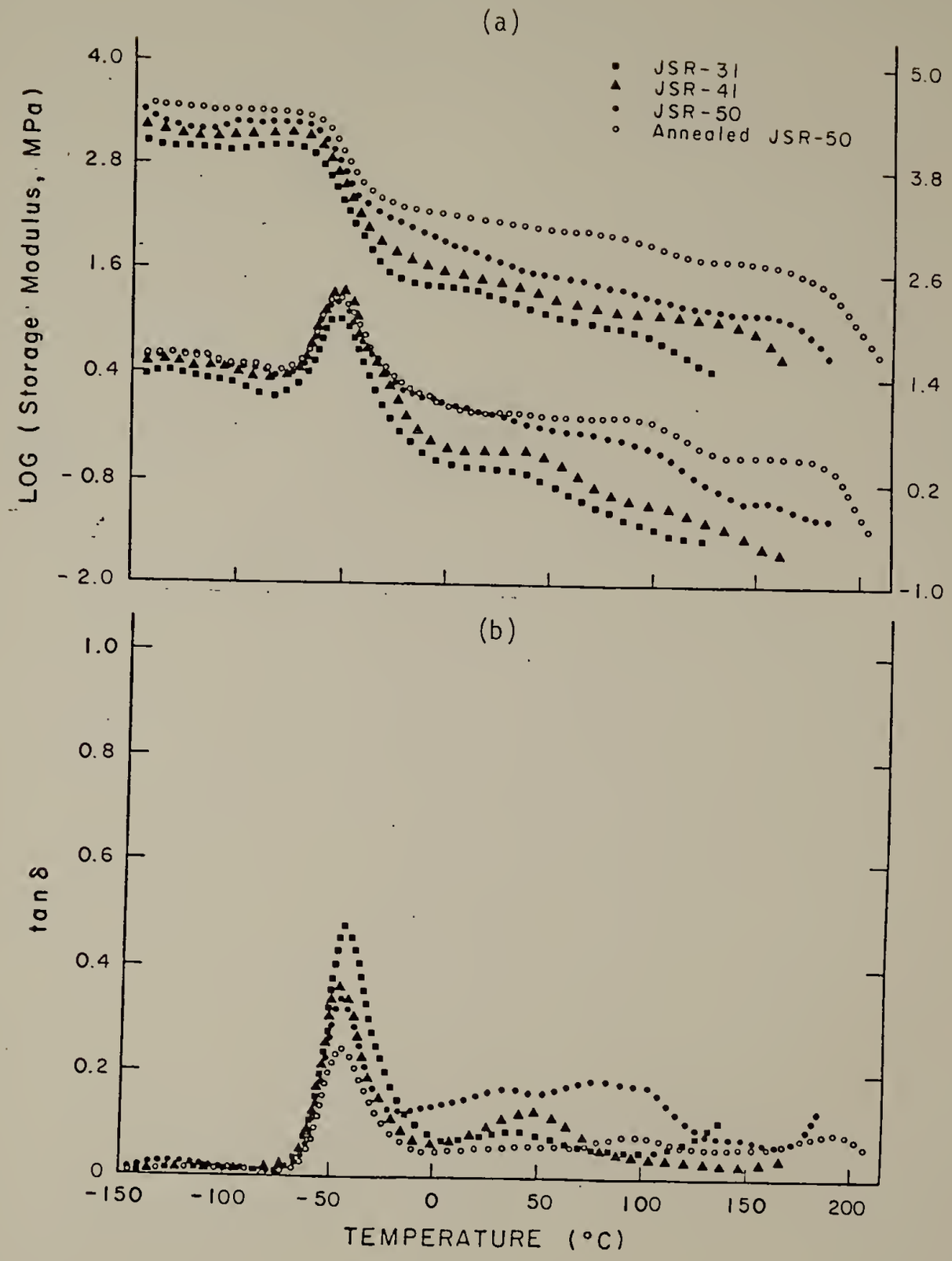

Fig. 4-6. Temperature dependence of (a) the storage and loss modulus and (b) the loss tangent for HTPBD-2,6-TDI-BDL polyurethanes.

Table 4-2

Dynamic Mechanical Relaxations in HTPBD-Polyurethanes

Sample	Relaxation[a]	Temperature (°C)	Activation Energy (kJ/mole)	Magnitude tan (δ)
JSR-31	α_s	-54 (-55)[b]	150 ±40	.460 (.350)
	α_h	42 (42)	---	
	δ	152 (173)	---	
JSR-42	α_s	-55 (-54)	140 ±20	.375 (.320)
	α_h	45 (45)	270 ±50	
	δ	170 (185)	---	
JSR-50	α_s	-54 (-54)	140 ±20	.345 (.240)
	α_h	40, 82 (105)	---	
	δ	185 (215)	---	

[a] α_s determined from E_{max}"

α_h from tan $(\delta)_{max}$

δ from log (E') - softening temp; all at 11 Hz

[b] Values in bracket- annealed at 155°C for 8 hrs.

over a temperature interval of 0-150°C while the temperature of the δ relaxation is shifted 20° to higher temperatures. The observed changes are most pronounced in JSR-50, the sample with the higher hard segment content. These effects can be attributed to an increase in the size and stability of the crystalline domains following annealing, as will be discussed below.

Discussion

The quantitative analysis of the melting and crystallization behavior by DSC in these 2,6-TDI polyurethanes suggests that the hard segments form crystalline domains whose size and therefore melting temperature is dependent on such factors as heating rate, annealing temperature, and hard segment length. Two melting endotherms (T_{m1} and T_{m2}) are observed at low heating rates while only T_{m1} persists at higher scanning rates (>80°C/min). Moreover, both endotherms appear at low annealing temperatures. At higher temperatures (T_a>140°C) a single endotherm (T_{m2}) can be obtained, the position and area of which increase with increasing annealing temperature. These results are interpreted to mean that at low heating rates and/or annealing temperatures, the original crystal distribution, corresponding to T_{m1}, can reorganize to increase its stability and consequently melt at higher temperatures (T_{m2}) with higher ΔH_m values. At higher scanning rates, the relatively slow recrystallization process is impeded. It is also concluded that crystalline domains formed at the higher annealing temperatures

(T_a>140°C) are not the result of reorganization during the scan in the DSC, but rather a new crystal distribution formed at T_a (hence, no T_{m1}). As indicated in Table 4-1, the degree of crystallinity, as measured by ΔH, is nearly the same for the reorganized structure, T_{m2}, whether formed during scanning at 20°/min or high annealing temperatures and appreciably higher than the original crystal distribution, T_{m1}.

The precise nature of the reorganization described above is shown to depend on hard segment composition. It will be recalled that the positions and areas of T_{m1} and T_{m2} in the control and annealed samples vary systematically with hard segment content, with T_{m2} occurring some 20° higher in JSR-50 as compared to JSR-31 and the enthalpy of fusion, ΔH_m, increasing from 1.37 to 5.63 cal/g. A similar increase in the δ relaxation temperature with hard segment content is also observed by rheovibron measurements. These effects can be assigned to an increase in the hard segment block length as the hard segment content is increased. The longer hard segments can then form better organized and more stable domains which melt at higher temperatures. Employing the number average hard segment length at 99% conversion and a μ value of 3 from Peebles theoretical data (8), the equation given by Flory (9) can be used to obtain the melting temperature for the infinite chain:

$$\frac{1}{T_m} = \frac{2R}{n\Delta H} + \frac{1}{T_m^{\infty}} \qquad (4\text{-}2)$$

A plot of the inverse of T_{m2} against the inverse of the hard segment length, n, is shown in Figure 4-8 for both control and fully annealed samples. The two sets of data were both found to fit a straight line

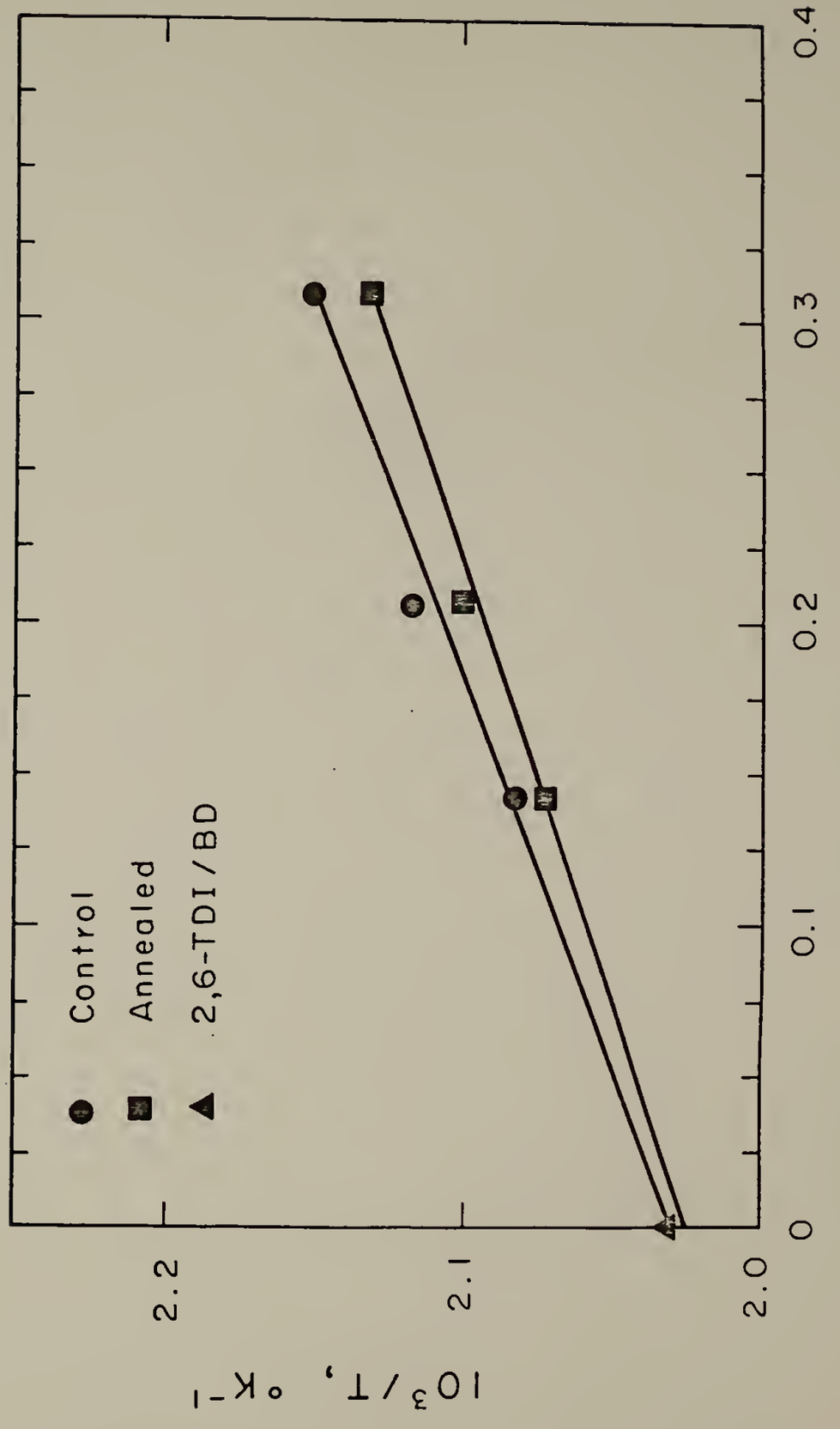

Fig. 4-7. Reciprocal of average hard segment length vs. $1/T_m$ for HTPBD-2,6 TDI-BDL polyurethanes.

with an identical value of T_m^∞ of 220°C, in good agreement with the experimentally determined T_{m2} of the TDI/BDL homopolymer. The depression of the melting points of the polymers over the value of the infinite chain can be accounted for by the presence of crystal defects and/or surface effects which are presumable more abundant in the shorter hard segment materials. From the slope of the line, the heat of fusion per repeat unit, ΔH_n, was calculated as 158 J/g in the control samples and 180 J/g in the annealed samples. The slight increase (ca. 10%) in ΔH_n of the annealed samples reflects an increase in the perfection and order of the crystalline domains as compared to those formed during scanning in the DSC. As in the controls, the extent of this perfection and/or reorganization is also governed by the hard segment length. Under the most severe annealing conditions, JSR-50 exhibits a single sharp melting peak (T_{m2}) while JSR-41 shows a double melting peak of enhanced breadth about 10° lower. In JSR-31, there is still evidence of a T_{m1} endotherm under these same conditions. These shorter sequences giving rise to T_{m1} presumably cannot co-crystallize with longer segments. Only crystals selectively built up of longer hard segments out of the total length distribution will contribute to higher melting behavior. These longer segments consequently yield a more ordered and well developed domain structure on annealing consistent with WAXS studies. Using the ΔH_m values at T_{m2} it was shown that the fraction of hard segments which form crystalline domains, w_c, relative to the pure homopolymer increases with hard segment content. Whether this is due to an increase in the degree of crystallinity or a consequence of an

increase in size of the crystalline domains cannot be answered unequivocally until further studies (i.e. SAXS) are made. In any event, w_c was found to be surprisingly high in JSR-50, nearly approaching that of the TDI/BDL homopolymer. These results must be attributed to the high degree of phase separation occurring in the materials, which facilitate reorganization and perfection of the hard segments.

Conclusions

As in the corresponding polyurethanes based on 2,4-TDI/BDL hard segments these materials consisting of crystalline hard segment domains are well phase separated as evidenced by the low and composition insensitive glass transition temperature, T_{gs}. Furthermore, thermal treatment was found to have negligible effect on T_{gs} both by dynamic mechanical and DSC measurements. In contrast to the completely amorphous systems whose hard segment glass transition temperature increases systematically with urethane content, all 2,6-TDI polyurethanes exhibit a glass transition at about 62°C. The invariance of T_{gH} in these materials would therefore suggest that the amorphous hard segment domain structure is not further improved by a longer hard segment length, within the composition range examined. On further heating, melting occurs (T_{m1}) followed by recrystallization and then a final melting process (T_{m2}). The positions of the melting peaks and the corresponding heats of fusion, ΔH_m, are shown to depend strongly on the hard segment content, annealing temperature and, to a lesser

degree, on heating rate. The data indicate that crystals of varying stability are formed at different annealing temperatures. Moreover, only those segments involved in the initial crystal distribution (T_{m1}) which are long enough will give rise to the higher melting crystals, the size and perfection of which are governed by the hard segment length.

References

1. N.S. Schneider and C.S. Paik Sung, Polym. Eng. Sci. 17, 73 (1977).
2. R.W. Seymour and S.L. Cooper, Macromolecules 6, 48 (1973).
3. K.H. Illers, Kolloid Z.Z. Polym. 250, 426 (1972).
4. C.E. Wilkes and C.S. Yusek, J. Macromol. Sci., Phys. 7, 579 (1973).
5. N.S. Schneider, C.S. Paik Sung, R.W. Matton, and J.L. Illinger, Macromolecules 8, 62 (1975).
6. R.R. Lagasse, J. Appl. Polym. Sci. 21, 2489 (1977).
7. T.R. Hesketh, J.W.C. Van Bogart, and S.L. Cooper, Polym. Eng. Sci. 20, 190 (1980).
8. L.H. Peeples, Macromolecules 7, 872 (1974).
9. P.J. Flory, "Principles of Polymer Chemistry", p. 570, Cornell University Press, Ithaca, New York (1953).

CHAPTER V

HYDROGEN BONDING PROPERTIES OF MODEL HARD SEGMENT COMPOUNDS IN POLYURETHANE BLOCK COPOLYMERS

Introduction

Segmented polyurethanes are extensively hydrogen bonded. In all cases, the N-H group of the urethane serves as the proton donor while the acceptor group may include the carbonyl and adjacent oxygen atom in the urethane group as well as the ester carbonyl or ether oxygen of the soft segment. Although hydrogen bonding is an important structural feature of segmented polyurethanes, its influence on their properties and morphologies is not clear. Working on a series of MDI-based polyurethanes, Seymour et al. (1) have concluded that the thermal behavior of hydrogen bonding is independent of morphology and depends primarily on the glass transition temperature of the hard segments. Investigations by the x-ray diffraction method (2,3) of hydrogen bonding and the orientation mechanisms of segmented polyurethanes have suggested otherwise; both crystallization of the hard segments as well as the observed orientation behavior have been explained by "restructuring" of the physical crosslinking caused by hydrogen bonding.

While hydrogen bonding in segmented polyurethanes has been the subject of numerous investigations using infrared spectroscopy, very little systematic interpretation has so far been made of the spectral features associated with the N-H absorption band. As in most hydrogen bonded

systems, this stretching mode displays well known and characteristic perturbations: frequency shift, increase in band width relative to the natural width and enhancement of intensity. The frequency shift has been generally accepted as a measure of the strength of the hydrogen bond, correlating well to hydrogen bond energy (4) and NH---O distance in solids (4-7). Although the origin of the latter two effects is less clear, changes in these properties are no doubt indicative of the structural and hydrogen bonding features of these systems and may therefore lead to additional information about the effects of hydrogen bonding on morphology.

The present work is concerned with a detailed analysis of the N-H stretching vibration in three copolymers based on MDI, 2,6-TDI and 2,4-TDI polymerized with butanediol (BD). They were selected to be representative of the chemical structures and morphologies of the hard segment units in polyurethane elastomers. As in these materials, the 2,4 TDI-BD copolymer is completely amorphous (8) while 2,6-TDI-BD and MDI-BD are capable of crystallizing under proper conditions (8,9). It was therefore of interest to examine changes in the spectroscopic properties of the N-H vibrations after annealing and determine whether additional information on the nature of hydrogen bonding and chain packing could be obtained from this type of analysis. The temperature dependence of hydrogen bonding in these mateials is also investigated. The results will be interpreted in light of current views on hydrogen bonded systems and compared to differential scanning calorimetry (DSC) studies.

Materials and Methods

The three model compounds were synthesized from 1,4 butanediol (BD) and each of the following diisocyanates: 2,4-toluene diisocyanate (2,4-TDI), 2,6-toluene diisocyanate (2,6-TDI) and p,p'-diphenylmethane diisocyanate (MDI).

2,4-TDI-BD

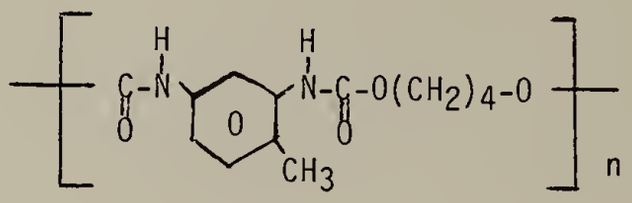

2,6-TDI-BD

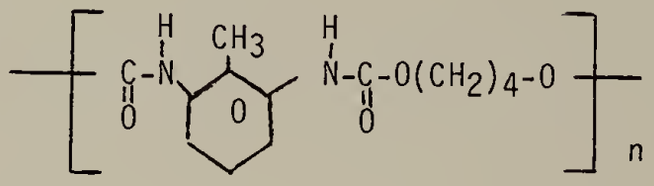

MDI-BD

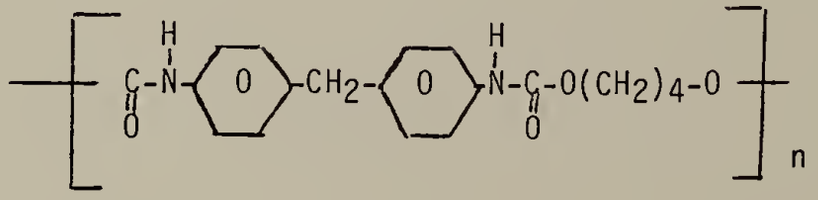

The solution polymerization of these polymers was carried out in a 50:50 mixture of dimethyl sulfoxide and methylisobutyl ketone following a procedure described by Lyman (10).

Infrared spectra (400-4000 cm^{-1}) were obtained with a Nicolet 7199 Fourier Transform Infrared spectrometer. Two hundred scans at 2 cm^{-1} resolution were signal averaged and stored on a disk for further analysis. Samples were prepared by solution casting 5% w/v of polymer

from N,N-dimethylformamide (DMF) directly onto KBr plates and vacuum drying for four days at 50°C. Survey spectra did not show any evidence of residual solvent (see Figure 5-1). The three samples were then placed in a vacuum oven and annealed at 150°C. Spectra were collected after various annealing times ranging from 30 minutes to 8 hours. Since rapid solvent evaporation is thought to be responsible for the lower melting points and heats of fusion of the solution cast MDI-BD copolymer compared to the as-polymerized material (11), a second drying procedure was used to circumvent this problem and facilitate crystallization. Here the KBr plate containing the polymer solution (5% w/v) was mounted in an evaporating dish, the bottom of which was covered with filter paper and saturated with DMF. The dish was then covered and placed in an oven for 24 hours at 100°C. Again no residual solvent was detected in the infrared spectrum.

For the temperature scans, the sample was placed in a variable temperature unit (Wilks Model No. 19) connected to the temperature controller (Wilks Model No. 37) and the temperature was monitored by a copper-constantan thermocouple junction placed directly on the sample. The temperature was held constant for about 5 min before spectra were collected. A dry nitrogen flow was maintained over the film throughout the measurements to avoid the condensation of moisture on the salt plate.

In the infrared analyses, absorption frequencies are accurate to ±1 cm^{-1} and widths at half peak height to about ±5 cm^{-1}. Frequency shifts are listed as $\Delta\nu = (\nu_f - \nu_b)$ where ν_f and ν_b are the frequencies of

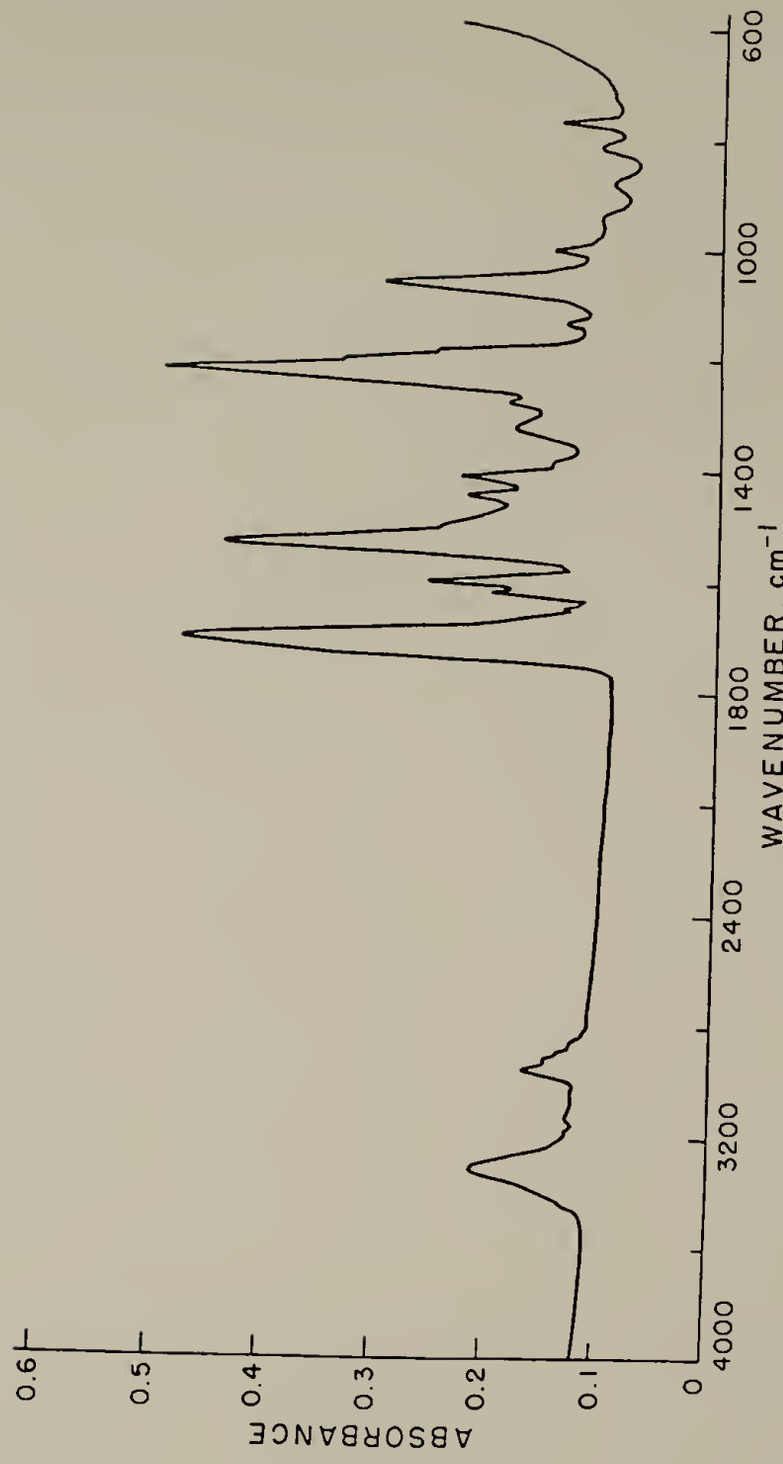

Fig. 5-1. Survey infrared spectrum of model hard segment compound 2,4-TDI-BD.

maximum absorption for the free and bonded N-H groups, respectively. Integrated intensities have been corrected for sample thickness differences using the CH_2 stretch near 2950 cm^{-1} as normalizing factors. These vibrational modes are very localized and, therefore, suitable for quantitative analysis (12). The fraction of hydrogen bonded N-H groups, X_b, is determined by a curve resolving technique based on a nonlinear least square analysis for the fitting of a combination of Lorenzian and Gaussian curve shapes. Values are reliable to within ±1%. The extinction coefficient difference between the free and bonded N-H absorption is also taken into account in the analyses (13,14).

Differential scanning calorimeter data were obtained on a Perkin-Elmer DSC-2. Runs were conducted on polymer samples of about 15 mg at a heating rate of 20°/min. The cell was calibrated for quantitative measurements using indium and tin standards. As in the infrared studies, polymers were cast from DMF solution (5% w/v) and subjected to the same thermal treatment.

Results

Infrared. All polymers when cast from DMF solution produced transparent films. Figure 5-1 shows a typical infrared spectrum (4000-600 cm^{-1}) of these materials. Although several vibrations are involved in hydrogen bonding, i.e carbonyl stretching (Amide I), N-H in plane bending (Amide II) and out of plane deformation (Amide V) (see Table 5-1), this study is principally concerned with the N-H stretching vibration. In each

Table 5-1

Band Assignments for Hard Segment Model Compounds

Frequency (cm^{-1})[a]	Assignment
	ν (N-H) free N-H
3450	in 2,6 and 2,4-TDI
3420	in MDI
	ν (N-H) bonded N-H
3330	in MDI
3310	in 2,4-TDI
3300	in 2,6-TDI
1735	ν (C=O) free C=O
	ν (C=O) bonded C=O
1708	in 2,4-TDI
1706	in 2,6-TDI
1703	in MDI
	δ (N-H) + ν (C-N)
1530	in MDI
1523	in 2,6 and 2,4-TDI
	δ (N-H) + ν (C-N)
1240	in 2,6-TDI
1230	in MDI
1225	in 2,4-TDI
1080	ν (C-O-C) in -C-O-C (O)
774	γ (-C-O-) (O)

[a] ν=stretching
δ=in plane bending
γ=out of plane bending

spectrum, the strong absorption peak centered around 3300 cm^{-1} is assigned to the hydrogen bonded N-H groups while the weak shoulder on the high frequency side of this peak corresponds to the free N-H groups. The spectral properties relating to this vibration are summarized in Table 5-2.

Prior to annealing, it is clear that the half-widths, $\Delta\nu 1/2$, frequency shift, $\Delta\nu$, and integrated intensities, B, of the N-H stretch are of comparable magnitude in the 2,4 and 2,6-TDI-BD copolymers; $\Delta\nu 1/2$ is in the range of 100-110 cm^{-1}, $\Delta\nu$ about 150 cm^{-1} and B, 3.6. The smaller values obtained in MDI-BD are presumably due to steric factors associated with packing. In agreement with earlier studies on the corresponding polyurethanes and model systems (13-15), 80-85% of the N-H groups are found to be hydrogen bonded in these materials.

Qualitative changes in the N-H stretching region after annealing are shown in Figure 5-2. Annealing at 150°C for as long as 8 hours produced no change in the intensity, shape or position in the 2,4-TDI-BD copolymer. In contrast, the N-H stretching vibration in 2,6-TDI-BD exhibited nearly a 50% reduction in half-width for the annealed sample. When compared to the initial solution cast material, there is also a 22 cm^{-1} shift in position to lower frequencies as well as an increase in intensity. These spectral properties are plotted as a function of annealing time in Figures 5-3 and 5-4. It is noted that the most significant changes occur during the first three hours of annealing in the 2,6-TDI copolymer after which these properties approach a nearly constant value. Similar changes are also observed in the carbonyl

Table 5-2

Changes of NH Stretching Vibration as a Function of Annealing Time

Annealing Time	$\Delta\nu$ (cm^{-1})	$\Delta\nu 1/2$ (cm^{-1})	I[a]
	2,6-TDI-BD		
0	150	105	3.75
30 min	152	102	3.95
90 min	160	92	4.35
4 hr	170	66	4.67
8 hr	172	58	4.82
	2,4-TDI-BD		
0	140	107	3.50
90 min	140	109	3.42
4 hr	140	111	3.30
8 hr	140	111	3.20
	MDI-BD		
0	90	92	3.09
90 min	90	92	3.21
4 hr	88	88	3.23
8 hr	88	88	3.26
24 hr[b]	102	56	4.10

[a]Normalized with respect to the 2950 cm^{-1} CH stretching vibration.

[b]Slow solvent evaporation technique.

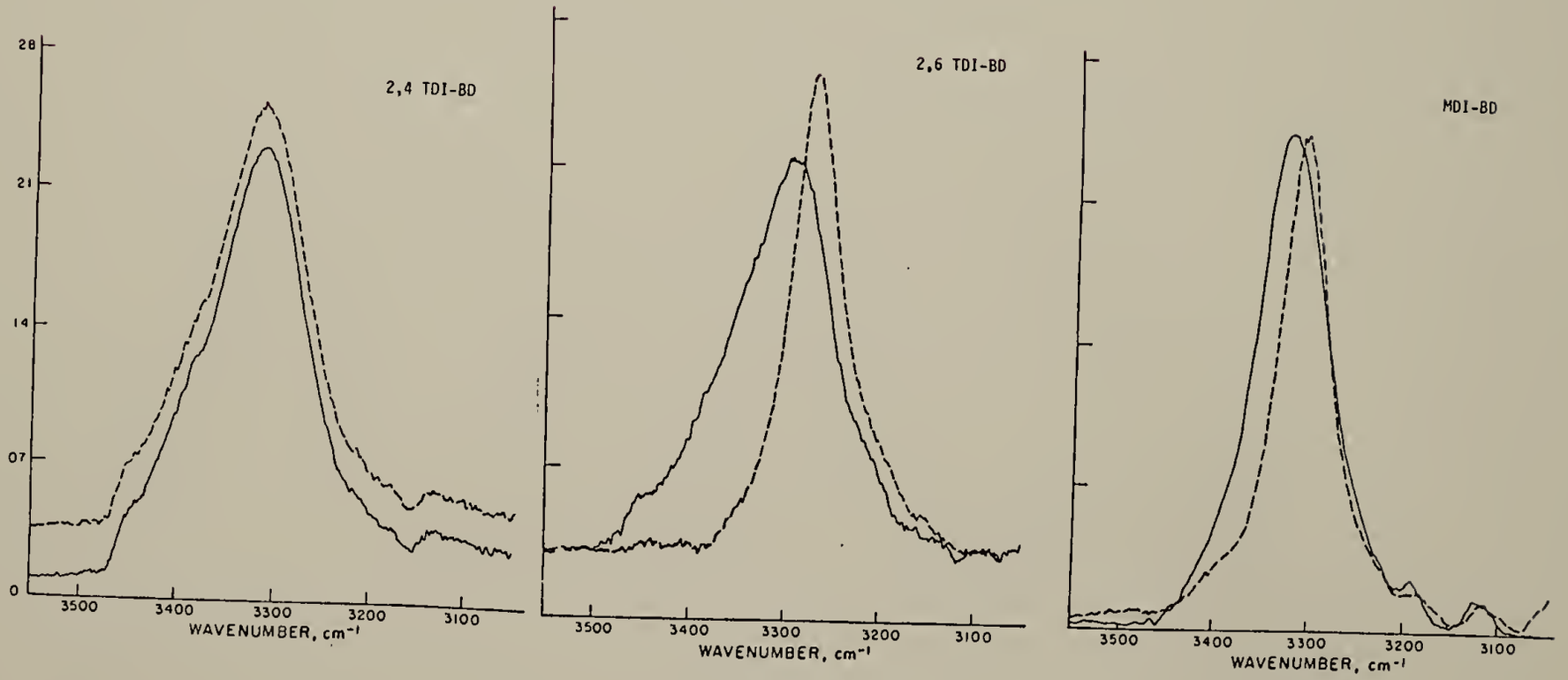

Fig. 5-2. Effect of annealing on the N-H stretching vibration of model hard segment compounds: (a) 2,4-TDI-BD; (b) 2,6-TDI-BD; (c) MDI-BD; (_____) control; (-----) annealed at 150°C for 8 hr in (a) and (b) and slow solvent evaporation technique in (c).

Fig. 5-3. Effect of annealing time on the position (ν_{NH}) and half-width ($\Delta\nu_{1/2}$) of the N-H absorption in model hard segment compounds; (-----) slow solvent technique.

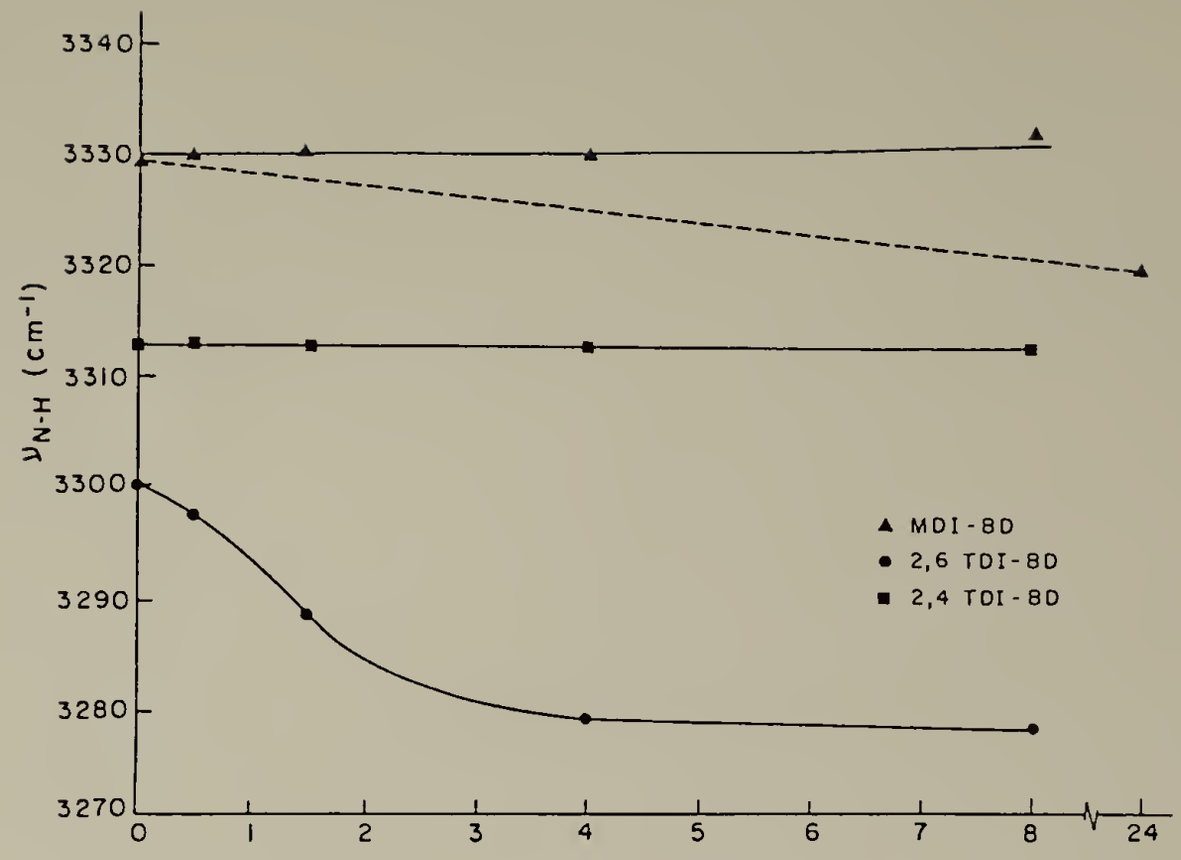
3340
3330
3320
3310
3300
3290
3280
3270
ν_{N-H} (cm^{-1})
0
1
2
3
4
5
6
7
8
24
▲ MDI-BD
● 2,6 TDI-BD
■ 2,4 TDI-BD

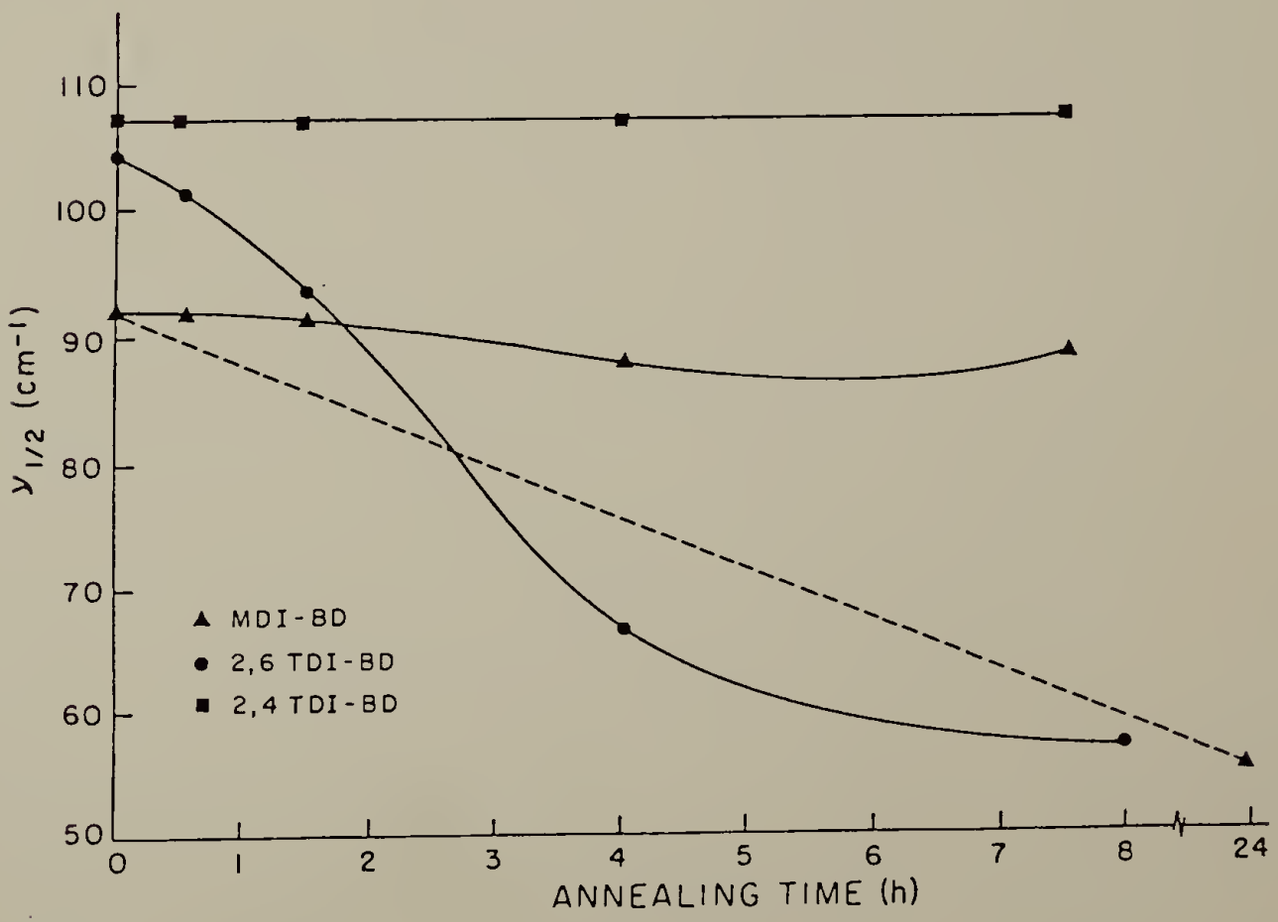
110
100
90
80
70
60
50
$\nu_{1/2}$ (cm^{-1})
0
1
2
3
4
5
6
7
8
24
ANNEALING TIME (h)
▲ MDI-BD
● 2,6 TDI-BD
■ 2,4 TDI-BD

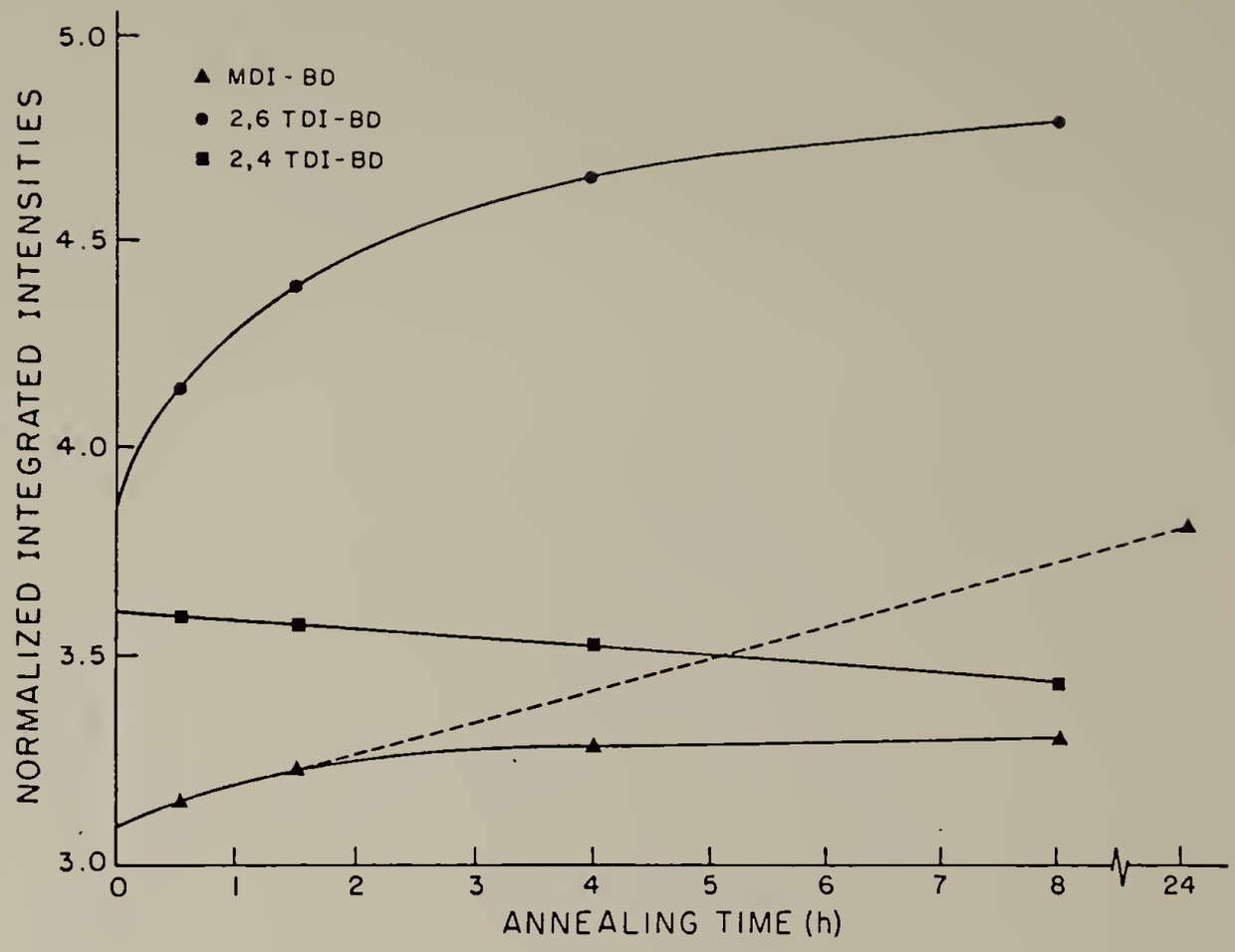

Fig. 5-4. Effect of annealing time on the normalized integrated intensity (B) of the N-H absorption in model hard segment compounds; (-----) slow solvent evaporation technique.

region of the 2,6-TDI-BD spectrum; the bonded C=O component decreases by 12 cm^{-1} and narrows. Consistent with this decrease in the stretching frequency, the bending vibrations at 1530 cm^{-1} and 760 cm^{-1} increase 2-3 cm^{-1}. The band shapes, however, remain essentially unchanged.

The magnitude of the spectral changes observed for MDI-BD are very sensitive to the annealing conditions. While a slight narrowing (<10 cm^{-1}) and frequency shift (2-3 cm^{-1}) are observed in samples annealed at 150°C, more dramatic changes occur in the slowly evaporated cast sample. Here the half-width of the N-H stretching vibration decreases by 36 cm^{-1} and the frequency by 12 cm^{-1}. The intensity also increases, comparable to the increase observed in the 2,6 TDI-BD sample. It is noted that these spectral changes are not accompanied by any measurable change in the fraction of hydrogen bonded N-H groups.

DSC. All hard segment copolymers display a glass transition, T_g between 90 and 100°C. These values are in good agreement with those reported in the literature (16,17). In addition, very weak transitions are observed for the 2,6 TDI-BD and MDI-BD samples between 135° and 200°.

Figure 5-5 shows the DSC scans for 2,6 TDI-BD following heat treatment. After 90 minutes annealing, the lower transition T_g is no longer discernible but a broad and well defined endotherm appears at 207° in addition to the weak endotherm at 160°C. At longer annealing times, both endotherms progressively shift to higher temperatures and become sharper. After a total of 8 hours annealing, the lower transition occurs at 195°C while the main peak has shifted to 218°C. Similar to the intensity variation of the N-H stretching vibration, the

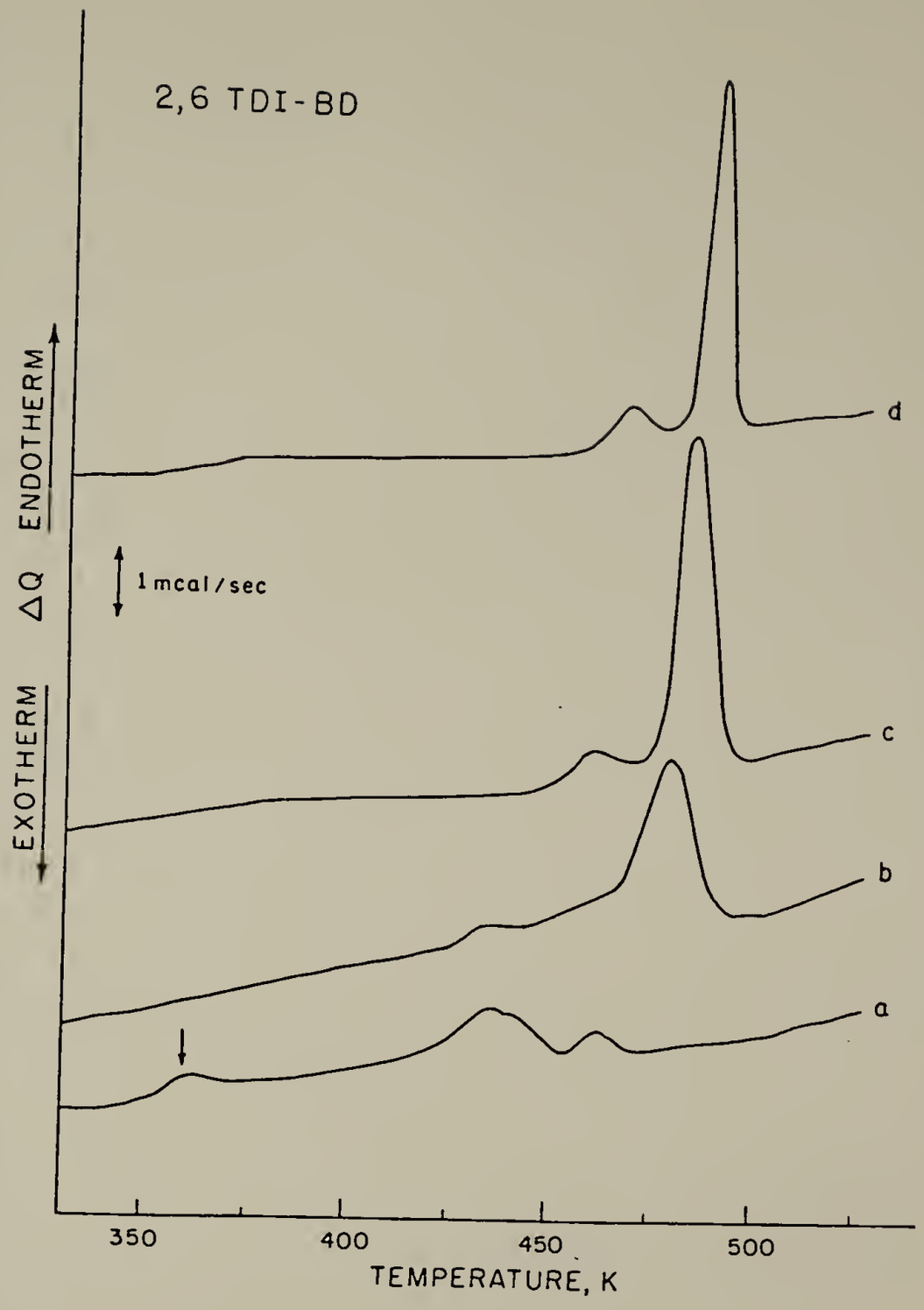

Fig. 5-5. DSC curves for 2,6 TDI-BD annealed at 150°C for various times (a) control; (b) 90 min; (c) 4 hr; (d) 8 hr.

area under the melting peak increases rapidly during the first 3 hours annealing after which it approaches a nearly constant value (see Figure 5-6). Both these effects can be attributed to improved ordering within the crystalline domains.

As shown in Figure 5-7, the melting endotherms in MDI-BD are much less pronounced than in the 2,6 TDI-BD samples. After 90 minutes annealing, the transitions at 94° and 135°C disappear while the melting endotherm at 202°C becomes more intense. Longer annealing times resulted in only minor changes in the position and area of this main peak. For the slowly evaporated sample, however, the DSC scan shows two sharp and overlapping peaks at 225 and 231°C and a corresponding increase in area. No change in the DSC behavior of 2,4 TDI-BD is observed following heat treatment. A summary of these transition temperatures is listed in Table 5-3.

Temperature dependence of hydrogen bonding. To determine whether the dissociation of hydrogen bonding in these treated samples is consistent with the observed spectral changes and DSC behavior, the temperature dependence of the N-H absorption band was investigated. Figure 5-8 shows a plot of the fraction of hydrogen-bonded N-H (X_b) groups versus temperature for the fully annealed 2,6 and 2,4-TDI-BD samples and slowly evaporated MDI-BD cast sample. For 2,4-TDI-BD, Figure 5-6 shows that X_b remains nearly constant below 100°C (corresponding to Tg) and decreases linearly above this temperature. In 2,6-TDI-BD and MDI-BD, the slope change at Tg is much less pronounced. There is, however, a marked decrease in X_b near the melting temperature which occurs at about

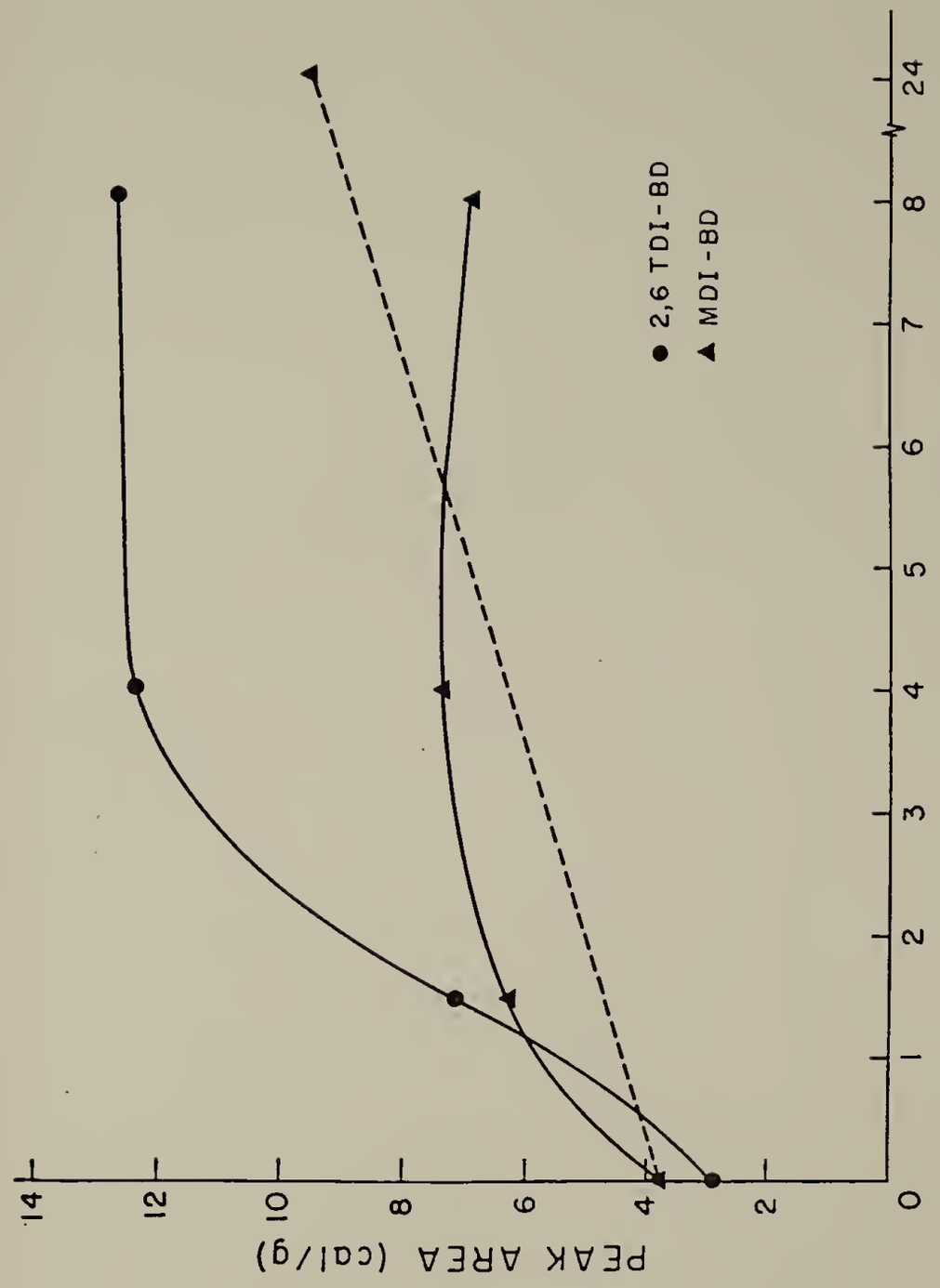

Fig. 5-6. Effect of annealing time on the area of DSC melting peaks; (-----) slow solvent evaporation technique.

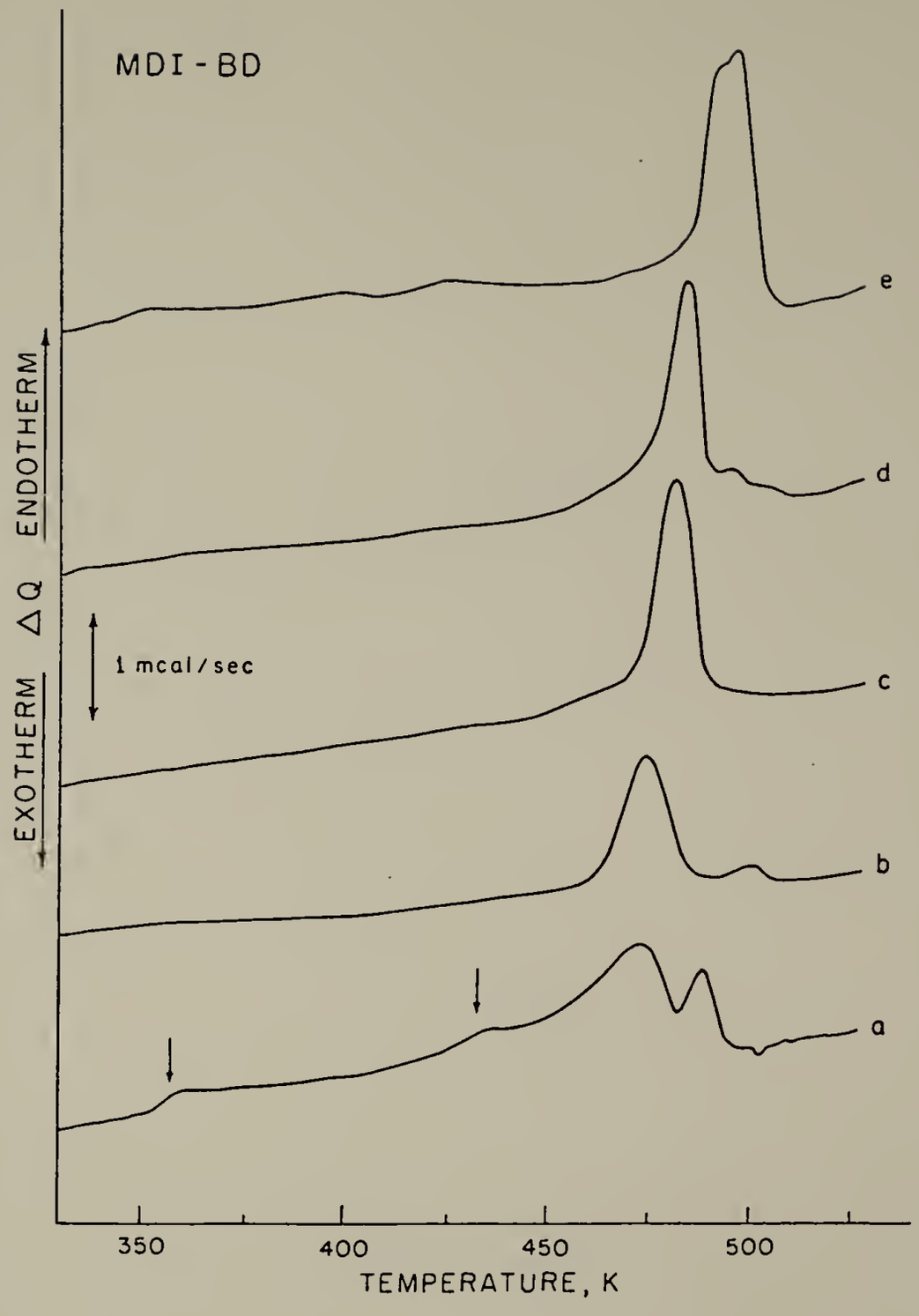

Fig. 5-7. DSC curves for MDI-BD annealed at 150°C for (a) control; (b) 90 min; (c) 4 hr; (d) 8 hr; (e) slow solvent evaporation technique.

Table 5-3

DSC Events as a Function of Annealing Time

Annealing Time	2,6 TDI-BD			MDI-BD				2,4 TDI-BD
Control	92[a]	160	195	94	135	200	217	101
90 min	-	160	207	-	-	202	227	104
4 hr	-	187	214	-	-	210	-	102
8 hr	-	195	218	-	-	210	-	102
24 hr[b]						225	231	

[a]Uncertainty for each temperature is ±2°C.

[b]Slow solvent evaporation technique.

200°C in 2,6-TDI-BD and 220°C in MDI-BD. Similar transitions have been reported earlier in nonsegmented polyurethanes based on 2,4-TDI and MDI and α,ω diols (13).

From the data shown in Figure 5-8 the equilibrium constant for the dissociation of hydrogen bonded N-H groups is determined:

$$K_d = \frac{[N\text{-}H]\ [O{=}C]}{[N\text{-}H\text{---}O{=}C]} = \frac{(1 - X_b)^2}{X_b} \qquad (5\text{-}1)$$

The change in enthalpy, ΔH, for hydrogen bond dissociation is then calculated from the temperature dependence of the equilibrium constant:

$$K_d = \exp\ (-\Delta H/RT + \Delta S/R) \qquad (5\text{-}2)$$

Figure 5-9 is a plot of $-\ln(K_d)$ vs. $1/T$. It should be noted that these curves exhibit transitions corresponding to those observed on the X_b curves. Values of ΔH were calculated from data above Tg in the 2,4-TDI-BD curve and above Tm in the 2,6-TDI-BD and MDI-BD curves shown in Figure 5-8. These values are listed in Table 5-4.

Discussion

A number of studies have reported substantial changes in the N-H stretching vibration in polyurethanes with both temperature (13,18,19) and deformation (20-23). These spectroscopic changes are undoubtedly correlated to changes in the uniformity and strength of the hydrogen bonds. It has been generally accepted that the shift, $\Delta\nu$, in the stretching frequency of the hydrogen bonded X-H group (X-H---Y) is a

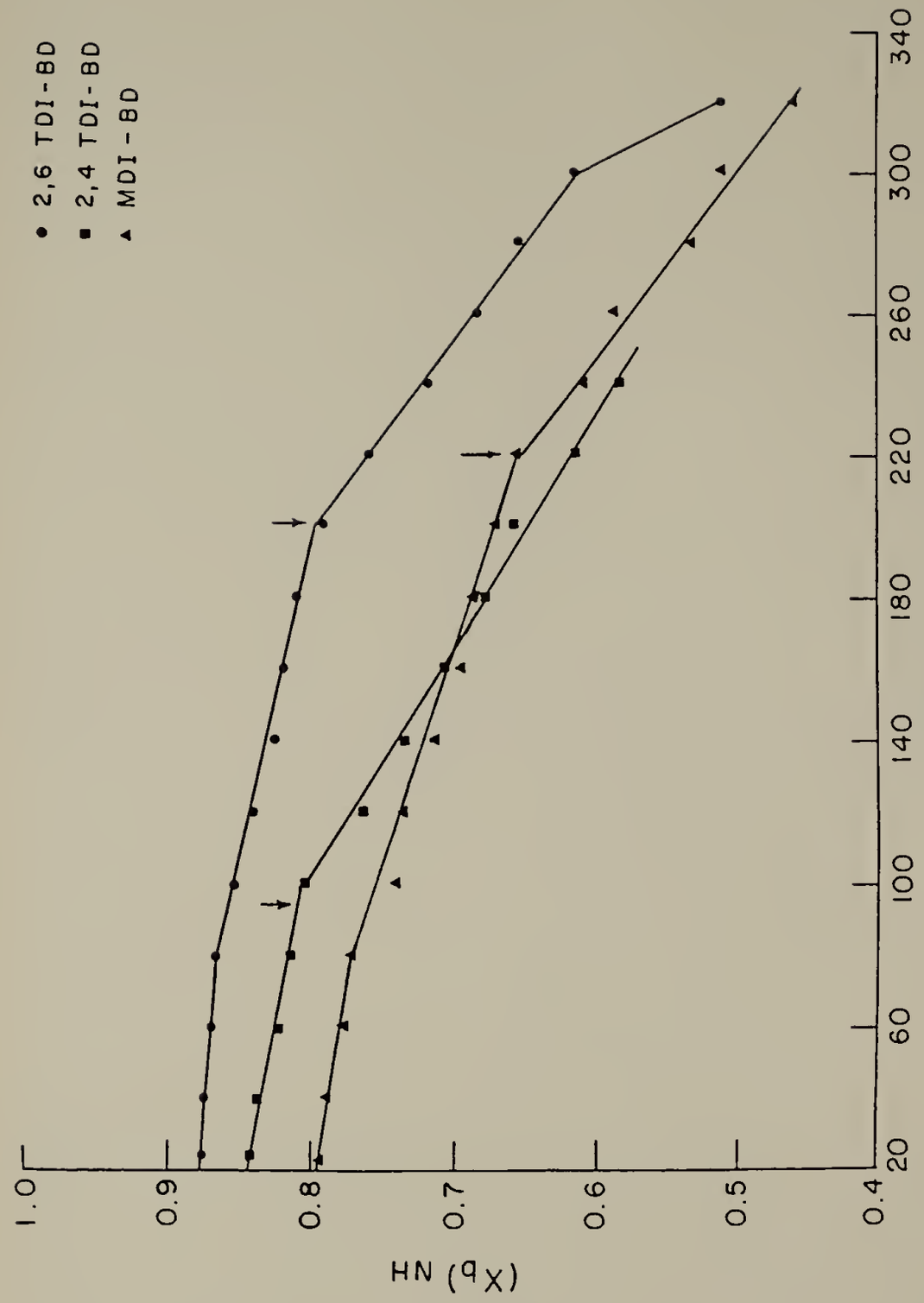

Fig. 5-8. Fraction of hydrogen-bonded NH (X_b) vs. temperature for model hard segment compounds.

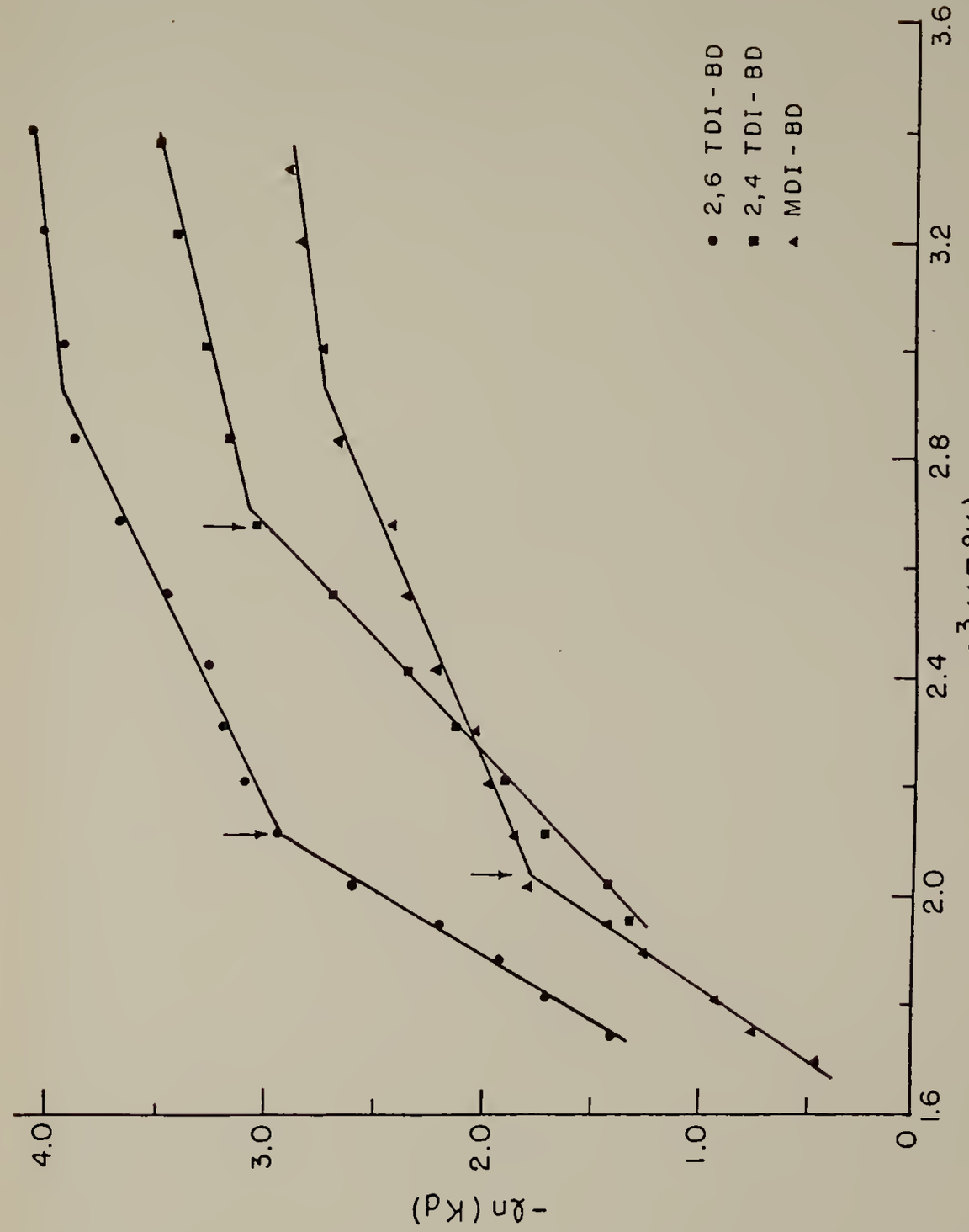

Fig. 5-9. Temperature variation of the hydrogen bonding equilibrium constant in model hard segment compounds.

Table 5-4

Enthapy of Hydrogen Bond Dissociation for Model Hard Segment Compounds

Sample	Onset Temperature (°C)	ΔH, kcal/mole NH
2,4-TDI-BD	100	4.6
2,6-TDI-BD	200	8.4
MDI-BD	220	7.5

measure of the strength of the hydrogen bond. With increasing hydrogen bond strength, the X-Y distance (R), measured in the solid state by x-ray crystallography, decreases and this decrease is usually accompanied by an increase in the difference between the bonded X-H stretching frequency and nonbonded X-H stretching frequency. In fact, a linear relationship between $\Delta\nu$ and R has been established for a number of hydrogen bonds of different types (5). For the NH--O hydrogen bond, bond distances were found to be in the range of 2.84-3.10 Å with corresponding $\Delta\nu$ between 170 and 60 cm^{-1} (6). Based on these average values of $\Delta\nu$ and R, Pimentel et al. have derived the following equation:

$$\Delta\nu = 0.548 \cdot 10^3(3.21 - R) \qquad (5\text{-}3)$$

describing a linear relationship between these two properties. Their data are reasonably consistent with that of Nakamoto, Margoshes and Rundle (7) and Lord and Merrifield (5). Changes in the average NH---O bond distance is also believed to be repsonsible for intensity variation of the N-H absorption band (23), while the considerable breadth beyond the inherent width is attributed to the presence of a very large number of differently hydrogen bonded species with a wide range of NH---O distances (24).

The spectral properties, $\Delta\nu$, $\Delta\nu_{1/2}$, and B have been examined here for the hydrogen bonded system N-H---O=C in three hard segment copolymers. Prior to annealing, these spectral features are nearly indistinguishable. Here the hydrogen bonds assume a wide distribution of lengths and

random orientation caused by structural disorder within the system. As shown in the DSC scans, all materials exhibit a well defined glass transition below 100°C, a further indication of their highly amorphous nature.

After annealing, the spectral properties of the N-H absorption band as well as DSC behavior vary markedly among the three related polymers. Differences in behavior are attributed to differences in the packing of the structural units. In 2,4-TDI-BD, asymmetric placement of the isocyanate residues with respect to the methyl group can result in head to tail isomerization within the repeat units. Variations in the orientation of these units causes immutable chain defects and consequently a noncrystallizable polymer. Thus annealing has no effect on the organization as evidenced by DSC or on the hydrogen bonding properties as shown by infrared. This behavior is consistent with that observed in the corresponding segmented polyurethane materials (25).

For 2,6-TDI-BD and to a lesser degree MDI-BD, changes in $\Delta\nu$, $\Delta\nu 1/2$, and B values show that hydrogen bonding properties of the urethane group are markedly affected by annealing. The decrease in the bonded N-H and C=O stretching frequency and the slight increase in Amide II and V vibrations indicate that the NH---O bond is significantly stronger following annealing. This presumably results from reorganization of the chains involving a shortening of the hydrogen bond. This change in bond distance would also be expected to alter the electronic charge distribution of the hydrogen bond and, therefore, the intensity (the intensity being proportional to the square of the change in dipole moment with

respect to the vibration). Using Equation 5-1 presented earlier, $\Delta\nu$ in 2,6-TDI-BD and MDI-BD corresponds to an average NH---O bond distance of 2.90 and 3.02 Å, respectively. These predicted values lie very close to those obtained by x-ray analysis on model hard segment compounds based on MDI-bismethylurethane (26,27). Here it was shown that MDI-urethanes can be formed in various modifications which differ by the type of hydrogen bond present. One modification consisted of strong hydrogen bonds, having a NH---O bond distance of 2.89 Å, while the other modification consisted of molecules bound by weak hydrogen bonds (2.99 Å). Although no detailed spectroscopic analysis has been carried out for these materials, the frequencies of the bonded components occurred at 3275 and 3325 cm^{-1}, respectively. While these frequencies and bond lengths are in good agreement with those obtained in this present study, additional experimental data using x-ray methods are needed to check $\Delta\nu$ - R correlation further for these materials. It is worth mentioning that the frequency of the bonded N-H component in 2,4-TDI-BD corresponds to a N-H---O bond distance of 2.96 Å. However, it should be recognized that the distribution of bond lengths is far greater in this amorphous system and therefore this value represents only a crude estimate.

An obvious explanation of the narrowness of the N-H band in 2,6 TDI-BD and MDI-BD after annealing is that the degrees of freedom normally responsible for the width have been "frozen out". That these degrees of freedom are not merely low frequency modes interacting in sum and difference combinations is indicated by the symmetrical narrowing. As in 2,4-TDI-BD, a wide variety of conformations having a range of

frequencies (associated with a range of NH---O distances) are possible in the amorphous 2,6-TDI-BD and MDI-BD solution cast samples. However, annealing and subsequent crystallization of these latter materials leads to homogenization of the hydrogen bonds. This process, as previously mentioned, is not accompanied by a change in the number of bonded N-H groups. The constancy in the degree of hydrogen bonding suggests that the hydrogen bonds assume a preferred length after annealing and that this is associated with the existence of a single conformation of the chain in the crystalline phase. This line of reasoning may also be applied to the corresponding segmented polyurethanes where hydrogen bonding occurs not only in the amorphous hard segment regions but also in the soft segment phase. In this case annealing also results in hard segment crystallization which in turn leads to improved phase separation with less interphase hydrogen bonding.

These spectral changes outlined above for 2,6-TDI-BD and MDI-BD are consistent with the thermal transition behavior observed by DSC. It will be recalled that the transition at about 90°C is obvious only in the initial solution cast samples. Apparently the non-crystalline domain structure converts to the crystalline state during annealing and gives rise to well defined high temperature transitions. Furthermore, after annealing these endotherms increase in magnitude and are shifted to higher temperature. It has been suggested that changes in the shape, size, and position of the melting peak are indicative of changes in the crystallite size and in the perfection of the hard segment structure (28,29). Since the packing of molecules is largely influenced by

hydrogen bonding (30), it is not surprising that changes in the hydrogen bonding properties are also observed. The increase in the melting temperature is consistent with the extra strength contributed by stronger, more uniformly distributed hydrogen bonds and possibly larger crystal size. As previously noted, the melting areas increase in an analogous way to the hydrogen bonding properties as a function of annealing time. This may also imply a certain contribution of hydrogen bond dissociation to the observed DSC curve. The more pronounced changes observed in 2,6-TDI-BD both by infrared and DSC are presumably a result of its smaller size and ease with which it crystallizes compared to the MDI-BD polymer.

The temperature dependence of hydrogen bonding in these polymers is also in accord with the above analysis. In 2,4-TDI-BD hydrogen bond dissociation occurs above Tg. It seems reasonable that the onset of segmental motion at Tg will allow a temperature dependent equilibrium to be established between free and hydrogen bonded N-H groups in this amorphous polymer. While some dissociation of the bonded N-H groups (<15%) occurs in the vicinity of Tg for 2,6-TDI-BD and MDI-BD, it is not until the melting point of the polymer is reached that the hydrogen bonding equilibrium is established. Any dissociation prior to melting may represent the disruption of weaker hydrogen bonds which possibly reside in the less ordered and amorphous regions.

It is also to be noted that ΔH, the enthalpy of hydrogen bond dissociation, is significantly higher in 2,6-TDI-BD and MDI-BD than in 2,4-TDI-BD. The results again suggest that stronger hydrogen bonds occur in the ordered crystalline region.

Conclusions

Changes in the frequency, band width and intensity of the bonded N-H absorption band following heat treatment have been studied in three model hard segment polymers and correlated to structural changes as evidenced by DSC. Variations in behavior among the three compounds is attributed to differences in packing and the ability and ease at which crystallization and/or regorganization of the repeat units occur. Annealing of 2,6-TDI-BD and MDI-BD results in a change in distribution towards stronger hydrogen bonds as measured by $\Delta\nu$ and corresponding increase in the melting temperatures. The half width and intensity of the N-H stretching band also show a strong dependence on annealing time as does the shape and size of the melting endotherms; they narrow and become more intense with longer annealing times. This indicates a uniformity in hydrogen bonds as well as in structure. The insensitivity of the 2,4-TDI-BD copolymer to thermal treatment is the result of poorer hard segment organization and inability to crystallize. Estimates of NH---O bond distances obtained from $\Delta\nu$-R correlation are in the range of 2.90-3.02 Å, in reasonable agreement with x-ray studies on urethane model compounds. The temperature dependence of hydrogen bonding shows transitions corresponding to Tg in all three polymers and to Tm in 2,6-TDI-BD and MDI-BD. The higher values of ΔH in the latter materials is also consistent with the increased strength of the hydrogen bonds and the higher degree of order present.

The present spectroscopic results on hard segment copolymer are also significant with work relating to corresponding polyurethane

elastomers. It is hoped that in these materials the detailed investigation of the positions and shapes of bands which are sensitive to the environment of the urethane group, i.e. the N-H stretching frequency near 3300 cm^{-1}, the amide I near 1700 cm^{-1}, the amide II near 1550 cm^{-1} and the N-H out of plane deformation near 700 cm^{-1} will lead to important structural and chemical information.

References

1. R.W. Seymour, G.M. Estes and S.L. Cooper, Macromol., 3, 579 (1970).
2. R. Bonart, J. Macromol. Sci., B2(1), 115 (1968).
3. R. Bonart, L. Morbitzer and G. Hentze, J. Macromol. Sci.-Phys., B3(2), 337 (1969).
4. R.M. Badger and S.H. Bauer, J. Chem. Phys., 5, 839 (1937).
5. R.C. Lord and R.E. Merrifield, J. Chem. Phys., 21, 166 (1953).
6. G.C. Pimentel and C.H. Sederholm, J. Chem. Phys., 24, 639 (1956).
7. K. Nakamoto, M. Margoshes and R.E. Rundle, J. Am. Chem. Soc., 77, 6480 (1955).
8. G.A. Senich, Ph.D. Dissertation, University of Massachusetts (1979).
9. D.S. Huh and S.L. Cooper, Polym. Eng. Sci., 11, 369 (1971).
10. D. Lyman, J. Polym. Sci., 45, 49 (1960).
11. A.L. Chang and E.L. Thomas, Adv. Chem. Ser., 176 (1979).
12. R.G. Snyder and J.H. Schachtschneider, Spectrochim. Acta, 19, 85 (1963).
13. W.J. MacKnight and M. Yang, J. Polym. Sci. C., 42, 817 (1973).
14. T. Tanaka, T. Yokoyama and Y. Yamaguchi, J. Polym. Sci., 6, 2137 (1968).
15. C.S. Paik Sung and N.S. Schneider, Macromol., 10, 452 (1977).
16. G.A. Senich and W.J. MacKnight, Adv. Chem. Ser., 176 (1979).
17. J.L. Illinger, N.S. Schneider and F.E. Karasz, Polym. Eng. Sci., 12, 25 (1972).
18. V.W. Srichatrapimuk and S.L. Cooper, J. Macromol. Sci.-Phys., B15(2), 267 (1978).

19. G.A. Senich and W.J. MacKnight, Macromol., 13, 106 (1980).

20. K. Nakayama, T. Ino and I. Matsubara, J. Macromol. Sci.-Chem., A3(5), 1005 (1969).

21. G.M. Estes, R.W. Seymour and S.L. Cooper, Macromol., 4, 452 (1971).

22. H. Ishihara, I. Kimura, K. Saito and H. Ono, J. Macromol. Sci.-Phys., B10(4), 591 (1974).

23. J.N. Finch and E.R. Lippincott, J. Phys. chem., 61, 921 (1957).

24. T.T. Wall and D.F. Hornig, J. Chem. Phys., 43, 2079 (1965).

25. N.S. Schneider, C.S. Paik Sung, R.W. Matton and J.L. Illinger, Macromol., 8 62 (1975).

26. K.H. Gardner and J. Blackwell, Polymer, 20, 13 (1979).

27. J. Hocker and L. Born, J. Polym. Sci.-Polym. Letters Ed., 17, 723 (1979).

28. T.R. Hesketh, J.W.C. van Bogart and S.L. Cooper, Polym. Eng. Sci., 20, 190 (1980).

29. L. Mandelkern, "Crystallization of Polymers", McGraw-Hill Inc., New York (1964).

30. G.C. Pimentel and A.L. McClellan, "The Hydrogen Bond", W.H. Freeman and Co., San Francisco (1960).

CHAPTER VI

INFRARED THERMAL ANALYSIS OF POLYBUTADIENE-POLYURETHANES

Introduction

In previous chapters, the thermal transition and relaxation behavior of HTPBD polyurethanes based on 2,4-TDI and 2,6-TDI have been reported. Irrespective of the hard segment structure, a high degree of phase segregation occurs as indicated by the low and compositionally insensitive soft segment Tg.

One method for quantitatively assessing the degree of phase segregation in segmented polyurethanes relies on the resolution of the NH and carbonyl absorption bands into their bonded and nonbonded components using infrared spectroscopy. Studies of a series of MDI polyurethanes by Seymour and coworkers (1) have shown that virtually all NH groups were hydrogen bonded but that only 60 percent of the urethane carbonyl groups participated in hydrogen bond formation. They suggested that the NH groups also hydrogen bond to the soft segment at the interface of the phase segregated structure or to the soft segment itself due to incomplete phase segregation. Similarly, in 2,6- and 2,4-TDI polyether urethanes (2), Sung and Schneider found that 95 percent of the NH groups were hydrogen bonded at room temperature but that only 80 and 50 percent of the carbonyl groups were similarly associated in the 2,6-TDI and 2,4-TDI polyurethanes, respectively. The greater degree of urethane to ether hydrogen bonding was also attributed to extensive hard segment

mixing with the soft segment phase. In subsequent temperature studies (3), they showed that bonded carbonyl in 2,4-TDI polyurethanes underwent little change to temperatures in excess of 150°C while 50 percent of NH groups had dissociated. It was concluded that NH to ether hydrogen bonding was responsible for most of the hydrogen bond dissociation in the NH spectra. In 2,6-TDI polymers, this hard segment-soft segment hydrogen bonding was also found to dissociate below 50°C. However, above 60°C dissociation of hydrogen bonding in the hard segments occurs, as indicated by the decrease in the bonded carbonyl band. It was suggested that hard segment-soft segment hydrogen bonding, being weaker than interurethane bonding does not require a hard segment transition process. The hydrogen bonding behavior in 2,6-TDI polyurethanes was attributed to more complete phase separation. However, owing to the number of possible acceptor sites in these materials, the observations were at best semiquantitative.

The analysis of the NH stretching vibration, the extent of hydrogen bonding and its temperature dependence by Fourier Transform Infrared (FTIR) spectroscopy is extended to butadiene soft segment polyurethanes. In contrast to previous studies, an accurate representation of the amount of hydrogen bonding in the hard segments and therefore in the extent of microphase segregation can be obtained; the only available proton acceptors are those residing within the hard segments. The absence of interphase hydrogen bonding should also simplify the thermal studies of hydrogen bonding in segmented polyurethanes. The structural implication of the results are discussed in conjunction with other properties studied via differential scanning calorimetry and dynamic

mechanical relaxation. Comparisons are made to model compounds described in Chapter V and to the more typical polyester and polyether polyurethanes.

Experimental

The three series of PBD-polyurethanes used in this study were those based on (Arco R45M)HYPBD-2,4-TDI (series A), (JSR)HTPBD-2,4-TDI (series B) and (JSR)HTPBD-2,6-TDI (series C) and which correspond to samples employed in the various mechanical and thermal studies detailed in Chapters II-IV. Table 6-1 reviews the compositon and thermal transitions of the polymers. All films, between 5-10 μm in thickness, were prepared by compression molding between teflon sheets and were subjected to the same thermal treatment as in the earlier studies.

Infrared spectra (4000-400 cm^{-1}) were recorded with a Nicolet 7199 Fourier Transform Infrared spectrometer by averaging 200 scans at a resolution of 2 cm^{-1}. For the temperature studies, the polymer film was placed between KBr windows in a variable temperature unit (Wilks Model No. 19) connected to the temperature controller (Wilks Model No. 37). Sample temperature was monitored by a copper-constantan thermocouple junction maintained in contact with the sample to ±1°C. The temperature was held constant for about 5 min before collecting spectra. A dry nitrogen flow was maintained throughout the chamber to avoid moisture and oxidation of the sample at higher temperatures. All data was stored on a disk for further analysis.

In the infrared analysis of the NH absorption band, frequencies

Table 6-1

Compositon and Thermal Transitions of PBD-Based Polyurethanes

Sample	Wt. % urethane	Hard Segment Transition Temperatures, °C (DSC) Tg	Tm
Series A 2,4-TDI-BDL-HYPBD (R45M)			
HY-50	26	40,74	
HY-51	37	37,71	
HY-52	43	38,74	
HY-53	48	59,78	
Series B 2,4-TDI-BDL-PBD (JSR)			
JSR-3	25	20	
JSR-4	32	20,55	
JSR-6	42	40,65	
JSR-8	49	74	
JSR-10	55	75	
Series C 2,6-TDI-BDL-PBD (JSR)			
JSR-31	31	64	142
JSR-42	42	60	144
JSR-50	50	63	148

(ν_{NH}) are accurate to ±1 cm^{-1} and widths at half peak height ($\Delta\nu_{1/2}$) to about ±5 cm^{-1}. Integrated intensities have been corrected for sample thickness differences, using the CH_2 stretch near 2950 cm^{-1} as a normalizing factor. Since considerable overlapping of the free and hydrogen bonded NH stretching band exists, values of the fraction of hydrogen bonded NH groups (X_b) were obtained using a curve resolving technique, based on a nonlinear least square analysis for the fitting of a combination of Lorentzian and Gaussian curve shapes. Details of the data analysis have been described in Chapter V. Values of X_b are reliable to within ±1%.

RESULTS

Survey spectra of typical 2,4-TDI and 2,6-TDI polybutadiene polyurethanes are presented in Figure 6-1 and the assignments of vibrational modes are collected in Table 6-2. The spectroscopic features of the bonded NH absorption band, namely the frequency (ν_{NH}), half-width ($\Delta\nu_{1/2}$) and integrated intensity, are comparable in magnitude to those of the corresponding model hard segment compounds described in Chapter V. The major NH absorption of the 2,4-TDI and 2,6-TDI series appears at 3310 and 3280 cm^{-1}, respectively, for the bonded component and that of the free NH, at 3450 cm^{-1}. The spectral parameters relating to this vibration are summarized in Table 6.3

In all series of polyurethanes studied, the fraction of hydrogen bonded NH groups, X_b [calculated from Equation (1) of Chapter V using a

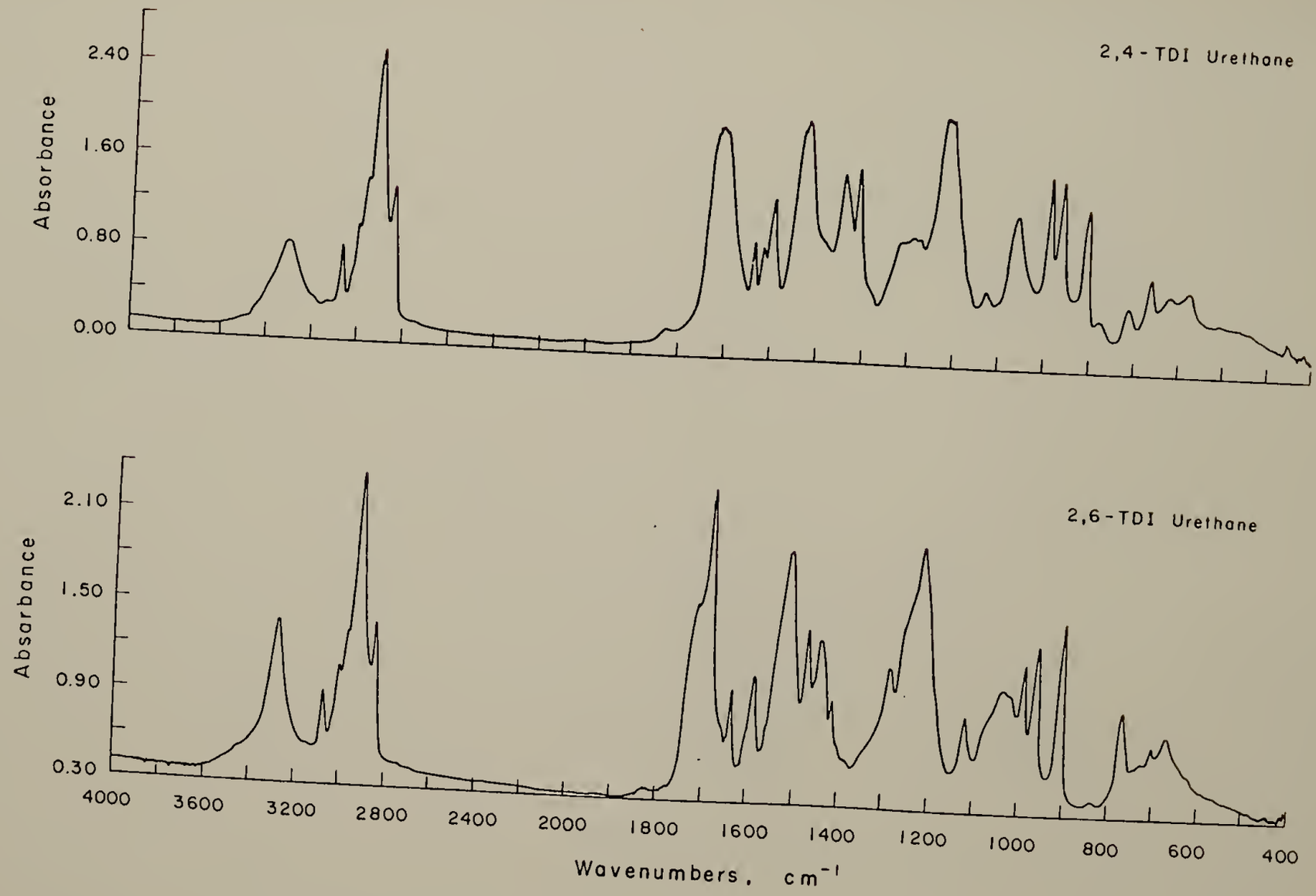

Fig. 6-1. Survey IR spectra of PBD-polyurethanes: (a) 2,4-TDI urethane; (b) 2,6-TDI urethane.

Table 6-2

Infrared Band Assignments for Segmented

Polyurethanes Containing Polybutadiene Soft Segments[a]

Frequency, cm^{-1}	Assignment[b]
3450 (w, sh)	free N-H str
3315-3280 (s)	bonded N-H str
3200 (vw)	trans-bonded N-H str
3130 (vw)	cis-bonded N-H str
2955 (m, sh)	CH_2 asymm. str
2925 (vvs)	CH_2 asymm. str
2855 (vs)	CH_2 symm. str
1735-1695 (vs)	free and bonded C=O str
1600 (m)	C=C str in aromatic group
1535 (vs)	N-H bend + C-N str
1455 (s)	CH_2 bend
1230 (vs)	N-H bend + C-N str
1065 (s)	trans C-C symm str
995 (w)	cis = CH vib
965 (s)	trans = CH out of plane wag
910 (w)	1,2 = CH_2 out of plane def.
816 (w)	C-H out of plane bend
720 (w)	-C-O- out of plane bend
721 (w)	CH_2 out of phase rock

[a]Key: s=strong; m=medium; w=weak; sh=shoulder; v=very.

[b]Ref.:Tanaka (4), Nakayama (5), Ishihara (6), Hsu (7), Binder (8).

Table 6-3

Spectral Properties of the NH Absorption Band in PBD-Polyurethanes

Sample	$\nu(cm^{-1})$	$\Delta\nu_{1/2}(cm^{-1})$	I[a]	Fraction of hydrogen bonded NH, X_b
Series A				
HY-50	3313	111	.450	.84
HY-51	3314	113	.476	.84
HY-52	3312	111	.466	.86
HY-53	3312	114	.428	.87
Series B				
JSR-3	3315	113	.462	.83
JSR-4	3314	115	.495	.82
JSR-6	3314	112	.491	.82
JSR-8	3311	111	.507	.84
JSR-10	3312	112	.512	.87
Series C				
JSR-31	3279	70	.89	.86
JSR-42	3278	68	1.10	.89
JSR-50	3278	67	1.25	.89

[a]Normalized Integrated Intensity

k value of 3.46] is found to be in range of 80-90 percent at room temperature. X_b for the 2,4-TDI series shows only a small increase over the full range of TDI concentration. In the 2,6-TDI series, no measureable change with composition is observed. Although this study has focused primarily on the NH stretching vibration, comparable amounts of hydrogen bonded carbonyl groups are also found (9). This indicates that the alkoxyl oxygen in the urethane accounts for less than 10 percent of the NH association in these PBD polyurethanes, in good agreement with earlier studies (2).

The infrared spectra collected at various temperatures were used to study the temperature variation of hydrogen bonding in these materials. Figures 6-2 and 6-3 show plots of X_b versus temperature for typical members of all three series of polyurethanes. At low hard segment concentrations, X_b shows approximately linear decreases with temperature in both series of 2,4-TDI samples. However, above a 35-40 weight percent hard segment, the onset of hydrogen bond dissociation, as noted by the transition in the slope, occurs around 70 to 80°C (see Table 6-4). For the 2,6-TDI series, most of the dissociation takes place at temperatures of about 125-135°C. It is noted that in all samples studied, a considerable amount of hydrogen bonding (~40-50 percent) still exists at temperatures as high as 200°C.

The dissociation of hydrogen-bonded NH groups follows an equilibrium process governed by Equation (2) of Chapter V. Plots of $-\ln(K_a)$ versus inverse temperature for these polymers are presented in Figures 6-4 and 6-5. The heats of hydrogen bond dissociation, ΔH, are

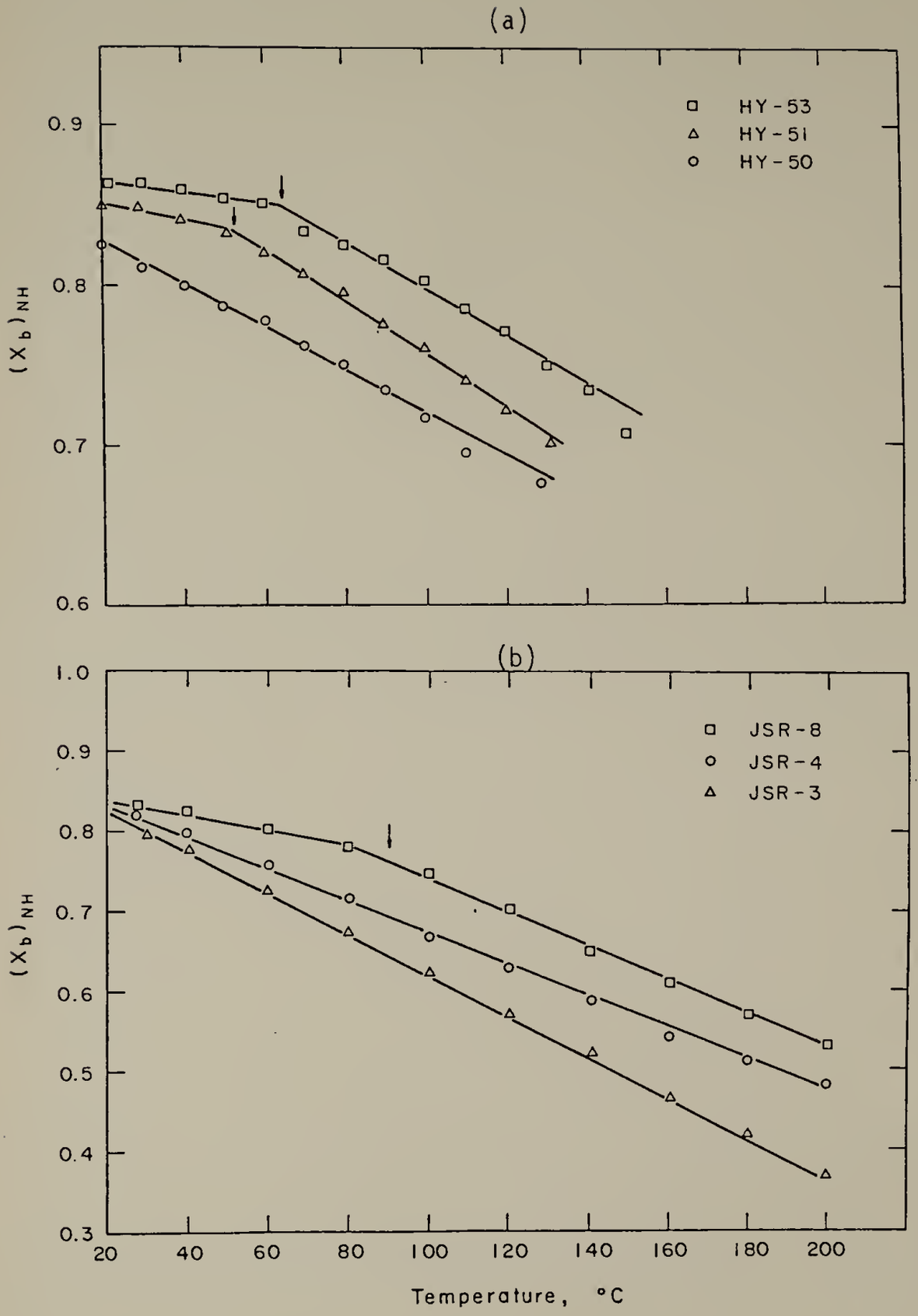

Fig. 6-2. Fraction of hydrogen-bonded NH (X_b) vs. temperature for (a) HYPBD-2,4-TDI and (b) HTPBD-2,4-TDI polyurethanes.

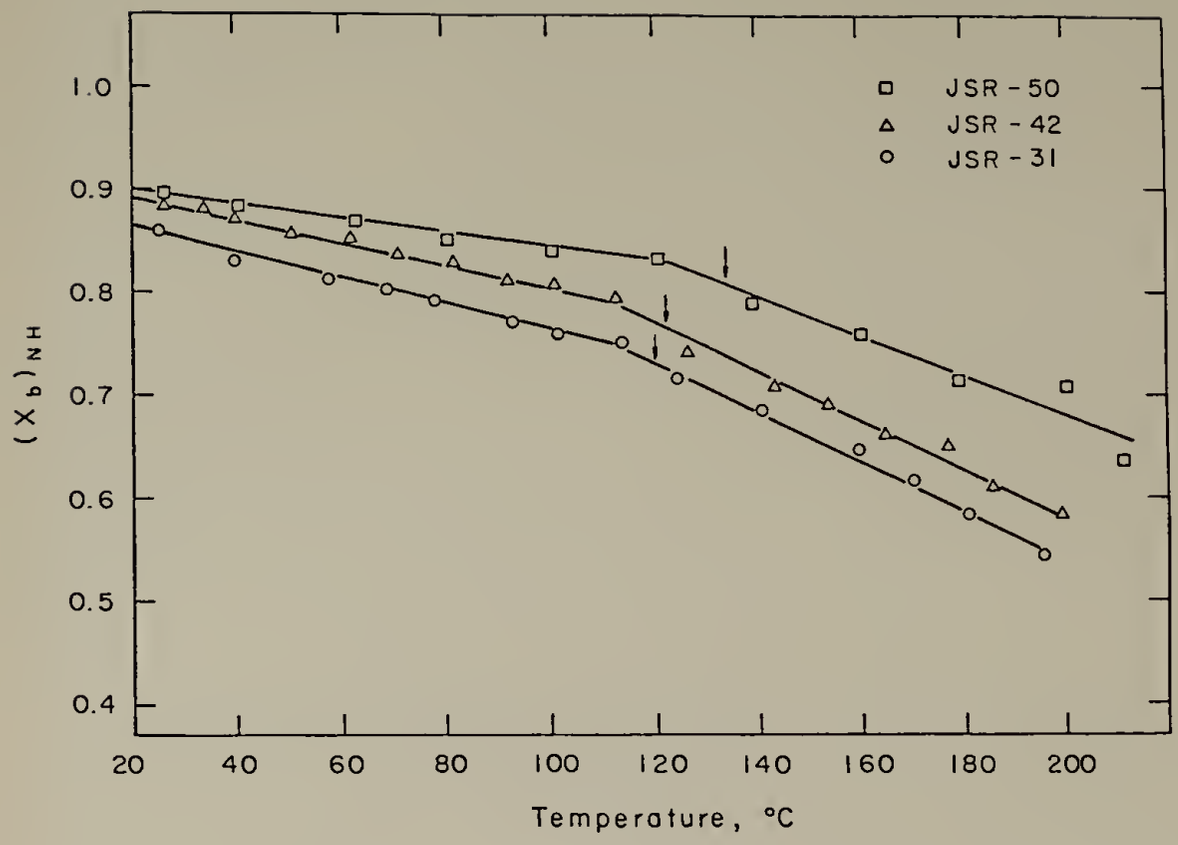

Fig. 6-3. Fraction of hydrogen-bonded NH (X_b) vs. temperature for HTPBD-2,6-TDI polyurethanes.

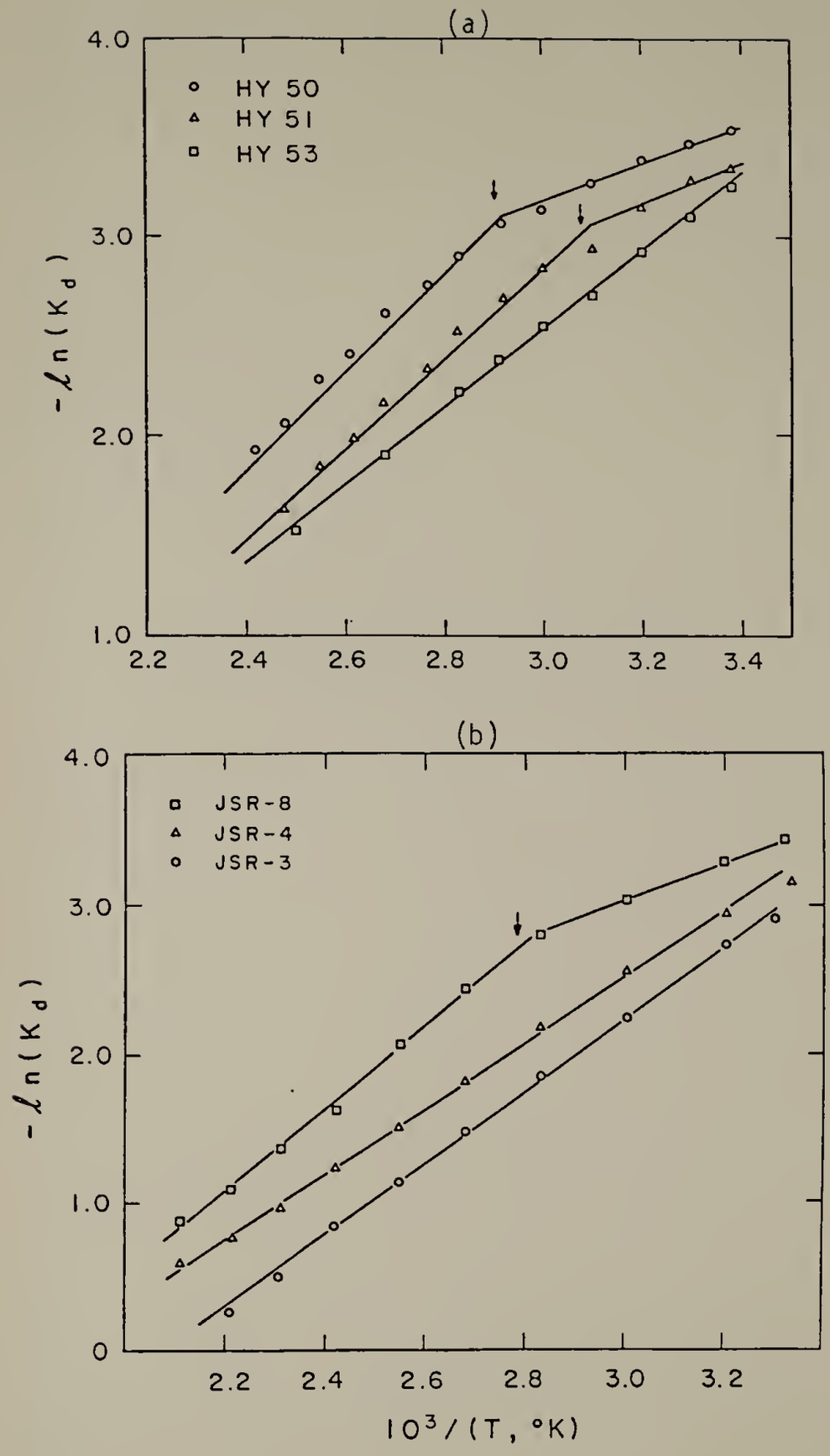

Fig. 6-4. Temperature variation of the hydrogen bonding equilibrium constant in (a) HYPBD-2,4-TDI and (b) HTPBD-2,4-TDI polyurethanes.

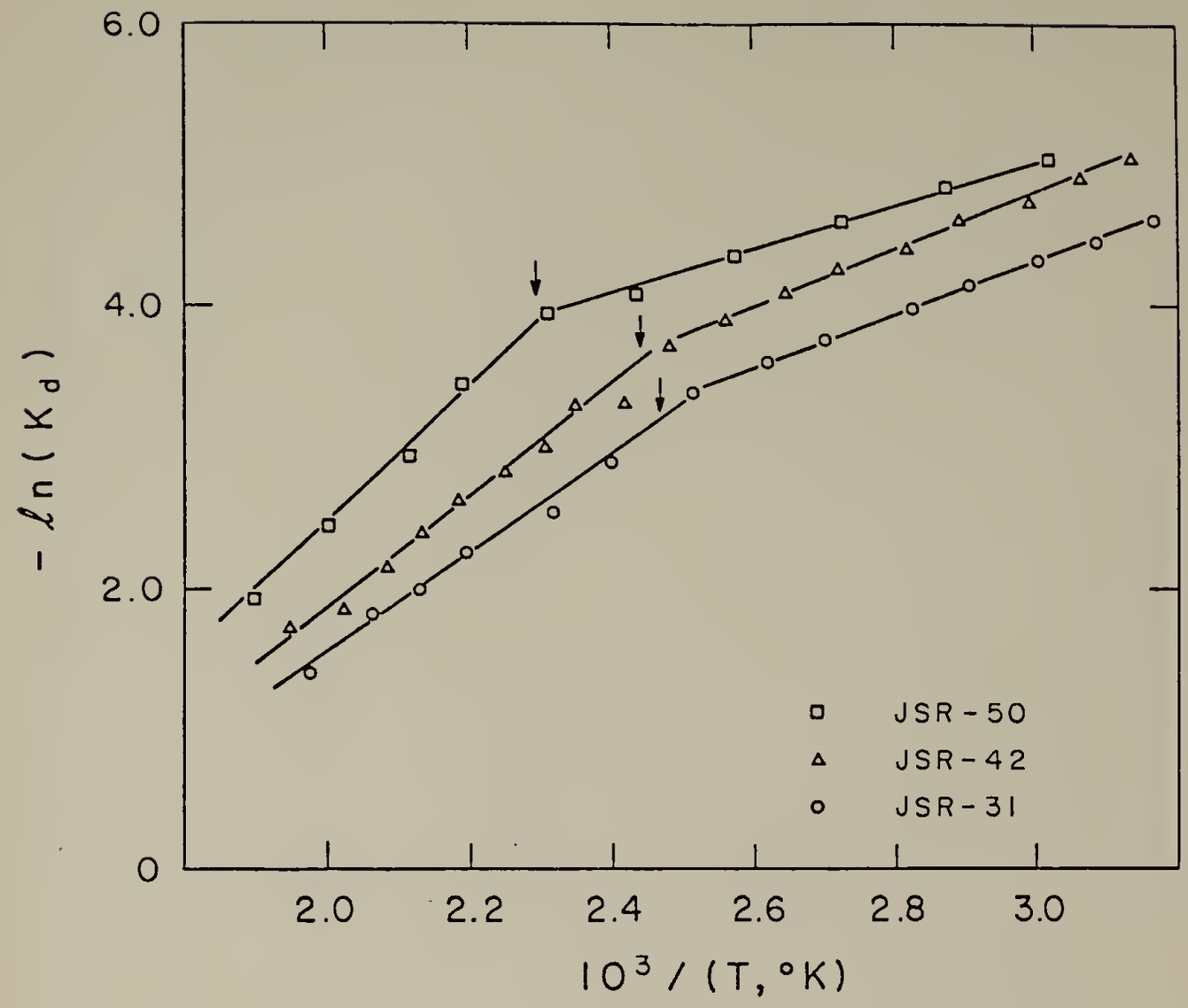

Fig. 6-5. Temperature variation of the hydrogen bonding equilibruim constant in HTPBD-2,6-TDI polyurethanes.

Table 6-4

The Onset Temperature and Enthapy of

Hydrogen Bond Dissociation in PBD-Polyurethanes

Sample	Onset temp., °C	ΔH, kcal/mole NH
Series A		
HY-50	27	3.5
HY-51	40	4.4
HY-52	70	4.3
HY-53	76	4.7
Series B		
JSR-3	28	4.7
JSR-4	27	4.4
JSR-6	30	4.4
JSR-8	75	4.8
JSR-10	75	4.8
Series C		
JSR-31	125	7.0 (4.0)[b]
JSR-32	123	7.5 (3.5)
JSR-50	133	7.6 (4.2)

[b] ΔH calculated below Tm.

then calculated from the slope of the line above the onset temperatures. It is noted that similar transitions appear in these plots as in the X_b versus temperature curves. A least squares fit to the 95% confidence level gave ΔH values of about 4-5 kcal/mole for the 2,4-TDI series and about 7-8 kcal/mole ±1% for the 2,6-TDI samples (Table 6-4). While the ΔH's are essentially independent of urethane concentration in the former series and comparable to ΔH of the 2,4-TDI/BDL homopolymer (4.6 kcal/mole), ΔH in the 2,6-TDI samples increases with urethane concentration. These values, however, are still lower than that of the corresponding 2,6-TDI/BDL homopolymer.

The temperature dependence of the frequency and half-width of the bonded NH absorption are shown in Figures 6-6 and 6-7. In 2,4-TDI polymer, ν_{NH} increases linearly with temperature, $d\nu/dT \simeq 0.2$ cm^{-1}/deg over the entire temperature range. Although the contour of the band changes with increasing temperature, in particular, the high frequency side, there is no detectable change within experimental error in the half-widths of the resolved peak. Apparently, the variety of configurations which is normally responsible for the band width is sufficiently complex at room temperture that no further change is observed on heating. In the 2,6-TDI series, both $d\nu/dT$ and $d\nu_{1/2}/dT \simeq .15$ cm^{-1}/deg below and above tempertures of about 120-130°C, the change in the half-width with temperature being slightly greater. The transitions observed in these spectral properties are consistent with those reported earlier in the temperature dependence of X_b.

The effects of thermal history on the NH absorption band are

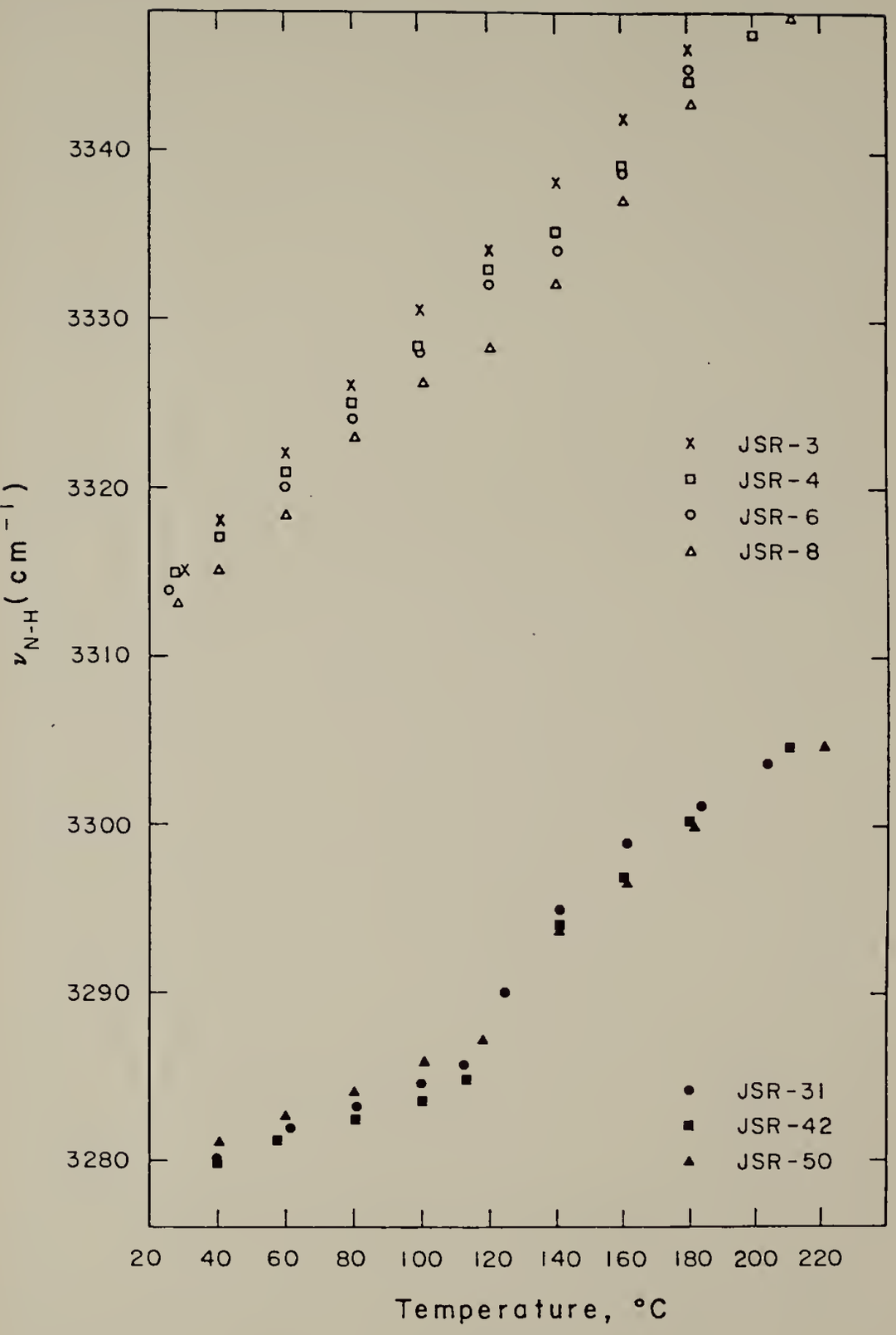

Fig. 6-6. Temperature dependence of the frequency (cm^{-1}) of the hydrogen bonded NH in 2,4-TDI and 2,6-TDI polyurethanes.

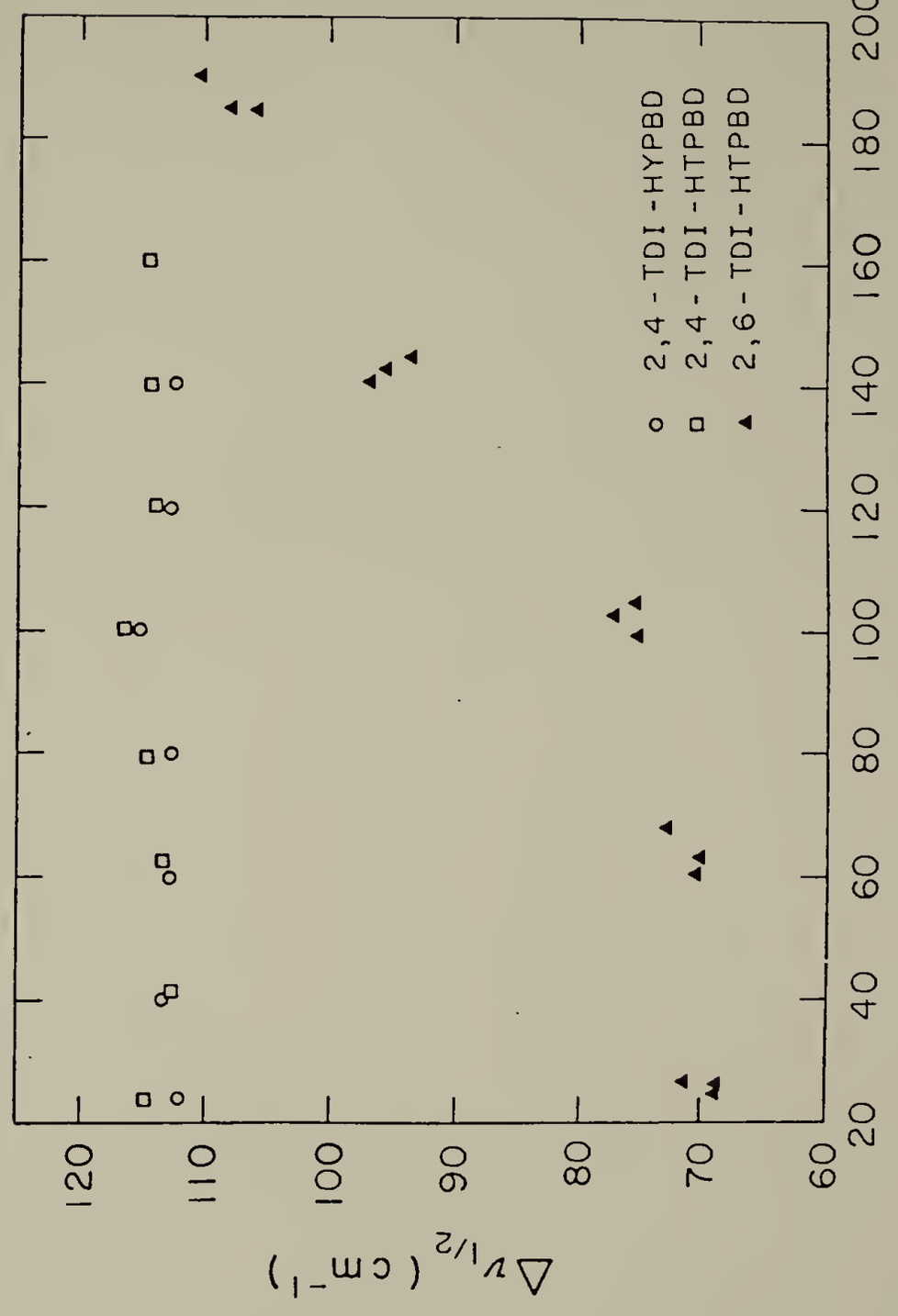

Fig. 6-7. Temperature dependence of the half-width (cm^{-1}) of the hydrogen bonded NH in 2,4-TDI and 2,6-TDI polyurethanes.

illustrated in Figure 6-8 and summarized in Table 6-5 for a representative 2,4- and 2,6-TDI polyurethane. Cooling from 250°C to room temperature produces negligible change in the infrared spectrum of the 2,4-TDI polymer when compared to the original spectrum before heating. In contrast, the spectral properties of the NH stretch in the 2,6-TDI polymer are markedly altered following the initial heating. Not only is there a significant decrease in the normalized intensity (ca. 60%) but the frequency increases 12 cm^{-1} and the half-width 40 cm^{-1}, relative to the control. On annealing at 140°C, however, the original spectroscopic features are restored. It is noted that similar changes are observed in the carbonyl region (1730-1690 cm^{-1}), though less pronounced.

Discussion

Before discussing the temperature dependence of hydrogen bonding in these PBD-polyurethanes and its structural implications, it is worthwhile to compare the spectroscopic features of the NH absorption band with those of the corresponding model hard segment compounds described in Chapter V. As in the 2,6- and 2,4-TDI/BDL homopolymers, the NH---O bond, as measured by $\Delta\nu$ (as well as ΔH), is considerably stronger in the 2,6-TDI polymers as compared to the 2,4-TDI polymers, both series of 2,4-TDI being approximately the same. Moreover, the half-widths in the 2,6-TDI series are narrower by some 40-50 cm^{-1}, but are increased (ca. 10 cm^{-1}) relative to the homopolymer. Comparable values of $\Delta\nu_{1/2}$ (110-115 cm^{-1}) are obtained for the 2,4-TDI systems as

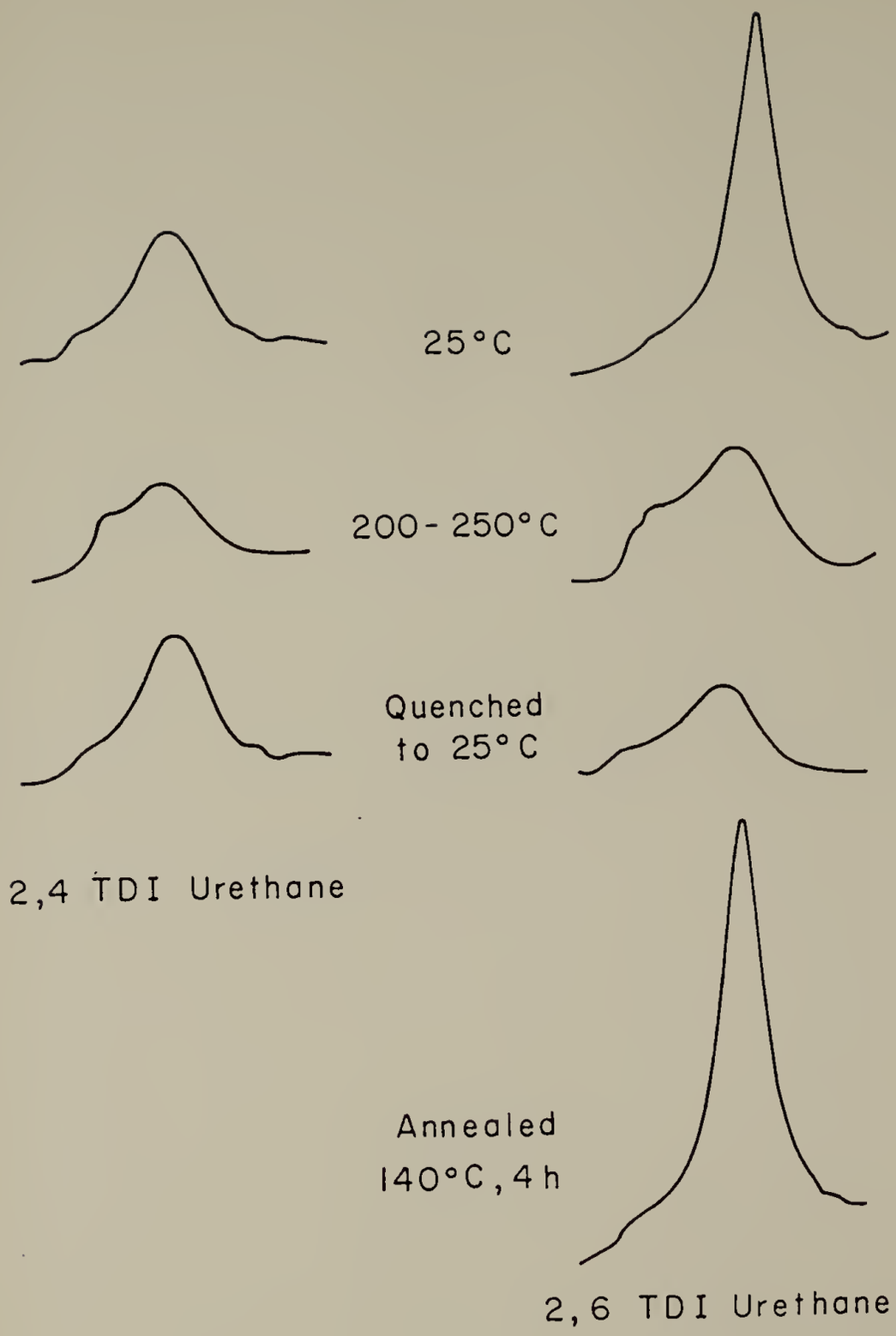

Fig. 6-8. Effects of thermal history on the NH absorption band in 2,4-TDI and 2,6-TDI polyurethanes.

Table 6-5

Effects of Thermal History on the NH Absorbtion Band

	2,4 TDI-PBD (HY-51)		2,6 TDI-PBD (JSR-42)		
	Control	Quenched to R.T.	Control	Quenched to R.T.	Annealed 140°C 4h
X_b	.87	.86	.89	.84	.91
ν_{NH} (cm^{-1})	3312	3312	3279	3295	3277
$\Delta\nu_{1/2}$ (cm^{-1})	110	112	64	100	60
Normalized Integrated Intensity	.301	.299	.407	.154	.426

compared to the corresponding 2,4-TDI/BDL compound. Borrowing from the concepts developed earlier in Chapter V, the considerable breadth of the NH absorption band in the 2,4-TDI polyurethanes can be attributed to the wide distribution of hydrogen bond lengths and random orientation caused by structural disorder within the system. The crystalline nature of the hard segments in the 2,6-TDI polyurethanes, however, results in uniformity of the hydrogen bonds and concomitant decrease in the bond length. The small but measurable increase in $\Delta\nu_{1/2}$ in these polymers relative to the homopolymer is probably due to the lower degree of order in the hard segment domains. This was also evident in DSC studied whereby the melting points and corresponding heats of fusion of these polymers were found to be lower than that of the pure 2,6-TDI/BDL.

As indicated in Table 6-3, all polymers are hydrogen bonded to the extent of 80-90 percent, regardless of whether they are semi-crystalline, i.e. 2,6-TDI polymer, or amorphous and crosslinked, i.e. 2,4-TDI polymers. Moreover, these values are comparable to those obtained in the corresponding TDI/BDL homopolymers. Since hydrogen bonding interactions are restricted to the hard segment components in PBD-polyurethanes, the high values of X_b support earlier conclusions based on DSC and dynamic mechanical measurements that the hard segment phase is relatively free of intermixed soft segments. This behavior may be contrasted to similar systems based on polyether soft segments (3). Here it was shown that the extent of interurethane hydrogen bonding was 30 percent higher in the 2,6-TDI than the corresponding 2,4-TDI polymers. These effects are undoubtedly attributed to the increased

tendency of hydrogen bond formation with the soft segment phase in the latter materials. It should also be mentioned that the above analysis does not differentiate between hydrogen bonded groups occurring within the hard segment domains and those at the interface between the phase segregated structure. It is likely that the occurrence of the latter would be appreciable in those materials of lower hard segment content and shorter hard segment lengths.

The temperature dependence of the NH absorption band will now be considered. In both series of 2,4-TDI polyurethanes and above a 35-40 weight percent hard segment, transitions in the X_b versus temperature curves [which are confirmed by the transitions in the $-(\ln K_d)$ versus 1/T plots] correlate well with the hard segment glass transition temperatures, as evidenced by DSC (Table 6-1). Consequently, the onset of segmental motion at Tg causes an acceleration of NH hydrogen bond dissociation at or above this temperature. The lower hard segments show only a continuous decrease in hydrogen bonding. This, too, is probably a consequence of the low values of the hard segment Tg's (in the range of 20-40°C) and dissociation at the interface which is not likely to be restricted by the glass transition. Since the degree of phase separation as measured by X_b is nearly complete and essentially independent of hard segment concentration, the higher transition temperatures observed in the higher hard segment materials may be attributed to a more stable hydrogen bonding system which occurs with increasing hard segment length and consequent improvement in the domain structure. The ΔH values calculated for the 2,4-TDI polyurethanes are within a reasonable range

to the value of 4.6 kcal/mole reported earlier for the TDI/BDL homopolymer and slightly higher than those found in the literature for similar systems based on polyether soft segments (2). Dissociation involving interphase hydrogen bonds occurs to the extent of 30 percent or more in these latter [illegible] account for the differences, the NH to [illegible] than interurethane bonding (3,10).

All polymers [illegible]

X_p versus temp[illegible]

[illegible]

hyd[illegible]

These ΔH values [illegible] concentration, ranging [illegible] material to 8.6 kcal/mole for the pure 2,6-TDI/BDL homopolymer. Consistent with DSC results, this again can be attributed to an increase in the perfection of the hard segment domains as the hard segment length (or content) increases.

Quite different results were reported by Sung and Schneider in a series of 2,6-TDI polyurethanes based on polyether soft segments (3). They found that the onset temperature for hydrogen bond dissociation occurs between 60 and 65°C, independent of urethane content and well

below the melting temperature of the crystalline hard segment structure. Values of ΔH were reported to be about 4 kcal/mole, close to those found in the corresponding amorphous 2,4-TDI series. These authors concluded that the thermal behavior of hydrogen bonding is independent of structure organization. More recently, Senich found that the temperature depencence of hydrogen bonded groups is without any discontinuity in a similar 2,6-TDI polyurethane and reported a value of 6.8 kcal/mole for ΔH (11).

Many of the discrepancies concerning the thermal behaivor of hydrogen bonding in 2,6-TDI polyurethanes can be accounted for by considering the nature of the hard segment structure. Unlike 2,4-TDI, the hard segments in 2,6-TDI polyurethanes are susceptible to crystallization. Therefore, the method of sample preparation and thermal history are likely to be determinants of the resultant morphology, and hence, hydrogen bonding properties. In contrast to this present study whereby films were compression molded and subjected to the same thermal treatment as those employed in the various thermal and mechanical studies, most previous IR studies were performed on samples prepared by solution casting. As shown by Chang et al. in a series of MDI-based polyurethanes (12), solution cast materials generally exhibit lower melting points and heats of fusion compared to the as-polymerized samples. Moreover, in Chapter V, it was found that solution cast 2,6-TDI/BDL homopolymer shows a distinct glass transition (ca. 90°C) and only until high annealing times and temperatures were employed did a well defined melting endotherm appear. Differences in sample morphology would certainly account for

the low ΔH values and onset temperatures which, incidently, fall in close line with the hard segment Tg in 2,6-TDI polyurethanes (13) as well as the considerable amount of dissociation (>50%) below Tm in earlier studies.

The above discussion raises another point concerning hydrogen bond dissociation in 2,6-TDI polyurethanes, or more generally, in semi-crystalline polymers. If the hypothesis is correct that these 2,6-TDI polymers based on PBD soft segment are three phase in nature without any significant interpenetration (as evidenced by the compositon invariant soft and hard segment Tg and higher melting endotherms, Chapter IV), it seems likely that below the melting point of the polymer a temperature dependent equilibrium between the free and bonded NH groups could be established in the amorphous hard phase. Presumably, this would involve dissociation of the weaker, distorted hydrogen bonds. Above the melting point, equilibrium between the free and bonded NH group is again established, involving the dissociation of stronger and more uniform hydrogen bonds which reside within the crystalline domains. As indicated earlier, the ΔH values corresponding to the dissociation of these bonds in the 2,6-TDI polymers are in the range of 7-8 kcal/mole; values calculated below the Tm transition are between 3.5 and 4.5 kcal/mole, comparble to those reported in the 2,4-TDI series (see Table 6-4). The occurence of two dissociation processes was also noted in an earlier study based on nonsegmented polyurethanes (14) as well as in the model hard segment compounds (Chapter V), thus supporting earlier conclusions on the two-phase nature of the hard segments in PBD-polyurethanes.

While the overall extent of hydrogen bonded groups in the polymer would remain unchanged, as noted by similarities in X_b for all polymers studied, the relative proportions of these groups residing within the amorphous or crystalline regions will vary depending on sample morphology. This, in turn, will undoubtedly influence the thermal behavior of hydrogen bonding in these (semi)crystalline polyurethanes.

The sensitivitiy of hydrogen bonding to structure organization was also evident in the quenching study. Upon cooling the 2,6-TDI samples to room temperature from 250°C a complete alteration of the NH spectrum is observed. In fact, its spectral features more closely resemble those of the corresponding amorphous 2,4-TDI systems. These effects can be directly attributed to the disruption of the crystalline domains and concomitant decrease in the strength and uniformity of the hydrogen bonds, as measured by $\Delta\nu_{NH}$ and $\Delta\nu_{1/2}$. The disappearance of the melting endotherm (Tm_1) and reduction in room temperture modulus following the initial heating in DSC and rheovibron measurements, respectively, further support these conclusions. As in the DSC study whereby the crystal distribution corresponding to Tm_1 reappears on annealing (140°C, 4h) the spectral features of the NH absorption band are also restored under these same conditions, with only minor variations. The absence of thermal history effects in the 2,4-TDI polymer is also consistent with DSC and dynamic mechanical studies reported earlier.

Conclusions

Resolution of the hydrogen bonded and free NH absorption band indicates that 80-90 percent of the NH groups are bonded at room temperature in 2,4-TDI and 2,6-TDI polyurethanes comprised of PBD soft segments. Since all the hydrogen bonding interactions are restricted to the hard segment domains in these polymers, the high extent of interurethane bonding confirms earlier conclusions by thermal and dynamic mechanical studies that these materials are well phase segregated. Above a 35-40 weight percent hard segment, the temperature dependence of the fraction of hydrogen bonded NH groups exhibits transitons corresponding to Tg in the 2,4-TDI polymers while all polymers in the 2,6-TDI series show transitions corresponding to Tm. The enthapies for hydrogen bond dissociation are found to be around 4 kcal/mole in both 2,4-TDI series and in the 2,6-TDI series below Tm; above Tm, ΔH values are between 7 and 8 kcal/mole. The higher ΔH values in the latter materials is attributed to the increase in perfection of the hard segment domain, which is accompanied by the increase in strength and uniformity of the hydrogen bonds. The strong dependence of the degree of order in the 2,6-TDI polymers on sample preparation and thermal history may account for some of the disagreement in previous studies.

Though the role of hydrogen bonding in determining the physical and mechanical properties remains unclear, it is apparent that hydrogen bonding is sensitive to structure organization, influencing the stability of the hard segment domains in amorphous polyurethanes and, more

obvious, chain packing in crystalline or partially crystalline polyurethanes. Moreover, in certain cases where hydrogen bonding can occur to the soft segment phase, i.e. polyester and polyether polyurethanes, hydrogen bonding can exert a profound role in determining the extent of phase segregation and, therefore, the overall properties of the polymer through its effects on the soft segment glass transition.

References

1. R.W. Seymour, G.M. Estes, and S.L. Cooper, Macromolecules, 3, 579 (1970).
2. C.S. Paik Sung and N.S. Schneider, Macromolecules, 8, 68 (1975).
3. C.S. Paik Sung and N.S. Schneider, Macromolecules, 10, 452 (1977).
4. T. Tanaka, T. Yokoyama, and Y. Yamaguchi, J. Polym. Sci., A-1, 6, 2153 (1968).
5. K. Nakayama, T. Ino, and I. Matsubora, J. Macromol. Sci., Chem., 13, 1005 (1969).
6. H. Ishihara, I. Kimura, K. Saito, and H. Ono, J. Macromol. Sci.-Phys., B10, 511 (1974).
7. C.M. Brunette, S.L. Hsu, W.J. MacKnight, and N.S. Schneider, Polym. Eng. Sci., 21, 163 (1981).
8. J.L. Binder, J. Polym. Sci., A3, 1587 (1965).
9. C.M. Brunette, S.L. Hsu, W.J. MacKnight, and N.S. Schneider, Polym. Eng. Sci., 21, 163 (1981).
10 V.W. Srichatrapimuk and S.L. Cooper, J. Macromol. Sci.,-Phys., B15(2), 267 (1978).
11. G.A. Senich and W.J. MacKnight, Macromolecules, 13, 106 (1980).
12. A.L. Chang and E.L. Thomas, Adv. Chem. Ser., 176 (1979).
13. G.A. Senich and W.J. MacKnight, Adv. Chem. Ser., 176 (1979).
14. W.J. MacKnight and M. Yang, J. Polym. Sci., 42, 817 (1973).

CHAPTER VII

RECOMMENDATIONS FOR FUTURE WORK

An obvious concern in the bulk polymerization of these polybutadiene-polyurethanes is the incompatibility of the HTPBD with other reactants at the outset of the reaction or at an early stage of molecular weight buildup. Incomplete mixing could be a contributing factor in producing a mixture of homopolymer which, incidently, might explain the granular and opaque appearance of these materials, as well as polydispersity in the hard segments. It is evident that more careful attention needs be given to the choice of composition and of reaction conditions. Perhaps some of these problems may be alleviated by carrying out the polymerization in solution.

A study of the hard segment length and distribution would be also of considerable aid in understanding kinetic aspects of the polymerization and micromorphology of the final polymer. A relatively straightforward method would be to selectively cleave the PBD segments, i.e. ozonolysis reaction, while leaving the urethane groups unchanged. The hard block distribution of diisocyanate residues can then be determined by gel permeation chromatography. Other techniques amenable to this type of analysis include high resolution carbon-13 and proton Nuclear Magnetic Resonance Spectroscopy. By treating these polyurethanes as two-phase systems, consisting of alternating hard and soft segments, an accurate determination of the composition and sequence length of the segments can be made. Moreover, it would be interesting to compare the

results with the theoretical calculations of hard segment distributions in block copolymers.

Techniques such as small angle x-ray scattering and diffraction and electron microscopy should provide significant information about the domain morphology, phase segregation, and the disruption of domain structure during deformation, and thus be used to complement DSC, dynamic mechanical, stress-strain, and infrared absorption measurements employed previously in studying PBD-polyurethanes. In addition, the use of infrared dichroism to follow the deformation behavior in specific domain locations can be done with relative ease for these polymers using Fourier Transform Infrared Spectroscopy. Such studies would also be of considerable aid in analyzing the mechanisms of domain reinforcement and large deformation mechanical behavior.